5-2015

The Role of OFD1 in the Pathogenesis of Polycystic Kidney Disease

Stephanie Jerman

STEPHANIE JUSTINE JERMAN
Candidate

BIOMEDICAL SCIENCES- PATHOLOGY
Department

This dissertation is approved, and it is acceptable in quality and form for publication:

Approved by the Dissertation Committee:

ANGELA WANDINGER-NESS, Ph.D., Chairperson

BRIDGET WILSON, Ph.D.

DIANE LIDKE, Ph.D.

LAURIE HUDSON, Ph.D.

ROLE OF OFD1 IN THE PATHOGENEIS OF POLYCYSTIC KIDNEY DISEASE

by

STEPHANIE JERMAN

B.B.A., Accounting, University of New Mexico, USA, 2003

DISSERTATION

Submitted in Partial Fulfillment of the
Requirements for the Degree of

Doctor of Philosophy
Biomedical Sciences

The University of New Mexico
Albuquerque, New Mexico

May, 2015

DEDICATION

To my parents, Stephen and Donna Jerman, my brother Greg Jerman, and sister Stacy Cecil for their unconditional love and support through all of my trials and tribulations. Lastly, I dedicate this to my godfather Dr. David Beaudoin, who always believed in me.

ACKNOWLEDGEMENTS

My sincere thanks go to my mentor, Dr. Angela Wandinger-Ness, who is a role model and inspiration to me and who encouraged me to be the best scientist that I could be. I owe it to her for many of the achievements I accomplished while obtaining my PhD and for always pushing me out of my comfort zone so that I could grow into an independent researcher. I will always aspire to live up to her exemplary level of caring, compassion, and intelligence. I would also like to acknowledge my dissertation committee members Dr. Laurie Hudson, Dr. Diane Lidke, and Dr. Bridget Wilson for all of their help and advice throughout these studies.

I would also like to thank my friend and teacher, Dr. Heather Ward, and my “lab mom” Elsa G. Romero, I could never thank you both enough for all of your help throughout the years. I thank my lab mate Yuna Guo who is an endless source of positive energy and can always put a smile on my face. Past members of the Wandinger-Ness lab that I had the pleasure to work with, Soumik Basuray and Jacob Agola, thank you for showing me the ropes and providing technical assistance whenever I would need it.

I thank Dr. Rebecca Lee and Genevieve Phillips for providing me the technical assistance in the microscope facility and help with image analysis. Finally, I would like to extend a special thanks to Nathan Smith, my good luck charm, without whom none of this would have been possible.

ROLE OF OFD1 IN THE PATHOGENESIS OF POLYCYSTIC KIDNEY DISEASE

by

STEPHANIE JERMAN

B.B.A., Accounting, University of New Mexico, USA, 2003

Ph.D., Biomedical Sciences, University of New Mexico, USA, 2015

Abstract

Oral-facial-digital syndrome type1 (OFD1) is an inherited disorder caused by expression of mutant OFD1 protein and results in abnormalities in facial and limb development and polycystic kidney disease that resembles Autosomal Dominant Polycystic Kidney Disease (ADPKD). The similarities in renal disease pathogenesis in patients with OFD1 and ADPKD suggest that the proteins implicated in these diseases, OFD1 and the polycystins, respectively, function on a common pathway in the affected cell types. This calls for an investigation to uncover the mechanism by which OFD1 contributes to polycystic kidney disease pathogenesis, which remains unknown. This thesis details for the first time the assembly of a ciliary signaling microdomain containing OFD1, the polycystins, the epidermal growth factor receptor (EGFR), and the domain organizing flotillin

proteins in renal epithelia and cells of the oral cavity. Also, the studies presented here provide a mechanism by which OFD1, a soluble protein, is trafficked to primary cilia via its interaction with polycystin-1 (PC1), a ciliary membrane protein. The presented data demonstrate the requirement of coiled coil domains found in both OFD1 and PC1 for OFD1 interaction with PC1 and proper localization of OFD1 to primary cilia. The composite work provides the foundation for identifying potential molecular targets for therapeutic interventions for the millions of individuals suffering from polycystic kidney disease worldwide.

TABLE OF CONTENTS

LIST OF FIGURES

LIST OF TABLES

ABBREVIATIONS

CKD: Chronic kidney disease

ESRD: End-stage renal disease

ICKD: Inherited cystic kidney disease

PKD: Polycystic kidney disease

ADPKD: Autosomal dominant polycystic kidney disease

ECM: Extracellular matrix

PCP: Planar cell polarity

Wnt: Wingless/Integrated

AQP: Aquaporin

OFD1: Oral-facial-digital syndrome type 1

PC1: Polycystin-1

PC2: Polycystin-2

GPS: G protein-coupled receptor proteolytic site

PLAT: Polycystin−lipoxygenase−alphatoxin

JAK: Janus Kinase

Ca^{2+}: Calcium

ER: Endoplasmic reticulum

mTOR: Mammalian target of rapamycin

MAPK: Mitogen-activated protein kinase

ERK: Extracellular signal-regulated kinase

EGFR: Epidermal growth factor receptor

STAT: Signal transduction and activator of transcription

PIP_2: Phosphatidylinositol-4,5-bisphosphate

PLC: Phospholipase C

PCM-1: Pericentriolar material 1

CC: Coiled coil

RCTE: Renal cortical tubular epithelial

RPTEC: Renal proximal tubule epithelial cells

MO6-G3: Odontoblast cells

Q4004X: Autosomal dominant polycystic kidney disease cystic epithelial cells

46M06: Polycystic kidney disease primary cell line

PFA: Paraformaldehyde

NA: Numerical aperture

ErbB: Erythroblastic Leukemia Viral Oncogene

IFT: Intraflagellar transport

V2R: Vasopressin type 2 receptor

Chapter 1: Introduction

Modified from: Stephanie Jerman, Angela Wandinger-Ness, and Heather H. Ward (2013). *Polycystins and the Pathophysiology of ADPKD.* In: Polycystic Kidney Disease: from Bench to Bedside. 1st edition electronic book. Editors: R.L. Bacallao and V.H. Gattone, II. Future Science Group, UK.

The number of individuals suffering from inherited, acquired, and developmental chronic kidney disease (CKD) is on the rise worldwide [1-3]. In 2014, the National Center for Chronic Disease Prevention and Health Promotion estimated that over 20 million people in the United States are living with some form of CKD [4]. CKD is characterized by decreased kidney function and is associated with co-morbities (such as cardiovascular disease, diabetes, anemia, and abnormalities of mineral absorption) and increased mortality [5]. Many patients living with CKD progress to end-stage renal disease (ESRD), ultimately requiring dialysis or kidney transplantation. This imposes a tremendous burden on the healthcare system accounting for over $32 billion dollars per year in healthcare expenditures for treatment of patients with ESRD [5-7]. With the number of cases of CKD expected to rise 5%-8% worldwide, it is clear that we need to better understand the mechanisms contributing to CKD to tackle this growing global concern [2]

1.1 Inherited cystic kidney disease

Inherited cystic kidney diseases (ICKD) are a group of common, hereditary, heterogeneous disorders characterized by the growth of numerous fluid-filled

cysts on both kidneys [3]. ICKD affect between 1:400-1:1000 individuals, which translates to approximately 6 million people worldwide [8]. With the advancement of modern genetics, at least 70 different genes have been found associated with ICKD in humans [9]. ICKD result in renal cysts that originate from the epithelial cells lining nephrons and collecting ducts of the kidney [10]. A delicate balance of cellular proliferation and differentiation is required for normal kidney function. Mutations causing ICKD disrupt these fundamental processes by altering normal signaling, which in turn increases proliferation and renal epithelial apoptosis, causes dedifferentiation and changes in cell polarity, and affects fluid secretion and cellular adhesion. The net effect is cyst formation and expansion within the renal tubules. While all patients with ICKD have kidney cysts, many also share similarities in kidney pathogenesis including chronic renal interstitial inflammation and fibrosis, renal dysmorphogenesis, and ultimate progression to ESRD. However, the pathophysiologies of these disorders lie on a varied spectrum. Cystic kidney disease can be inherited in an autosomal dominant, autosomal recessive, or X-linked mode of inheritance, and vary greatly in the age in which in the disease presents, severity of symptoms, and extent of extrarenal involvement [11]. Symptoms of some forms of ICKD are not obvious until adulthood and primarily only involve the kidneys; while other forms of ICKD are present from birth or early adolescence and, in addition to cystic kidney disease, these forms of ICKD oftentimes include extrarenal manifestations including retinal degeneration, cardiovascular and skelatal abnormalities, and developmental disorders. A detailed list of the different forms of ICKD is given in **(Table 1)**. This

dissertation will focus on two common forms of ICKD that produce a similar kidney phenotype, Autosomal Dominant Polycystic Kidney Disease and Oral-Facial-Digital Syndrome Type 1. The mechanism by which mutations in different genes that cause two distinct diseases, yet result in indistinguishable kidney disease, remains unclear and is the focus of the studies presented here.

Different Forms of ICKD

Disease	Inheritance	Genes	Protein Products
Autosomal Dominant Polycystic Kidney Disease	Dominant	*PKD1* or *PKD2*	Polycystin-1 or Polycystin-2
Autosomal Recessive Polycystic Kidney Disease	Recessive	*PKHD1*	Fibrocystin/Polyductin
Oral-Facial-Digital Syndrome Type 1	Dominant	*OFD1*	OFD1
Nephronopthisis	Recessive	*NPHP1*	Nephrocystin-1
Autosomal Dominant Polycystic Liver Disease	Dominant	*PRKCSH* or *SEC63*	GIIβ or SEC63
Medullary Cystic Kidney Disease	Dominant	*MCKD1/MUCI* or *MCKD2/UMOD*	Mucin-1 or Uromodulin (Tamm-Hoesfall)
Tuberous Sclerosis Complex	Dominant	*TSC1* or *TSC2*	Hemartin or Tuberin
von Hippel-Lindau Disease	Dominant	*VHL*	pVHL
Bardet-Biedl Syndrome	Recessive	*BBS*	BBS
Meckel-Gruber Syndrome	Recessive	*MKS1*	Meckel Syndrome Type 1

Table 1. Different forms of ICKD. Table lists different forms of inherited chronic kidney diseases, their mode of inheritance, and the genes and protein products affected in the disease.

1.2 Autosomal Dominant Polycystic Kidney Disease and Oral-Facial-Digital Syndrome Type 1

1.2.1 Autosomal Dominant Polycystic Kidney Disease

Autosomal dominant polycystic kidney disease (ADPKD) is the most common form of ICKD. ADPKD is a slowly progressive disease characterized by cardiovascular and renal abnormalities. ADPKD is caused by mutations in the *PKD1* gene located on chromosome 16p13.3 (~85% of reported cases) or *PKD2* gene located on chromosome 4q21-23 (~15% of reports cases) [10]. Mutations in *PKD1* or *PKD2* result in indistinguishable disease phenotypes; however, patients with *PKD2* mutations often present later in life and have a better disease prognosis [10]. The hallmark of ADPKD is the presence of hundreds of fluid-filled renal cysts that can exceed two inches in diameter **(Figure 1)**.

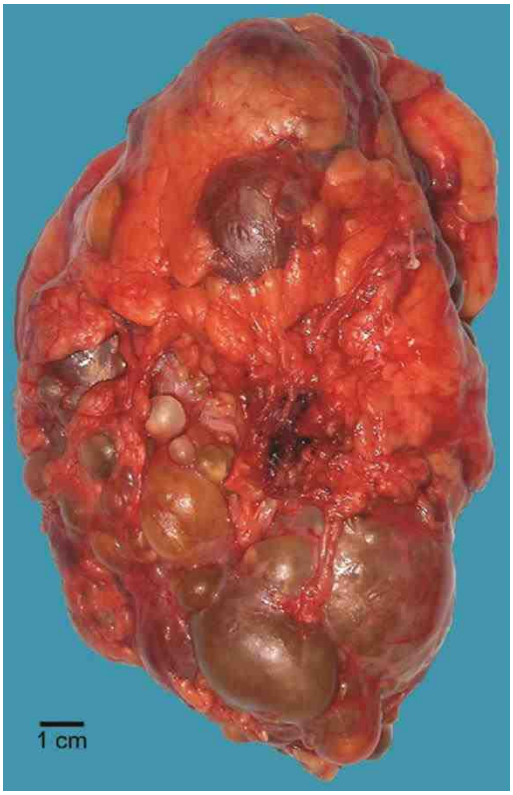

Figure 1. ADPKD kidney. ADPKD kidneys enlarge during disease progression. Kidney weights range from a normal 150g to 4000g, and cysts of differing sizes can be found throughout the nephrons and collecting ducts. Cysts may be filled with clear cyst fluid, blood, or white, opaque fluid, which is an indication of infection. ADPKD cysts increase in size during disease progression and obstruct functional regions of the kidney. Scale bar = 1 cm, photo provided by Indiana University Department of Pathology.

Renal cysts form *in utero* and throughout a patient's lifetime and recent imaging studies revealed that cysts which form early in life have the most dramatic impact on disease progression [12-14]. Cysts form in less than 1% of the 0.5-2 million nephrons [15] and more cysts initiate from collecting ducts than the nephron proper [14]. Given the low incidence of cyst formation (when compared to the number of nephrons present in both kidneys), scientists have postulated that additional genetic hits, local injury through renal ischemia, epigenetic, or other environmental factors are necessary to initiate cyst formation. This hypothesis is known as the "two-hit" mechanism, in which the first hit is an inherited genetic mutation on one allele followed by a somatic mutation on the second allele. Cyst formation likely instigates local renal fibrosis and inflammation, and the consequent cyst expansion represents an interplay between defective signaling cascades generated by dedifferentiated cystic epithelia, remodeling of the basal interstitium, and signaling activation caused by ligands present in apically-secreted cyst fluid.

Cyst expansion and concurrent renal fibrosis and interstitial inflammation promote kidney enlargement. ADPKD kidneys enlarge at an average rate of 5% per year [16] with cyst enlargement occurring at an average growth rate of 12% per year [12]. However, this average rate is actually punctuated by periods of more rapid growth as evidenced in human studies [14]. As cysts grow, they impinge upon normal tubules and renal blood vessels, resulting in decreased renal function and blood flow. Cysts are highly susceptible to infection and

hemorrhage; hence additional ADPKD renal symptoms include hematuria and urinary tract infections along with the occurrence of kidney stones, polyuria and flank pain.

Though the renal pathology is the most striking feature of ADPKD, multiple extrarenal manifestations do occur contributing to morbidity of ADPKD patients. Indeed, cardiovascular complication is a leading cause of death in ADPKD patients [17] and a majority of ADPKD patients present with hypertension even before renal function declines [18,19]. Decreased nitric oxide production results in increased vascular resistance, which in combination with renal factors, leads to hypertension [18,20,21]. ADPKD patients are at greater risk for large artery and cerebral aneurysms [17,22], likely due to aberrations in vascular smooth muscle and endothelial cells resulting in matrix rearrangements that lead to weakening of the vascular wall and abnormal pressure sensing [23]. Additional extrarenal manifestations of ADPKD include mitral valve prolapse and other valve abnormalities, inguinal and ventral hernias, occurrence of gastrointestinal diverticuli, and formation of cysts in epithelial-lined ductal organs such as the liver, pancreas, seminal vesicles and ovaries (among others). The pathophysiology resulting from ADPKD is well documented; however, the links between *PKD1* and *PKD2* gene mutations and the onset and progression of ADPKD remain an area of active study in order to develop a complete picture of disease pathogenesis.

Altered Kidney Function in ADPKD

ADPKD is a pleiotropic disease causing cellular, molecular, and structural changes in the kidney. The dysregulated kidney functions that lead to cyst formation in ADPKD can be divided into four general categories: (1) loss of cell polarity, (2) aberrant fluid transport, (3) basement membrane and matrix abnormalities, and (4) increased cell proliferation (discussed further in Section 1.3.3 *Signaling Pathways Regulated by the Polycystins*).

Maintenance of apico-basal polarity is necessary for normal tubule function. Loss of cell polarity and altered cellular differentiation are common features observed in cystic renal epithelial cells. For example, in normal renal epithelia the Na^+-K^+-ATPase localizes exclusively to the basolateral plasma membrane. However, in ADPKD cystic epithelial cells, the Na^+-K^+-ATPase is mislocalized to the apical surface [17]. Additionally, in ADPKD cystic epithelia, E-cadherin is replaced with N-cadherin, adopting a phenotype similar to that found during fetal development [17,24]. Changes in cadherin expression may in part enable cystic epithelial cells to preferentially associate with each other and, coupled with increased proliferative potential, cause cysts to pouch out and wall off from the tubule of origin **(Figure 2)**. The secreted extracellular matrix (ECM) underlying cystic epithelium also resembles that secreted by immature cells [24,25]. Collectively, these studies show that cystic epithelia adopt an immature phenotype with different cell polarity than that of mature renal epithelial cells.

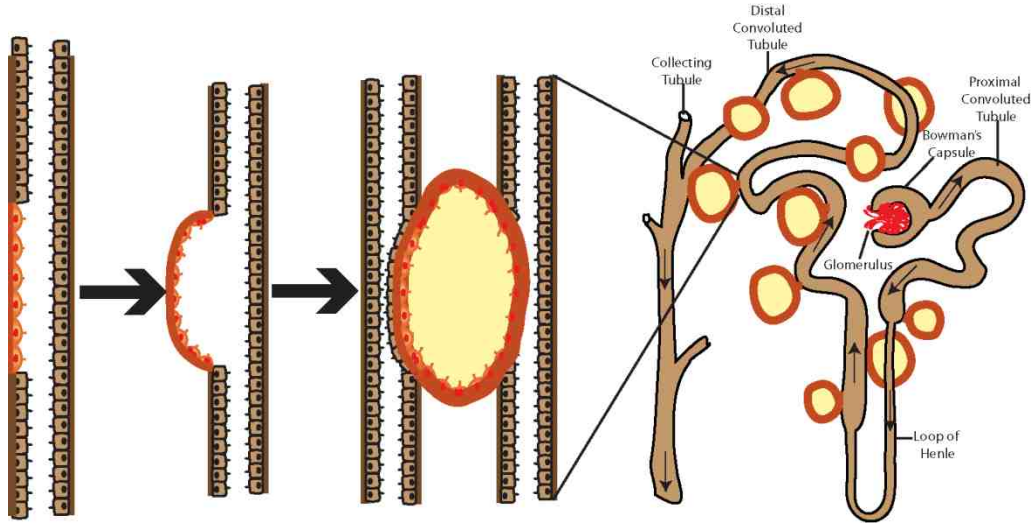

Figure 2. Cyst growth. ADPKD renal cysts pouch out, then wall off from the tubule from the tubule of origin. Cyst expansion causes tissue distortion and impedes kidney function.

In addition to apico-basal polarity, tissue integrity is also dependent on planar cell polarity (PCP), which is defined as the uniform organization of cells within a plane of a mature epithelial monolayer, such that all cells are oriented in a similar asymmetrical pattern, parallel to the basement membrane and perpendicular to apico-basal polarity [26]. Correct PCP is crucial for proper orientation of the mitotic spindle to ensure kidney tubular cells divide to increase tubule length while maintaining a constant tubule diameter [26]. The contribution of dysregulated PCP in the formation of cysts is not completely understood, however, evidence suggests that cystic epithelia exhibit PCP defects [27]. While loss of PCP in itself is not sufficient to initiate cyst formation, PCP dysregulation may contribute to overall cyst expansion. Dysregulation of noncanonical wingless/integrated (Wnt)/PCP signaling in cystic epithelia can lead to misorientation of mitotic spindles and subsequent cell division out of the plane of the epithelium, increasing tubule diameter and contributing to cyst expansion. PCP is regulated, in part, by noncanonical Wnt/PCP signaling, and altered regulation of Wnt signaling cascades is implicated in the cellular dedifferentiation of cystic epithelia [28]. Wnt signaling cascades are critical in the regulation of embryogenesis and the establishment and maintenance of cellular polarity and differentiation, and thus, tight regulation of these pathways are required for maintenance of tubular integrity [28].

Further contributing to cyst expansion in ADPKD is the observation that cystic epithelia exhibit aberrant expression and activation of ion transporters and water channels. Normal kidney epithelia primarily function to reabsorb water and small

molecules from the kidney ultrafiltrate and the renal tubular reabsorption process is accomplished through ion transporters and channels located in the epithelial plasma membrane **(Figure 3A)**. Cystic epithelia switch their primary function from ion absorption to ion secretion resulting in fluid accumulation in the intracystic region. The aberrant expression, activation, and mislocalization of multiple ion transporters results in the secretion of fluid into the cyst lumen [29]. Secretion of water by cystic epithelia is facilitated by mislocalization and over activation of aquaporin (AQP) water channels AQP1 and AQP2, respectively. Cumulatively, the aberrant apical secretion of ion transporters and AQP water channels maintain the cyst lumen and promote cyst expansion **(Figure 3B)**.

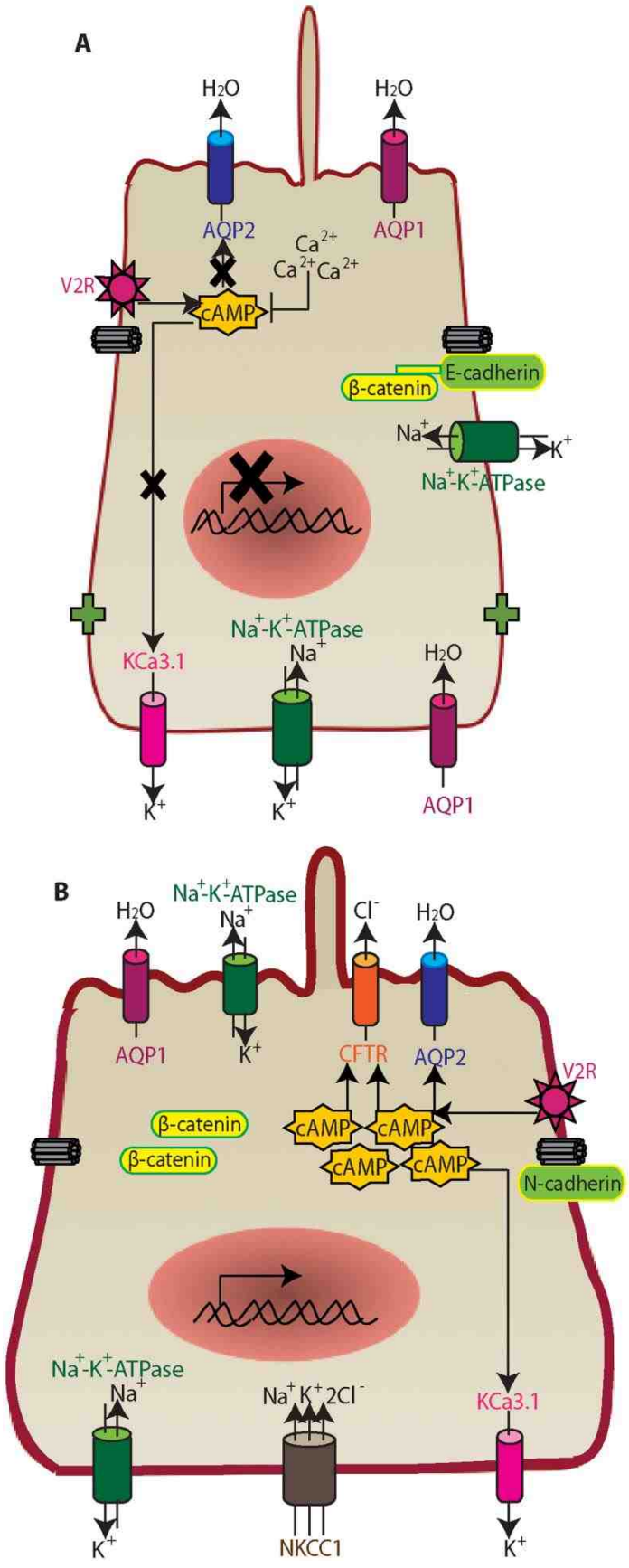
A
H2O
H2O
AQP2
AQP1
Ca2+
Ca2+ Ca2+
V2R
cAMP
E-cadherin
β-catenin
Na+
K+
Na+-K+-ATPase
Na+-K+-ATPase
KCa3.1
Na+
H2O
K+
K+
AQP1
B
Na+-K+-ATPase
H2O
Na+
Cl-
H2O
AQP1
K+
CFTR
AQP2
V2R
β-catenin
β-catenin
cAMP
cAMP
cAMP
cAMP
N-cadherin
Na+-K+-ATPase
Na+
Na+ K+ 2Cl-
KCa3.1
K+
NKCC1
K+

Figure 3. Altered localization and regulation of proteins and ion transporters contribute to cyst initiation and expansion in ADPKD. Normal renal epithelial cells primarily absorb ions and water from kidney ultrafiltrate (A). Crosstalk between intracellular Ca^{2+} and cAMP regulates intracellular cAMP levels, which are produced in part by vasopressin receptor, V2R, signaling. Maintaining intracellular cAMP homeostasis decreases activation of the cAMP-induced K^+ transporter, KCa3.1, and water channel, AQP2. Basolateral and apical AQP1 channels regulate and maintain water reabsorption processes in tubular epithelia. Basolateral Na^+-K^+-ATPase reabsorbs Na^+. Cystic renal epithelia switch their main function from ion absorption to ion secretion (B). Decreases in intracellular Ca^{2+} levels, in combination with V2R activation, increases intracellular cAMP and activates cAMP-induced KCa3.1 transporter, thus causing an efflux of K^+ and creating negative intracellular membrane potential. Negative membrane potential causes Cl^- secretion into the cyst lumen by cAMP-activated CFTR. CFTR is absent from mature kidney tubules, but expressed at the apical membrane in the majority of cystic epithelia. AQP1 is enriched at the apical membrane and Na^+-K^+-ATPase mislocalizes to the apical surface in cystic epithelia resulting in apical secretion of water and Na^+. Loss of β-catenin transcriptional regulation leads to aberrant expression of target genes. E-cadherin is replaced with N-cadherin at adherens junctions, which causes the cystic epithelia to preferentially associate with each other and form cysts.

Renal fibrosis is concurrent with cyst expansion in ADPKD [24]. Fibrosis in ADPKD is similar in some ways to other chronic forms of kidney disease in terms of progression and composition [24,30], yet distinct due to changes in matrix synthesis and cytokine secretion profiles of cystic renal epithelia [24,25]. Classically, chronic renal fibrosis is characterized by: increased synthesis and secretion of matrix components accompanied by decreased matrix degradation; recruitment and activation of fibroblasts and inflammatory cells to the renal interstitium; proliferation of interstitial cells; and, impingement on renal tubules and capillaries [24,31,32]. Cell signaling and protein expression changes in polycystic tubular epithelial cells, along with alterations in the tubular basement membrane, likely trigger renal fibrosis in ADPKD **(Figure 4)**.

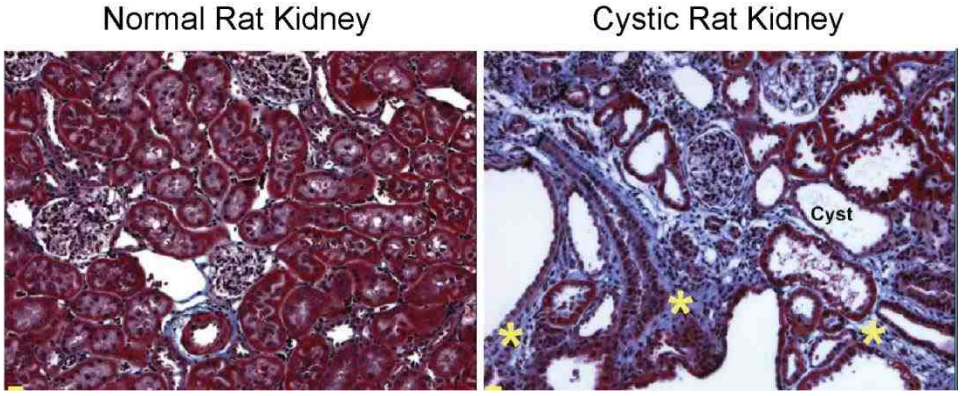

Figure 4. Fibrosis in ADPKD rat kidney. Thickening of the interstitium (*) in three-month-old male Han:SPRD Cy/+ cystic rat kidneys (Scale bar = 20 µm). Note the difference in renal ECM content between normal and cystic littermates.

Cyst growth and expansion of the basement membrane and renal interstitium causes tissue distortion through compression of renal tubules, lymphatics, and vasculature **(Figure 5)**. These events cause local renal ischemic injury, which in turn promotes pathogenesis both within the kidney and to the vascular system as a whole [33]. Since cyst expansion, inflammation, and fibrotic progression all contribute to disease pathogenesis and renal decline, exclusive targeting of cyst growth has not been sufficient to halt disease progression in human ADPKD. A detailed exploration of the mechanisms contributing to cyst formation is necessary to gain further insight into ADPKD pathophysiology.

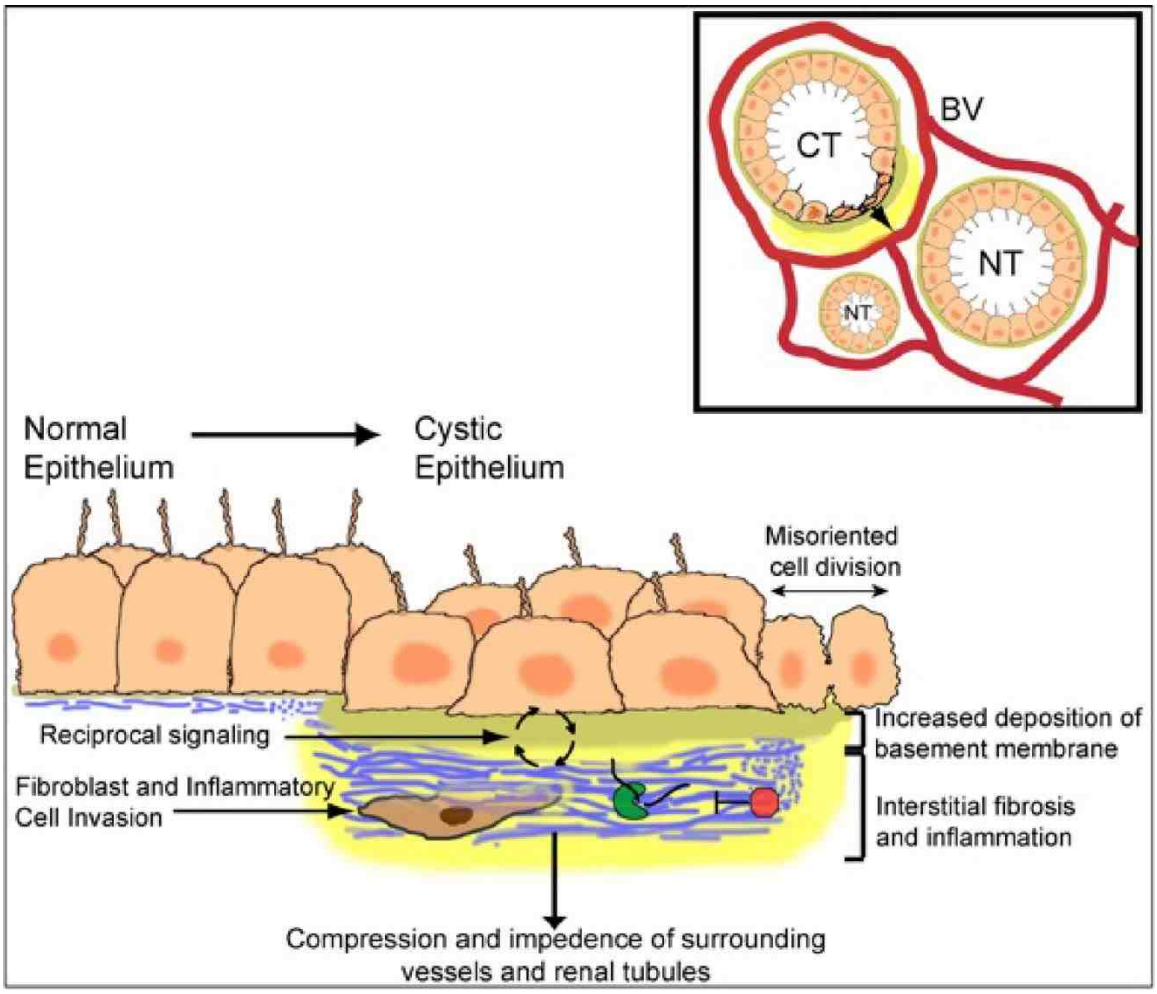

Figure 5. ADPKD tubular and interstitial pathogenesis. Renal epithelial cells undergo dedifferentiation and exhibit cellular polarity defects and increased proliferation. Cells lose the ability to respond to PCP cues, and thus, cell division of cystic epithelia extends tubule diameter. As cysts enlarge, cystic epithelia lose the cuboidal/columnar phenotype and adopt a more squamoid or endothelial appearance. Cystic epithelial cells synthesize and secrete alternative basement membrane and ECM proteins, which causes thickening of the basement membrane and underlying interstitial space. Expanded interstitium and cyst growth ultimately compress surrounding vasculature, lymphatics, and renal tubules (inset). Cytokines and growth factors recruit monocytes and fibroblasts and subsequently promote fibroblast proliferation and activation. Myofibroblasts also secrete matrix components and proteins involved in regulating matrix metabolism (activators and inhibitors). Matrix metalloproteinases and protease activators cleave and activate latent cytokines and growth factors resident within the matrix. Aberrant signaling and response to signaling from cystic epithelia and interstitial cells, combined with altered matrix metabolism, causes a feedback loop that promotes cyst expansion and fibrotic progression.

1.2.2 Oral-facial-digital syndrome type 1

Oral-facial-digital syndrome type 1 (OFD1) is an ICKD that occurs in 1:50,000 births [34]. OFD1 is caused by mutation of the *OFD1* gene, also called *CXORF5*, (located on the chromosome Xp22.2-Xp22.3) [35]. OFD1 is an X-linked, systemic disease that is embryonic lethal in males [36]. Affected females exhibit malformation of the face, oral cavity, hands and feet, as well as polycystic kidney disease (PKD) [34,35]. Genetic links between tooth defects and kidney disease were determined through mouse models with *OFD1* mutations or conditional knockout of *OFD1*. Mutant animals have disease mimicking human X-linked OFD1 including impaired odontoblast differentiation and dentin deposition, missing/supernumerary teeth, and cystic kidneys [36,37].

The advancement of high definition renal ultrasound scanning has shown that PKD is much more intimately associated with OFD1 than we were previously aware. In fact, the renal symptoms in patients with OFD1 are frequently proven to dominate the clinical course of the disease, ultimately causing ESRD requiring dialysis and transplantation [38]. Because of this, it is now recommended that an OFD1 diagnosis should be suspected in families with PKD affecting only the females. Due to the low rate of kidney transplantation, many patients with OFD1 will eventually die of renal failure. The slow progression and variability in kidney disease severity caused by mutant OFD1 closely resembles that seen in ADPKD, suggesting that the proteins that cause these diseases, OFD1 and the polycystins, respectively, may function in a similar pathway. The focus of the dissertation is to assess the similarities in protein composition and trafficking in

the cell types affected in ADPKD and OFD1 (renal epithelia and odontoblasts, respectively), and determining how these processes become dysregulated in both cell types to result in similar kidney pathogenesis.

1.3 The Polycystin Proteins

ADPKD results from expression of mutant polycystin-1 (PC1) protein, encoded by the *PKD1* gene, or polycystin-2 (PC2) protein, encoded by the *PKD2* gene. Overall, the polycystins play multifunctional roles in signaling during embryonic development, establishment of tissue polarity and differentiation, and homeostatic regulation.

1.3.1 Structure and Function of the Polycystin Proteins

PC1 is a large multi-spanning integral membrane glycoprotein with a predicted molecular mass of ~460 kDa. Due to its considerable size, the exact structure of PC1 has been difficult to characterize and only recently has atomic force microscopy of purified protein given us some insight into the domain organization and architecture of PC1 [39]. PC1 has a long extracellular N-terminus (>3000 aa), eleven transmembrane domains (~1030 aa), and a short (~200 aa) intracellular C-terminus **(Figure 6)**.

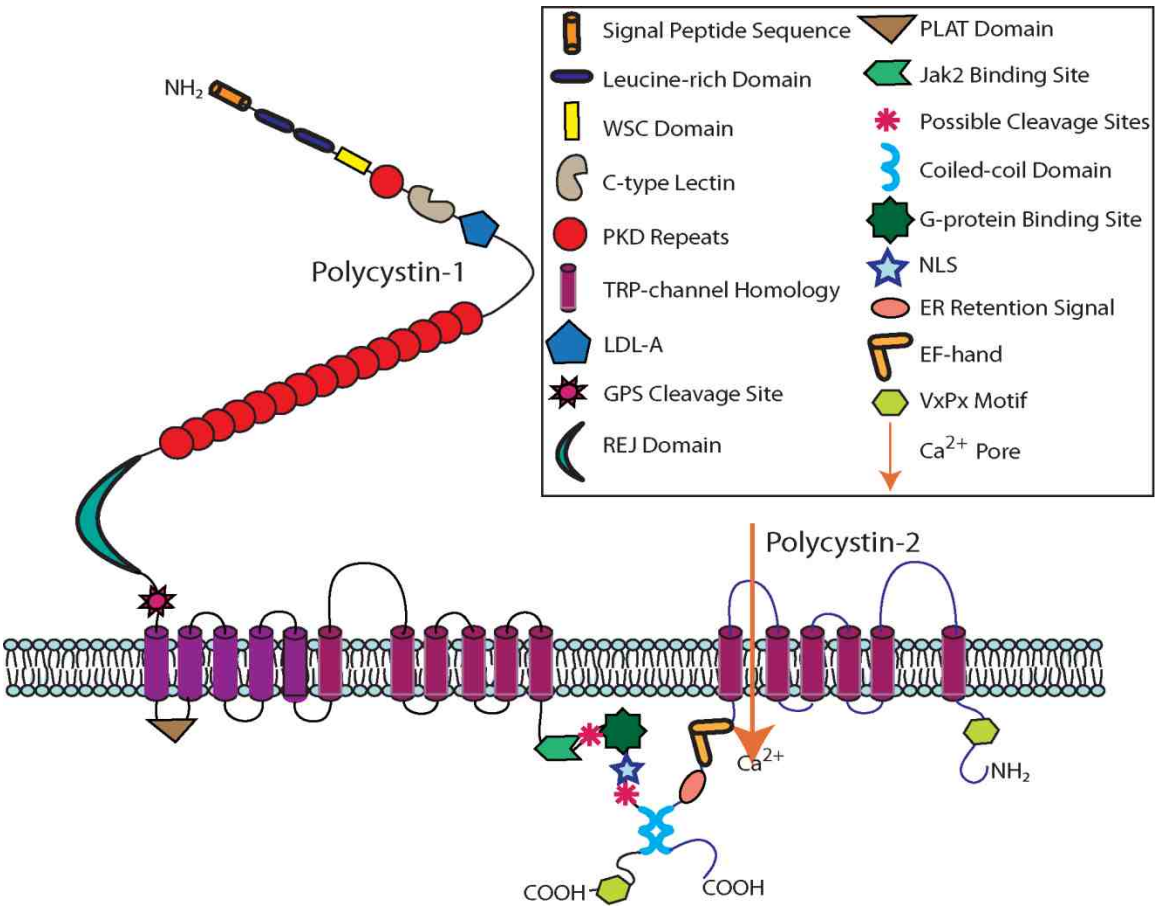
Signal Peptide Sequence
Leucine-rich Domain
WSC Domain
C-type Lectin
PKD Repeats
TRP-channel Homology
LDL-A
GPS Cleavage Site
REJ Domain
PLAT Domain
Jak2 Binding Site
Possible Cleavage Sites
Coiled-coil Domain
G-protein Binding Site
NLS
ER Retention Signal
EF-hand
VxPx Motif
Ca2+ Pore
NH2
Polycystin-1
Polycystin-2
Ca2+
NH2
COOH
COOH

Figure 6. Structural representation of PC1 and PC2. PC1 is an integral membrane protein with a long extracellular N-terminus, eleven transmembrane domains, and a short cytoplasmic C-terminal tail. The N-terminus of PC1 extends into the extracellular space and contains several structural domains, including a signal peptide sequence, and leucine-rich repeats surrounded by two cysteine-rich domains. The PC1 N-terminus contains a cell wall integrity and stress response component (WSC domain) and a C-type lectin domain, and both are implicated in carbohydrate binding. The PC1 N-terminus also contains a low-density lipoprotein (LDL) domain, 16 immunoglobulin-like PKD domains, a receptor for egg jelly (REJ) domain, and a G protein-coupled receptor proteolytic site (GPS). The polycystin−lipoxygenase−alphatoxin (PLAT) domain located on the first intracellular loop may mediate membrane attachment via other protein binding partners. PC1 contains eleven transmembrane domains; the final six share sequence homology with PC2. The intracellular C-terminus of PC1 contains multiple protein-protein interaction domains including a JAK binding domain, a G-protein binding domain, and a coiled coil domain. The C-terminal tail also contains two proposed cleavage sites, a nuclear localization signal (NLS), and a VxPx ciliary targeting motif. PC2 is an integral membrane protein with an intracellular N-terminus, six transmembrane domains, and an intracellular C-terminus. The N-terminus of PC2 contains a VxPx ciliary targeting domain. PC2 is a member of the Ca^{2+}-permeable channel with the ion pore predicted to reside between the 5^{th} and 6^{th} transmembrane domains. The intracellular C-terminus contains a Ca^{2+}-binding EF hand domain, an ER retention signal, and a coiled coil domain which interacts with the coiled coil domain of PC1 to form a heterodimeric complex.

PC1 has a structure similar to that of an adhesion molecule or cell surface signaling receptor, however a ligand has not been identified for PC1. The N-terminus of PC1 contains various interaction domains, motifs, and a G protein-coupled receptor proteolytic site (GPS). The PC1 N-terminus is predicted to sense extracellular mechanical stimuli, suggesting that PC1 acts as a mechanosensor to relay information from the extracellular environment into the cell to regulate cellular activities [40]. A portion of the cellular pool of PC1 undergoes cis-autoproteolysis at the GPS domain, which cleaves the N-terminal extracellular portion from the remainder of PC1, resulting in two separate cleavage products that remain noncovalently tethered. In the kidney, the cleaved version of PC1 likely plays a role in signaling pathways important for cell differentiation, whereas uncleaved PC1 appears to function primarily during embryonic development [12]. The first cytoplasmic loop in the transmembrane domain contains a polycystin−lipoxygenase−alphatoxin (PLAT) domain, which likely enables PC1 association with the plasma membrane. The final six transmembrane domains of PC1 share significant homology with the transmembrane regions of PC2 [12]. The C-terminus of PC1 contains various functional domains important for protein-protein interactions. Both a Janus Kinase 2 (JAK2) and G-protein binding domain were identified in the PC1 C-terminus, suggesting that PC1 is involved in the regulation of various signaling pathways. The C-terminal tail contains cleavage domains, producing tail fragments that can translocate to the nucleus to modulate transcriptional activities [41]. The first cleavage site liberates the entire C-terminus (p200), while

further cleavage of the C-terminus produces a 150 kDa fragment and a 112 amino acid fragment (p112) of PC1 [12,42]. The PC1 C-terminus contains a ciliary targeting VxPx motif [43] as well as a nuclear localization signal, which highlights the complexity of this molecule. Finally, the C-terminus of PC1 contains a coiled coil (CC) domain by which it interacts with the CC domain of PC2.

PC2 (968 aa) is an integral membrane protein with an intracellular N-terminus, six transmembrane domains, and an intracellular C-terminus **(Figure 6)**. PC2 has a predicted molecular mass of ~110 kDa and is a member of the Transient Receptor Potential (TRP) family of ion channels. PC2 is a non-selective, calcium (Ca^{2+}) permeable cation channel capable of modulating intracellular Ca^{2+} levels [44]. Like PC1, PC2 also contains a ciliary targeting VxPx motif; however, in PC2, this sequence is found in the N-terminus [12,27]. PC2 bears a Ca^{2+} channel pore predicted to reside between the 5^{th} and 6^{th} transmembrane domains. The cytoplasmic C-terminus of PC2 contains the CC PC1 interacting domain. Although there is conflicting data, it appears that the interaction between PC2 and PC1 via the C-terminal CC domain is crucial for PC2 channel regulation [45]. Furthermore, the CC region is connected to a Ca^{2+}-binding EF-hand domain by a flexible acidic linker. PC2 Ca^{2+} channel activity is dependent on binding of intracellular Ca^{2+} to the EF-hand, which then induces a conformational change in PC2 facilitated by the flexible linker region and an influx of Ca^{2+} [46].

1.3.2 Expression and Localization of the Polycystin Proteins

PC1 expression is greatest during embryonic development and decreases in adult tissues. The subcellular localization of PC1 is spatiotemporally regulated based on discrete functions during cell polarization **(Figure 7)**. PC1 is important for cell-matrix interactions and co-localizes with focal adhesions proteins, including integrins, at early time points in cell polarization [17,24]. Later, PC1 is important for establishing adherens junctions and desmosomes and relocates to the forming cell-cell contacts [12]. Once, the adherens junctions are fully established and stabilized by cytoskeletal interactions, PC1 disappears from the lateral membrane. In fully polarized cells, PC1 localizes to the nucleus, Golgi apparatus, cytoplasmic vesicles, and the primary cilium [12,17,47].

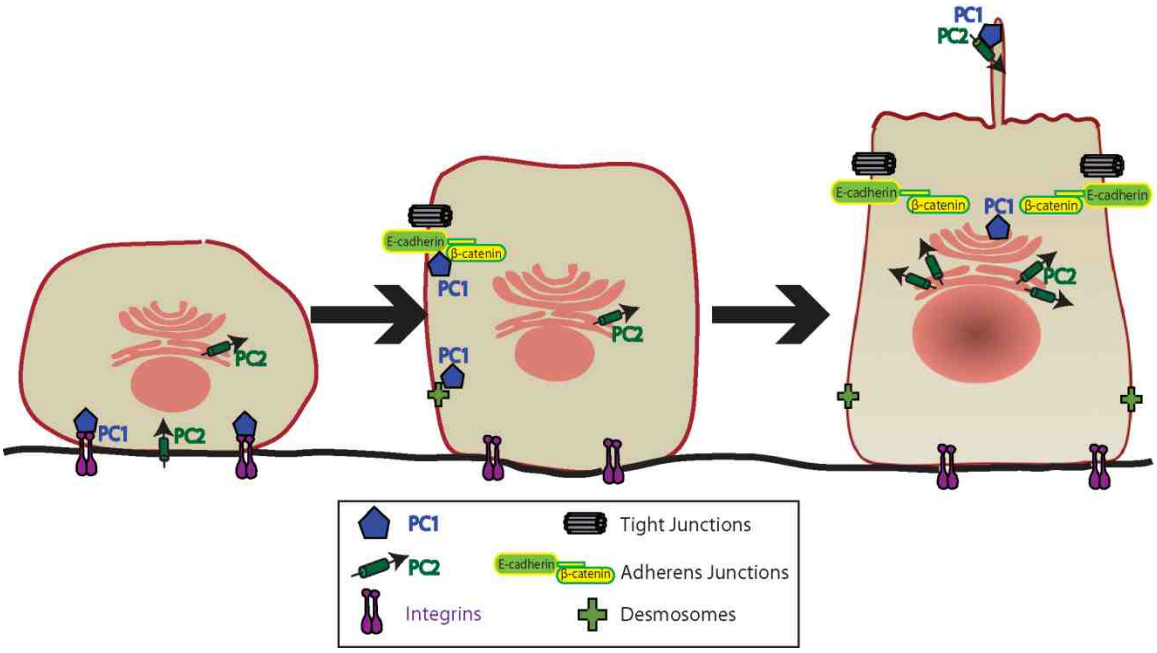

Figure 7. Subcellular localization of polycystins is spatiotemporally regulated. In normal renal epithelial cells, expression and localization of the polycystins is spatially regulated depending on the state of cell polarization. PC1 and PC2 are highly expressed during renal development. In the mature kidney, expression of PC1 is significantly decreased, while PC2 expression remains high. Spatiotemporal localization of PC2 is still under investigation but PC2 is known to reside in ER and cilia. In contrast, at early stages of cell polarization, PC1 is found at cell-matrix interactions and associates with focal adhesion proteins. As cells form cell-cell contacts, PC1 localizes to lateral membrane and associates with desmosomes and adherens junction proteins. Once cells are fully polarized, PC1 predominately localizes to the primary cilium where it forms a complex with PC2.

Like PC1, PC2 has multiple subcellular localizations including the endoplasmic reticulum (ER), Golgi apparatus, apical and basolateral plasma membranes, centrosomes, mitotic spindles, and the primary cilium [12,28] **(Figure 7)**. Determining how PC2 is delivered to and functions within different subcellular regions remains an active area of study; however, certain trafficking mechanisms and functions of PC2 have been defined. Corresponding with its role in intracellular Ca^{2+} regulation, there is a large resident population of PC2 in the ER. PC2 contains an ER retention signal in the C-terminus and is shuttled by the PIGEA protein from the ER to the Golgi apparatus. Retention of PC2 in the trans-Golgi and ER is facilitated by PACS proteins (PACS1; PACS2), which actively retrieve PC2 back to these compartments [12,27]. Although still debated, PC2 transport to the primary cilium is suggested to depend on an N-terminal sorting signal and the expression of PC1 [27]. Both PC1 and PC2 are present in urinary exosomes, suggesting a mechanism by which these proteins may be secreted and contribute to signaling to nearby cells [48].

The expression and localization of the polycystins has proved complex and dynamic during development and cell differentiation and polarization. This complexity likely reflects the pivotal functions that the polycystins serve both at the cellular level in the regulation of cell polarization, growth and differentiation, and at the organ and system level in sensing and communicating signaling events.

1.3.3 Signaling Pathways Regulated by the Polycystins

PC1 and PC2 act as sensors of external cues that feed into multiple signaling cascades and serve to control diverse cellular processes. The polycystins are upstream of pathways governing cellular proliferation, differentiation, and polarity **(Figure 8)**. Polycystin regulation of intracellular Ca^{2+} levels [12], G-protein signaling [27,49], mammalian target of rapamycin (mTOR) signaling [26,50] and growth factor signaling cascades such as the mitogen-activated protein kinase (MAPK)/extracellular signal-regulated kinase (ERK) [51-54] all serve to control the rate at which cells grow and divide **(Figure 8)**, and dysregulation of these cellular processes are implicated in ADPKD. The polycytins are crucial for the regulation of both canonical and noncanoical Wnt signaling pathways **(Figure 8)** and aberrant regulation of Wnt signaling results in loss of cell polarity and altered differentiation states [28,41]. Therefore, abnormal expression of PC1 or PC2 results in dysregulation of not one, but many, important cellular processes leading to the formation and progressive enlargement of the fluid-filled cysts characteristic of ADPKD.

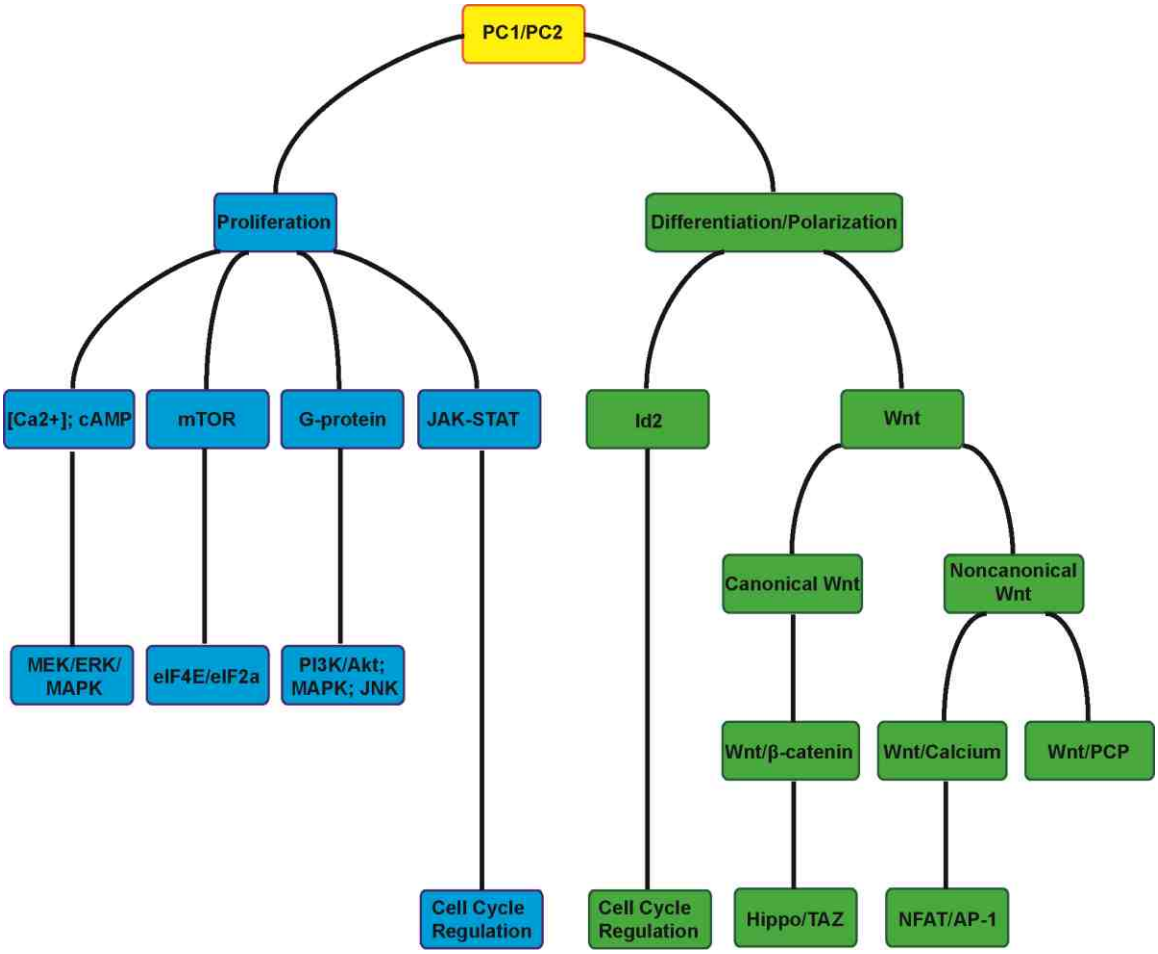

Figure 8. The polycystins regulate multiple signaling pathways. PC1 and PC2 are sensory proteins that function upstream and downstream of signaling pathways important for cellular proliferation, polarization, and differentiation.

A defining feature of ADPKD is increased cell proliferation along with increased apoptosis. Normal, full-length PC1 increases resistance to apoptosis through G-protein-dependent activation of the PI3K/Akt pathway. Mutant PC1 expression interferes with this normal regulation resulting in increased apoptosis of ADPKD renal epithelia [44]. PC1 functions as a negative regulator of G-protein signaling and this control is lost in cystic epithelia leading to increased apoptosis [27,49].

There are several known signaling pathways that contribute to increased cell proliferation in ADPKD. Abnormal activation of a serine/threonine protein kinase, mTOR, is one contributing factor to ADPKD disease progression. Activation of mTOR signaling results in diverse cellular processes including cell proliferation and protein synthesis. In ADPKD, mutant PC1 may contribute to aberrant activation of mTOR leading to cellular proliferation [26,27]. Additionally, mTOR activity is crucial for the phosphorylation of key components of the translation initiation complex, resulting in assembly and initiation of protein translation and cell growth [55]. Both PC1 and PC2 can negatively affect the protein synthesis machinery by inhibiting activation of the eukaryotic translation initiation factors eIF4E and eIF2a, respectively [56]. The negative regulation of eIF4E and eIF2a imposed by PC1 and PC2 is disrupted in ADPKD resulting in increased cellular proliferation **(Figure 8)**.

PC1 also modulates cellular proliferation via regulation of the Janus kinase (JAK)-signal transduction and activator of transcription (STAT) signaling cascade

(Figure 8), a pathway that is involved in the regulation of cell cycle progression [27]. PC1 contains a JAK binding domain, and PC1-JAK interaction causes activation of JAK and STAT. PC1 is involved in regulating both the upstream and downstream JAK-STAT signaling pathway to induce p21 expression and decrease cellular proliferation. Evidence suggests that the nuclear C-terminal fragment of PC1 is overexpressed in ADPKD, thus causing aberrant STAT activation and this dysregulation may contribute to the proliferative phenotype of cystic epithelia [57].

PC1 and PC2 form a receptor-channel complex in primary cilia of renal epithelial cells to facilitate Ca^{2+} influx and intracellular Ca^{2+} homeostasis [58] **(Figure 9A)**. Sustained intracellular Ca^{2+} levels activate the PI3K/Akt pathway to inhibit B-Raf. B-Raf is a protein kinase involved in the activation of the MAPK signaling pathway leading to increased cellular proliferation. Since expression of mutant PC1 or PC2 causes decreased intracellular Ca^{2+} concentrations in cystic epithelia, inhibition of B-Raf is decreased, and thus contributes to increased proliferation [44]. Crosstalk between intracellular Ca^{2+} levels and cAMP signaling also impacts cellular proliferation [59]. In normal renal epithelia, cAMP inhibits cellular proliferation by repressing the Raf-1/MEK/ERK signaling cascade. In cystic epithelia, decreased intracellular Ca^{2+} levels and changes in V2R activity cause an accumulation of intracellular cAMP and differential effects of cAMP signaling relative to normal renal epithelia. In the disease state, loss of intracellular Ca^{2+} homeostasis causes ADPKD cells to respond abnormally to

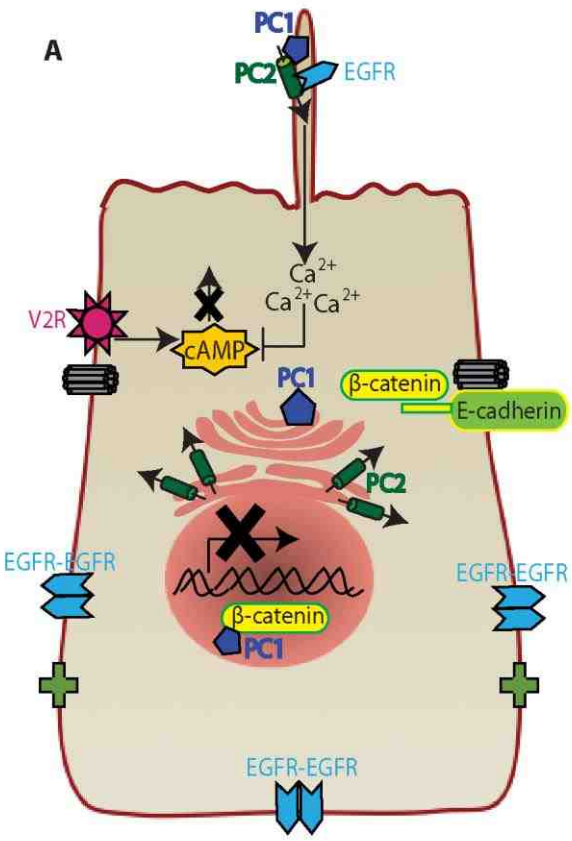
A
PC1
PC2
EGFR
Ca2+
Ca2+ Ca2+
V2R
cAMP
PC1
β-catenin
E-cadherin
PC2
EGFR-EGFR
EGFR-EGFR
β-catenin
PC1
EGFR-EGFR

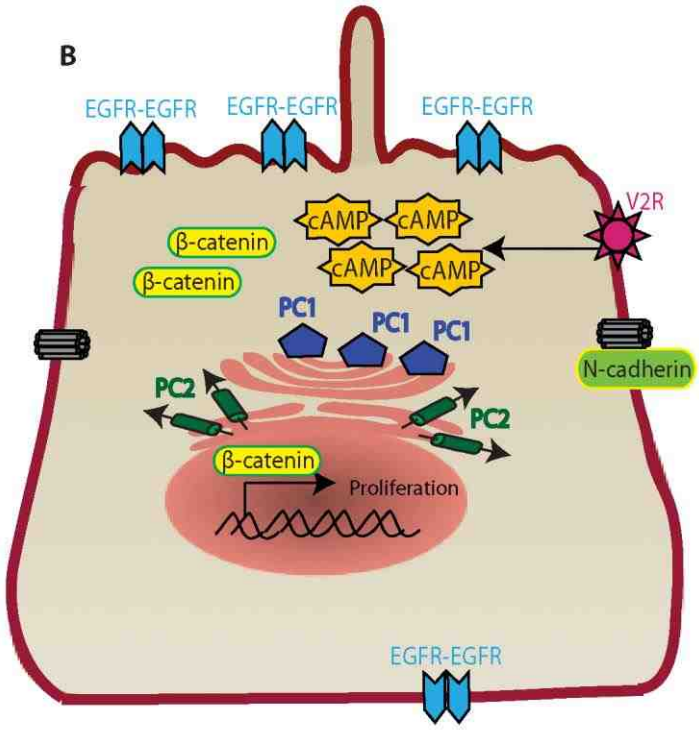
B
EGFR-EGFR
EGFR-EGFR
EGFR-EGFR
V2R
cAMP
cAMP
cAMP
cAMP
β-catenin
β-catenin
PC1
PC1
PC1
N-cadherin
PC2
PC2
β-catenin
Proliferation
EGFR-EGFR

Figure 9. Loss of ciliary signaling regulation results in aberrant cellular proliferation in ADPKD. PC1 and PC2 form a receptor-channel complex in primary cilia of renal epithelial cells to facilitate Ca^{2+} influx and intracellular Ca^{2+} homeostasis (A). Crosstalk between intracellular Ca^{2+} levels and cAMP signaling causes inhibition of target gene transcription resulting in inhibition of cellular proliferation. EGFR normally localizes to basolateral surface and primary cilia of renal epithelia. In cilia, EGFR interacts with PC2 to regulate Ca^{2+} channel activity from that that ciliary location. In ADPKD cystic epithelia, loss of intracellular Ca^{2+} homeostasis causes ADPKD cells to respond abnormally to cAMP and stimulate cell proliferation through activation of the MEK/ERK signaling pathway (B). Additionally, EGFR is mislocalized to the apical membrane of renal epithelia where it can bind EGF ligand present within cyst fluid, thus causing activation and prolonged signaling from the wrong membrane domain, which contributes to unregulated cell proliferation in ADPKD.

cAMP and stimulate cell proliferation through activation of the MEK/ERK signaling pathway [59] **(Figure 9B)**. Treatment of ADPKD cystic cells with a Ca^{2+} ionophore to increase intracellular Ca^{2+} levels can reverse cAMP-stimulated cellular proliferation and may offer a new approach to the treatment of ADPKD [59].

Importantly, aberrant activation and mislocalization of the Epidermal Growth Factor Receptor (EGFR) is a major contributor to cyst epithelial proliferation in ADPKD. During renal development, EGFR forms heterodimers with ErbB2 at the apical plasma membrane. As cells polarize and differentiate, ErbB2 disappears and EGFR localizes exclusively to the basolateral membrane of normal kidney epithelia where it's signaling is tightly regulated **(Figure 9A)**. In ADPKD, EGFR is mislocalized to the apical membrane of cystic epithelial cells [17] **(Figure 9B)**. Missorted apical EGFR binds EGF ligand present within cyst fluid, thus causing activation and prolonged signaling from the wrong membrane domain, which contributes to unregulated cell proliferation in ADPKD. Furthermore, EGFR has a unique role in primary cilia to lower the threshold for PC2 activation. In cilia, PC2 calcium channel activity is inhibited by the binding of phosphatidylinositol-4,5-bisphosphate (PIP_2) to PC2. Activated EGFR forms a binding site for the catalytic enzyme phospholipase C (PLC) which cleaves PIP_2 and allows for a PC2-mediated Ca^{2+} influx [52]. In the primary cilium, PC2 co-localizes with PC1 and other signaling molecules, such as EGFR, to form a signaling complex [52,60]. Mislocalization of EGFR in kidney epithelia causes global defects in the

regulation of this signaling pathway (both at cell membrane and within primary cilia) leading to increased proliferation, a major contributor to disease progression in ADPKD.

Collectively, the polycystins are crucial to the regulation of multiple signaling pathways controlling cellular proliferation, including mTOR, G-protein, JAK-STAT, and MAPK/ERK. PC1 and PC2 regulation begins at the plasma membrane with the upstream activation of these cascades and continues all the way to the nucleus to modify gene transcription and subsequent protein synthesis. The net effect resulting from the loss of these sensor proteins is uncontrolled proliferation, an altered differentiation state, loss of polarity, and fluid secretion in the affected cells, which promotes cyst formation and expansion in ADPKD

1.4 OFD1 protein

1.4.1 Expression of OFD1 protein

Oral-facial-digital syndrome type 1 results from mutations in the *OFD1* gene, which encodes OFD1 protein. OFD1 is a cytosolic protein whose expression is tightly regulated during development. OFD1 is highly expressed during human organogenesis in the metanephros, gonads, brain, tongue, and limbs, and at lower levels in the liver, pancreas, heart, and lung [61,62]. Studies have shown that OFD1 is expressed ubiquitously, albeit at lower levels, in adult tissues [62].

1.4.2 Structure and function of the OFD1 protein

The 1011-amino acid OFD1 protein contains an N-terminal LisH motif (which helps facilitate OFD1 interaction with microtubules) as well as five or six predicted C-terminal CC domains that enable OFD1 protein-protein interactions. OFD1 localizes to the centrosome during cell division, where it controls mother/daughter centriole length [63]. OFD1 has been shown to localize to the distal end of centrioles where it is important for distal appendage formation [63]. After the cells have finished dividing and become fully polarized, OFD1 can be found localized to basal bodies at the base of the primary cilia [64]. OFD1 is required for primary cilia formation and left-right axis specification [36,65]. OFD1 also localizes to centriolar satellites where autophagy-specific degradation of OFD1 is a requisite step in ciliogenesis [66].

OFD1 interacts with the centriolar protein PCM-1 and the intraflagellar transport protein IFT88 via OFD1 CC domains. In fact, targeting of IFT88 to the centrosome is dependent on its interaction with OFD1 through the OFD1 second CC domain [63,64]. The polycystins also contain CC domains, which mediate their protein-protein interactions, and are hypothesized to interact with OFD1 via these domains [64]. However, many important details about the interconnection between membrane proteins (such as polycystins) and soluble proteins (such as OFD1) that result in multi-organ diseases remain unclarified.

1.5 Primary Cilia Link ADPKD and OFD1 Diseases

The primary cilium is an antennae-like, microtubule-based protrusion from the apical cell surface of nearly every vertebrate cell. For decades after its discovery, the 9+0 primary cilia was largely ignored by scientists; believed to be a relic left over from our evolutionary past. However, recent studies have shown that mechanical bending of primary cilia in cultures kidney cells resulted in an increase in intracellular calcium that propagated out to neighboring cells [67]. These observations led to a renewed interest in this once ignored cellular organelle that has since produced evidence that primary cilia are crucial in a number of cellular processes, both during development and later for maintaining cellular homeostasis. The primary cilium is crucial during development where it plays a major role in Hedgehog and Wnt signaling cascades [37,68]. Primary cilia sense changes in the extracellular environment and relay extracellular cues into the cell. The primary cilium houses many important signaling proteins and functions as a signaling hub. The primary cilia contain ICKD proteins including PC1 and PC2. Not surprisingly, a multitude of human diseases caused by defects in ciliary proteins, termed ciliopathies, have been identified. ADPKD was the founding member of an ever-expanding list human ciliopathies, including OFD1.

Research into the primary cilium over the last decade has revealed some striking similarities in the mechanism whereby odontoblasts and renal epithelial cells respond to external stimuli. The function of the primary cilium of odontoblasts is

believed to closely mimic the sensory function of cilia in renal epithelial cells [69-71]. It is hypothesized that, in both cell types, the primary cilium is the critical link between extracellular mechanical stimuli and initiation of an intracellular signaling cascade in response. The primary cilium of an odontoblast is crucial for sensing the extracellular environment to regulate the formation of dentin and in tooth pain transmission. Similarly, the primary cilium in renal epithelial cells functions as a mechanosensor of external fluid flow to regulate cell differentiation and polarization. Odontoblasts and renal epithelial cells both display voltage-gated calcium channels and mechanosensitive potassium channels in their plasma membranes which are believed to act with primary cilia to transmit external messages into the cell [69,70]. Thus, in these two very different cell types the primary cilium serves a similar function for sensing and communicating changes in the external environment. Furthermore, ciliary protein defects often result in multi-organ involvement. This evidence highlights the importance of elucidating the commonalities between renal epithelia and cells of the oral cavity in order to gain a molecular understanding for how and why these diseases, such as OFD1 and ADPKD, result in multi-organ pathologies.

1.6 Overall Hypothesis

Many proteins associated with craniofacial and cystic kidney disease localize to and function within the primary cilium, including OFD1 [72,73] and the polycystins. The role of OFD1 in oral and renal pathologies is likely linked to its conserved expression and function, along with the polycystins, in the cilia of

odontoblasts and renal epithelia though the mechanistic underpinnings are unclear [37,64,74]. The polycystins and OFD1 are likely part of a conserved ciliary signaling microdomain in renal epithelia and cells of the oral cavity; which would explain the overlapping PKD patholodies observed in ADPKD and OFD1 diseases. Based on the available literature, the overall hypothesis for the dissertation is that **OFD1 is trafficked to the primary cilium in odontoblast cells using a conserved trafficking mechanism where it is assembled into distinct microdomains constituted of signaling and lipid scaffolding proteins.**

Specific Aims

Specific Aim 1: To characterize the ciliary signaling domains shared between kidney epithelial cells and cells of the oral cavity.

Specific Aim 2: To determine the interdependence of OFD1 and PC1 for OFD1 trafficking to primary cilia.

1.7 Significance

Findings over the last eight years show that many of the proteins associated with craniofacial and cystic kidney disease localize to and function in the primary cilium and when defective result in significant developmental defects and multi-organ failure [72,73]. Although the connection between OFD1 and renal disease has been known for many years [62], there has yet to be a conclusive investigation into the shared mechanisms in different cell types affected in these

diseases; cells of the oral cavity and renal epithelia, respectively. Past studies have focused mainly on the role of OFD1 at the centrosome and basal bodies and have shown that OFD1 is required for ciliogensis; however, OFD1 also localizes to the shaft of primary cilia, suggesting that OFD1 has a role beyond ciliogenesis and performs a distinct function in the primary cilium [64]. However, it is unknown how OFD1 arrives at the primary cilium or whether OFD1 is organized into ciliary microdomains with proteins implicated in PKD, either of which could explain similarities in disease pathology.

This research is significant because it, for the first time, probed for interconnections in the ciliary transport and functional assembly of OFD1 and the polycystins in specialized ciliary membrane domains. Innovative technologies were used to bridge gaps in the mechanistic details of how defects in cells of the oral cavity and kidney are related, leading to multi-organ disease. Characterizing this pathway may in the long term identify new therapeutic interventions for enhancing protein function in and/or targeting to the cilia.

Chapter 2: Materials and Methods

2.1 Cells and Reagents

Dental pulp-derived odontoblasts were used as representative neural crest derived cells from the oral cavity. The previously characterized MO6-G3 immortalized mouse dental pulp-derived odontoblast cell line was used as described [75]. MO6-G3 cells were grown in alpha-MEM supplemented with 10% FCS, 100 units/ml penicillin and streptomycin, 50 µg/ml ascorbic acid at 33°C in a humidified atmosphere of 95% air and 5% CO_2, with media changes every two days. The previously characterized PKD Q4004X PKD cells [76] were a generous gift from Dr. Robert Bacallao (Indiana University School of Medicine, Indianapolis, IN). Primary human cell line 46M06 was obtained from renal cysts of an ADPKD kidney. Human cell lines from renal cortical tubular epithelia (RCTE) were immortalized and cultured as previously described (Nauli, 2006, Ward 2011}. Renal proximal tubule cells (RPTEC) were purchased from Lonza (Walkersville, MD) and cultured using RCTE conditions. Cell culture reagents were purchased from Invitrogen/Gibco (Carlsbad, CA). Rabbit pAb directed against PC1 NM005 raised by immunizing rabbits with a distal carboxy-terminal fragment of polycystin-1 (amino acids 4070-4302) (Roitbak, 2004); rabbit anti-PC1 NM002 and NM032 raised in rabbits immunized with a peptide corresponding to aa 3633–3645 of human PC1, and with an N-terminal cysteine (CKRLHPDEDDTLVE; Suzanna Horvath, California Institute of Technology, Pasadena, CA). The peptide was conjugated to keyhole limpet hemocyanin using

benzoquinone and was used to immunize rabbits NM002 and NM032 (Covance, Denver, PA). For affinity purification, the same peptide was conjugated to Sulfalink gel (#20401; Pierce) according to the manufacturer's instructions (1 mg peptide/1 ml resin bed volume). Ten ml NM002 serum was incubated with 5 ml resin and washed to remove unbound immunoglobulin and serum proteins. Bound immunoglobulin was eluted with 0.1 M glycine (pH 2.5), immediately neutralized with Tris base, and used for immunoblotting and immunostaining experiments at a concentration of 10 µg/ml. (Ward, 2011); rabbit pAb against polycystin-1 (PC1-FP-LRR antibody) was generated against a fusion protein containing residues 27 to 360 of human polycystin-1 [77]. Primary antibodies were purchased from the following vendors: mouse mAb directed against acetylated α-tubulin (Sigma-Aldrich T7451, St. Louis, MO); rabbit pAb directed against α/ß-tubulin (Cell Signaling Technology #2148, Danvers, MA); mouse mAb anti-actin, clone C4 (Millipore #MAB1501, Temecula, CA); goat pAb directed against Lamin B (Santa Cruz sc-6217, Santa Cruz, CA); mouse mAb anti-polycystin-1 (Santa Cruz Biotechnology sc-130554, Santa Cruz, CA); mouse mAb anti-CD16 (Santa Cruz Biotechnology sc-20052, Santa Cruz, CA); mouse mAb anti-Giantin (AbCam ab37266, Cambridge, MA); mouse mAb anti-GST (Santa Cruz Biotechnology sc-138, Santa Cruz, CA); rabbit pAb anti-polycystin-2 (AbCam ab78622, Cambridge, MA); rabbit pAb anti-polycystin-2 (Santa Cruz Biotechnology sc25749, Santa Cruz, CA); rabbit pAb anti-EGFR (GeneTex GTX121919, Irvine, CA); rabbit pAb anti-EGFR (Santa Cruz Biotechnology sc-03, Santa Cruz, CA); rabbit pAb anti-ErbB2 (US Biological E3451-27, Swampscott,

MA); rabbit mAb anti-ErbB2 (Epitomics #2064-1, Burlingame, CA); rabbit pAb anti-OFD1 (Novus Biologicals NBP1-89355, Littleton, CO); goat pAb anti-OFD1 (Santa Cruz Biotechnology sc-168837, Santa Cruz, CA); rabbit pAb anti-Flotillin-1 (AbCam ab-50671, Cambridge, MA); mouse mAb anti-Flotillin-1 (BD Transduction Laboratories 610820, San Jose, CA); rabbit mAb anti-Flotillin-2 (Cell Signaling Technology #3436, Boston, MA); mouse mAb anti-Flotillin-2 (BD Transduction Laboratories 610383, San Jose, CA). Secondary antibodies were purchased from the following vendors: ECL Anti-Rabbit IgG-HRP (GE Healthcare NA934V, Little Chalfont, Buckinghamshire); ECL Anti-Mouse IgG-HRP (GE Healthcare NA931V, Little Chalfont, Buckinghamshire); donkey anti-goat IgG-HRP (Santa Cruz sc-2020, Santa Cruz, CA); Rabbit TrueBlot ULTRA: Anti-Rabbit Ig HRP (eBioscience 18-8816, San Diego, CA); Mouse TrueBlot ULTRA: Anti-Mouse Ig HRP (eBioscience 18-8817, San Diego, CA); mouse IgG2a, κ mouse isotype control (Sigma-Aldrich M5409, Saint Louis, MO) normal rabbit IgG isotype control (Santa Cruz Biotechnology sc2027, Santa Cruz, CA). The following fluorophore-conjugated secondary antibodies (Alexa Fluor dyes) were used for immunofluorescence assays: Alexa Fluor 488 Donkey Anti-Mouse IgG (Invitrogen A-21202, Grand Island, NY); Alexa Fluor 488 Donkey Anti-Rabbit IgG (Invitrogen A-21206, Grand Island, NY); Alexa Fluor 555 Donkey Anti-Mouse IgG (Invitrogen A-31570, Grand Island, NY); Alexa Fluor 488 Donkey Anti-Goat IgG (Invitrogen A-11055, Grand Island, NY); Alexa Fluor 555 Donkey Anti-Rabbit IgG (Invitrogen A-31572, Grand Island, NY); Alexa Fluor 647 Donkey Anti-Mouse IgG (Invitrogen A-31571, Grand Island, NY); Alexa Fluor 647 Donkey Anti-Rabbit IgG

(Invitrogen A-31573, Grand Island, NY); Alexa Fluor 647 Donkey Anti-Goat IgG (Invitrogen A-21082, Grand Island, NY).

2.2 Immunofluorescence Staining

For ciliary immunolocalization experiments, cells were grown on glass coverslips or 0.4 μm filter supports (Falcon-BD 353090, Franklin Lakes, NJ) for 4-6 days post-confluence and fixed with 3% paraformaldehyde (PFA) and processed for immunostaining as previously described [47]. Briefly, cells were permeabilized using 0.1% Triton-X 100 in 0.2% cold fish gelatin (blocking agent), and primary and secondary antibody incubations were performed in a humidified chamber at 37°C. Cells were labeled with antibodies directed against OFD1, EGFR, ErbB2, PC1, PC2, flotillin-1, or CD16. Cells were co-labeled with anti-acetylated α-tubulin or anti-α/β-tubulin to identify primary cilia. Controls for specificity and auto-fluorescence included staining with secondary antibodies alone. Ciliary colocalization of proteins with acetylated α-tubulin or α/β- tubulin was defined as exhibiting colocalization of the two signals across at least two pixels within the cilium as imaged in the confocal Z-stack data. Confocal immunofluorescence images were collected using a Zeiss LSM510 or Zeiss LSM 510-META laser-scanning confocal microscope (Carl Zeiss, Thornwood, NY) with 40x, 1.3 numerical aperture (NA) or 63x, 1.4 NA oil immersion objectives. LSM 510 Image Acquisition software (Carl Zeiss) was used to acquire images. Confocal Z-stacks were processed with the Zeiss Image Browser or Voxx2 (provided freely for noncommercial use by the Indiana Center for Biological Microscopy,

Indianapolis, IN, www.nephrology.iupui.edu/imaging/voxx/index.htm), and assembled using Adobe Photoshop and Illustrator (Adobe, San Jose, CA). Quantification was performed by importing z-stack images (all taken at identical settings) into SlideBook software (Intelligent Imaging) and creating a ciliary mask based on acetylated α-tubulin or α/β-tubulin staining. Ciliary protein (OFD1, PC1, PC2, flotillin-1, EGFR, GFP-OFD1, and CD16) staining intensities within the ciliary mask were quantified and normalized based on ciliary volume. At least 30-100 cilia were quantified from multiple experiments.

Movies were generated using the movie maker feature in Voxx2 software, and converted to .avi and .mpg file formats using QuickTime Player (Apple, Cupertino, CA) and TMPGEnc (Pegasys, Tokyo, Japan), respectively.

2.3 Proximity Ligation Assay (PLA)

PCR-based visualization was performed using Duolink II Rabbit/Mouse Red Kit (Olink Bioscience #92101) following manufacturer's instructions **(Figure 10)**. Cells were grown on coverslips 5 days post-confluency to allow for ciliogenesis and then fixed with 3%PFA. Primary antibodies used were: rabbit anti-EGFR (GeneTex GTX121919, Irvine, CA) and anti-polycystin-1 (Santa Cruz Biotechnology sc-130554, Santa Cruz, CA).

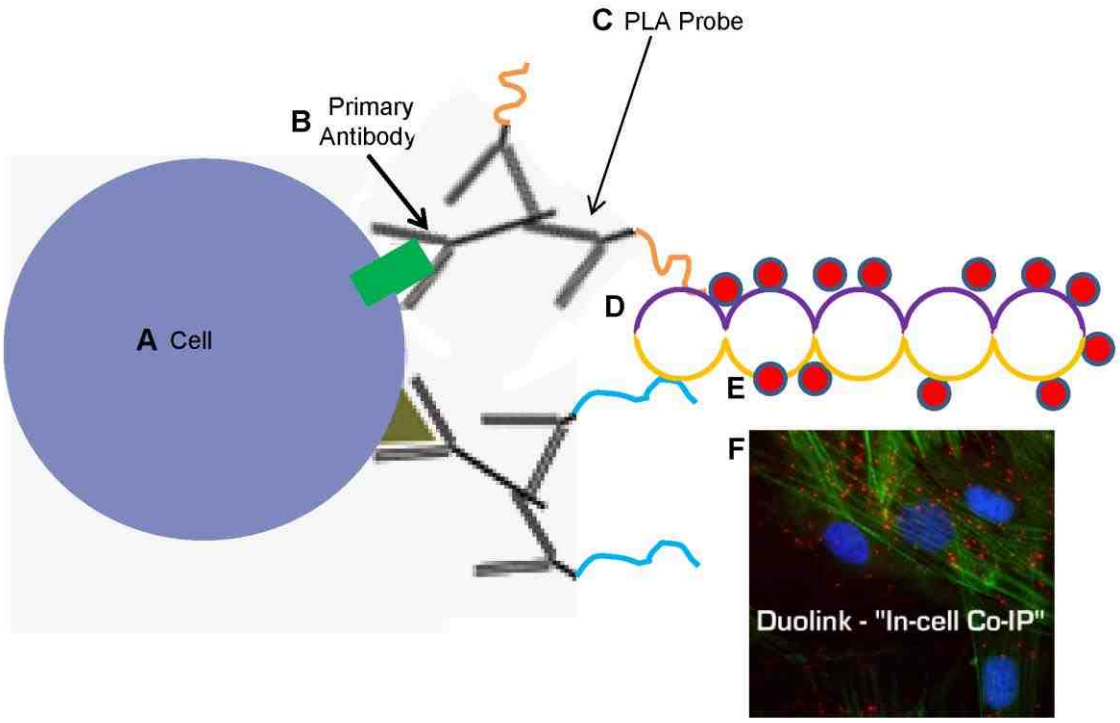

Figure 10. Duolink proximity based ligation assay. RCTE and MO6-G3 cells were plated on glass coverslips and grown 4-6 days post-confluency to allow for ciliogenesis (A). Cells were then fixed with 3% PFA and labeled with the following primary antibodies: rabbit anti-EGFR and mouse anti-PC1 (B). Secondary anti-rabbit and anti-mouse proximity ligation probe antibodies bound to specific PCR primers were added (C). When two proteins reside within <40nm, a rolling circle amplification reaction occurs (D) that integrates a fluorescent probe (E), which can be visualized using confocal microscopy (F).

2.4 Immunoprecipitations

Cells were grown 3-5 days post-confluency to ensure cilial formation. Cells were washed in PBS and lysed on ice in lysis buffer (0.5% NP40, 10 mM Tris-HCL pH 7.4, 150 mM NaCl, 5 mM EDTA, 50 mM NaF, 1mM Na_3VO_4, 60 mM n-octyl-β-D-glucopyranosid (AppliChem A1010, Saint Louis, MO), supplemented with protease inhibitor cocktail (Calbiochem/EMD Chemicals, Gibbstown, NJ). Lysates were precleared by centrifugation at 10,000 rpm in an Eppendorf microcentrifuge for 10 minutes and pretreated with protein G Sepharose or protein A Sepharose (Amersham Biosciences/GE Healthcare, Piscataway, NJ); 500 µg of total protein was used for immunoprecipitations. 500 µg cell lysate/40 µg protein A Sepharose or protein G Sepharose at 4˚C for 3 hours on a rotator. Precleared lystate supernatant was transferred to a clean microfuge tube and incubated with 1-3 µg of antibody directed against specified protein at 4˚C for 2 hours with gentle rotation. Antibody complexes were recovered by incubation with Protein G or Protein A Sepharose beads at 4˚C overnight. The immunoprecipitates were washed three times in lysis buffer and supplemented with SDS-PAGE loading buffer, heated for 5 minutes at 94˚C, and resolved by SDS gel electrophoresis.

2.5 Deciliation Assay

Renal epithelial cells were deciliated using 1.5 mM dibucaine-HCl for 5 minutes or 5 mM dibucaine-HCL in culture media for 5 minutes or 15 minutes, both of which rapidly and selectively caused the intact shedding of primary cilia from the

cell surface as was observed previously for IMCD3 cells [78,79]. Dibucaine treatment conditions were optimized by testing different concentrations and treatment times with the goal of promoting cilial release without cell detachment. A stock solution of dibucaine HCl (25 mM) was diluted to 1.5 mM or 5 mM in Tyrodes balanced salt solution. RCTE and MO6-G3 cells were grown on 60mM collagen-1 coated cell culture dishes for 5-6 days post-confluency to allow for ciliogenesis. Media was aspirated and cells were washed three times in PBS^{+} (PBS with 1 mM Ca^{2+} and 1 mM Mg^{+} added). Dibucaine was then added for 5-15 minutes with agitation causing deciliation. Tyrodes/dibucaine-HCl solution containing the cilia were then collected and centrifuged at 850 g_{max} for 10 minutes to collect cell bodies. The supernatant containing the ciliary fraction was collected and cilia were harvested by centrifugation at 28,000 g_{max} for 30 minutes. Supernatant was removed and pellet containing ciliary fraction was resuspended using 30 µl of lysis buffer and run on a SDS-PAGE gel.

2.6 Transient transfections with flotillin-2-GFP or GFP-OFD1

Flotillin-2–EGFP (where EGFP stands for enhanced green fluorescent protein) encoding full-length rat flottilin-2 fused in frame at the C-terminus to EGFP was provided by Dr. Ritva Tikkanen [80]. GFP-OFD1 encoding full-length OFD1 fused in frame at the N-terminus to pEGFP-N1 vector [81] was provided by Dr. Andrew Fry. Cells were plated at confluency on filter supports and cultured as described above 4-6 days post-confluency to ensure ciliogenesis. Transfections were performed by electroporation (iPoration-Primax Biosciences, Menlo Park, CA)

according to the manufacturer's instructions. The iPorator (Primax Biosciences, Inc.) yields 40-60% transfection efficiency in both cell types **(Figure 11)**. Flotillin-2-GFP and GFP-OFD1 transfection efficiency of ~40% was consistently observed. Cells were fixed with 3% PFA 16 h post-transfection, and viewed directly or processed for co-immunostaining.

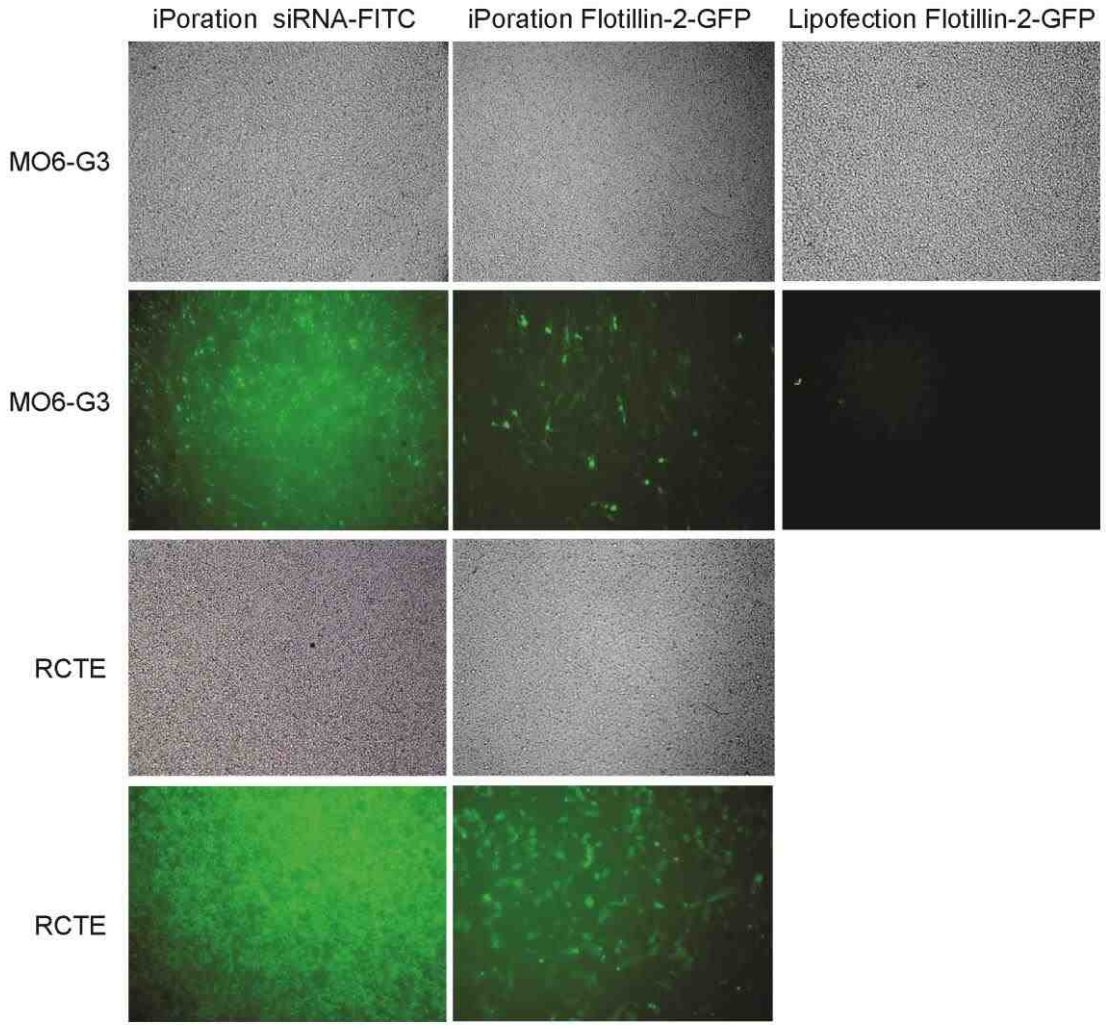

Figure 11. iPoration yields high transfection efficiencies for plasmid expression vectors and siRNA in post-confluent, polarized MO6-G3 and RCTE cells. MO6-G3 odontoblasts are an inherently more difficult cell line to transfect. This problem is compounded further by the necessity to transfect these cells after they are 100% confluent and have a completely polarized phenotype with very tight cell-cell contacts. With iPoration transfection efficiencies were 60-70% for FITC-labeled siRNA and 40-60% for flotillin-2-GFP in both MO6-G3 and RCTE cell types. As a comparison, traditional lipofection using Lipofectamine 2000 (Life Technologies) resulted in transfection efficiencies that were consistently <10%.

2.7 iDimerize-CD16.7-PC1-PC1 constructs

Purple: DmrD domain

Yellow: Preferred Furin cleavage site R-x-K-R

Red: CD16 without leader

Italics : *CD7*

Underline: PC1 WT

MATGSRTSLLLAFGLLCLPWLQEGSASRGVQVETISPGDGRTFPKRGQTCVVH

YTGMLEDGKKMDSSRDRNKPFKFMLGKQEVIRGWEEGVAQMSVGQRAKLTIS

PDYAYGATGHPGIIPPHATLVFDVELLKLETRGVQVETISPGDGRTFPKRGQTC

VVHYTGMLEDGKKMDSSRDRNKPFKFMLGKQEVIRGWEEGVAQMSVGQRAK

LTISPDYAYGATGHPGIIPPHATLVFDVELLKLETRGVQVETISPGDGRTFPKRG

QTCVVHYTGMLEDGKKMDSSRDRNKPFKFMLGKQEVIRGWEEGVAQMSVGQ

RAKLTISPDYAYGATGHPGIIPPHATLVFDVELLKLETRGVQVETISPGDGRTFP

KRGQTCVVHYTGMLEDGKKMDSSRDRNKPFKFMLGKQEVIRGWEEGVAQMS

VGQRAKLTISPDYAYGATGHPGIIPPHATLVFDVELLKLETSARNRQKRDLPKAV

VFLEPQWYSVLEKDSVTLKCQGAYSPEDNSTQWFHNESLISSQASSYFIDAATV

NDSGEYRCQTNLSTLSDPVQLEVHIGWLLLQAPRWVFKEEDPIHLRCHSWKNT

ALHKVTYLQNGKDRKYFHHNSDFHIPKATLKDSGSYFCRGLVGSKNVSSETVNI

TITQGLAVSTISSFSPPGAD*PPRASALPAPPTGSALPDPQTASALPDPPAASALP*

*AALAVISFLLGLGLGVACVLAR*TRSQLDGLSVSLGRLGTRCEPEPSRLQAVFEA

LLTQFDRLNQATEDVYQLEQQLHSLQGRRSSRAPAGSSRGPSPGLRPALPSRL

ARASRGVDLATGPSRTPLRAKNKVHPSST

The iDimerize-PC1-CD16.7-PC1-WT and iDimerize-CD16.7-PC1-359 (deletion of last 20 amino acids of the PC1 C-terminus) constructs were prepared under contract with Clonetech Laboratories Inc. (Mountain View, CA 94043). Each vector was fully sequenced by the University of New Mexico Health Sciences Center (UNM HSC) Research Services.

2.8 Transient co-transfections with GFP-OFD1 and either CD16.7-PC1 tripartite fusion proteins or iDimerize-CD16.7-PC1 constructs

GFP-OFD1 encoding full-length OFD1 fused in frame at the N-terminus to pEGFP-N1 vector [81] was provided by Dr. Andrew Fry. CD16.7-PC1-WT (CD16.7-PKD1(115-226)) and CD16.7-PC1-L152P (CD16.7-PKD1(115-226) L152P) described in Vandorpe et al., 2001 [82] were a generous gift from Dr. Seth Alper. CD16.7-PC1-WT tail (total length 379 amino acids) and CD16.7-PC1-359 (total length 359 amino acids- lacking the last 20 amino acids (ATGPSRTPLRAKNNKVHPSST) of the PC1 tail) fusion proteins used for the cloning of iDimerize-CD16.7-PC1 constructs described in Ward et al., 2011 and Vandorpe et al., 2001 [43,82]. Cells were plated at confluency on filter supports and cultured as described above 4-6 days post-confluency to ensure ciliogenesis. Transfections were performed by electroporation (iPoration-Primax Biosceinces, Menlo Park, CA) according to the manufacturer's instructions. The iPorator (Primax Biosciences, Inc.) yields ~40% transfection efficiency in RCTE cells [60]. GFP-OFD1 and iDimerize-CD16.7-PC1-WT, iDimerize-CD16.7-PC1-359, CD16.7-PC1-WT, or CD16.7-PC1-L152P co-transfection efficiency of ~40%

was consistently observed. 16 hours post-transfection cells were either processed for Golgi Lock assay or (iDimerize-PC1-CD16.7 constructs were treated +/- solubilizer) fixed with 3% PFA and viewed directly or processed for co-immunostaining. For iDimerize-CD16.7-PC1 constructs, 16 hours post-transfection cells were washed three times with PBS+ and treated +/- 250 nM solubilizing ligand in normal kidney media for 2 hours to allow for ciliary transport.

2.9 Golgi Lock Assay

Golgi lock experiments were performed as described in Matlin and Simons, 1983 [83]. Briefly, RCTE cells were grown on 0.4 µm filter supports (Falcon-BD 353090, Franklin Lakes, NJ) for 6 days post-confluence. Cells were then transfected with GFP-OFD1 and either iDimerize-CD16.7-PC1-WT or iDimerize-CD16.7-PC1-359 and cultured in normal kidney media (DMEM/F12, 10% Fetal Bovine Serum, 2 mM L-glutamine) for 20 hours post-transfection. Cells were then washed three times with DMEM/F12 Wash Buffer (0.35g DMEM/F12, 60mg KH_2PO_4, 10mM Hepes pH 7.4, 0.2% Pen/Strep) and treated with or without 250 nM iDimerize solubilizing ligand in DMEM/F12 Wash Buffer and placed immediately in a 20ºC water bath for 60-90 minutes. Cells were then washed three times with PBS, fixed with 3% PFA and processed with co-immunstaining as described above.

2.10 GST Pulldown

RCTE cells were grown on 100 mm cell culture dishes for 3-5 days post-confluency to ensure cilia formation. Cells were washed in PBS and lysed on ice in lysis buffer (200 mM Tris-HCl pH 8.0, 200 mM NaCl, 0.5% NP-40, 1 mM EDTA, 1 mM PMSF and supplemented with protease inhibitor cocktail (Calbiochem/EMD Chemicals, Gibbstown, NJ). Lysates were precleared by centrifugation at 10,000 rpm in an Eppendorf microcentrifuge for 10 minutes and pretreated with glutathione Sepharose beads (GE Healthcare, Piscataway, NJ); 500 µg of total protein was used for GST pulldown experiments. 500 µg cell lysate/40 µg glutathione Sepharose beads at 4˚C for 2 hours on a rotator. Precleared lystate supernatant was transferred to a clean microfuge tube. GST only, GST-OFD1-CTD and GST-OFD1-NTD were purified using 1 µg DNA to 50 µl of chemically competent Rosetta cells (defrosted on ice) (*E. coli* Rosetta 2(DE3) pLysS from Novagen) mixed gently and incubated on ice for 5 minutes, heat shocked at 42ºC for 30 seconds, and incubated on ice for another 2 minutes. Transformed cells were added to 250 µl of pre-warmed LB media and incubated at 37ºC, 225 rpm for 1 hour. 100 µl of cells were spread onto LB agar plates containing the appropriate antibiotic for selection and incubated at 37ºC overnight. Individual colonies were used to inoculate cultures of LB supplemented with the appropriate antibiotics. Cultures were grown at 37ºC, 225 rpm until an OD600 of ~0.5 was reached and expression was induced using 0.1 mM IPTG for 3 hours. NOTE: The temperature was then either kept at 37ºC for GST, GST-OFD1-NTD or adjusted to 22ºC for GST-OFD1-CTD. Cells harvested

by centrifugation and resuspended in lysis buffer (PBS containing 1 mM PSMF, 1 mM EDTA, 5 mM DTT, 200 µg/ml lysozyme) and sonicated on ice using 10 cycles of 10 second sonication followed by 20 seconds cooling. Centrifuged at 15000 g for 30 minutes at 4ºC. Supernatant was mixed with 1 ml of glutathione sepharose 4B beads (GE Healthcare) (pre-washed in 1x PBS three times) and rotated at 4ºC for 1 hour. Lysate with bead slurry was loaded onto a column and washed two times with ice cold 1x PBS. Bound protein was eluted in elution buffer (50 mM Tris-HCl pH 8.0, 25 mM reduced glutathione, 100 mM KCl, 1 mM DTT, 1 mM PMSF; pH adjusted to 8.0) in several 1 ml fractions. Protein recovery was determined by SDS-PAGE and Coomasie Blue analysis of aliquots of each fraction and those containing highest protein levels were pooled and dialysed against 1x PBS

Purified GST-tagged protein (100 µg) or equimolar GST alone was incubated for 1 hour at 4°C with glutathione Sepharose 4B beads (GE Healthcare) that had been pre-washed with NETN buffer (200 mM Tris-HCl pH 8.0, 200 mM NaCl, 0.5% NP-40, 1 mM EDTA). Beads were then washed four times with NETN buffer, resuspended in NETN buffer plus inhibitors (1 mM PMSF and 1mM Sigma Protease Inhibitor Cocktail) and incubated with 1 mg of pre-cleared RCTE cell lysate overnight at 4°C. The next day, beads were washed four times with NETN buffer and resuspended in protein sample buffer for analysis by SDS-PAGE and western blotting.

2.11 Statistical Analysis

For biochemical assays, means and standard errors were used to summarize the data from each experiment. For immunofluorescence experiments a minimum of 30-100 cells/condition were counted. All experiments were repeated at least three times. For immunoprecipitations and GST pulldown assays, comparisons across groups were made using one-way analysis of variance (ANOVA) to determine whether the group means were significantly different. When significant differences in group means are found, post-hoc multiple comparison tests (e.g., Tukey's test) were used to determine which groups are significantly different from one another. For protein expression analyses and immunofluorescence quantifications differences were analyzed by unpaired, two-tailed Student's *t* test. GraphPad Prism version 5.0 was used to perform statistical analyses.

Chapter 3: Results-OFD1 and Flotillins are Integral Components of a Ciliary Signaling Protein Complex Organized by Polycystins in Renal Epithelia and Odontoblasts

Stephanie Jerman, Heather H. Ward, Rebecca Lee, Carla A. M. Lopes, Andrew M. Fry, Mary MacDougall and Angela Wandinger-Ness (2014). *OFD1 and Flotillins are Integral Components of a Ciliary Signaling Microdomain Organized by Polycystins in Renal Epithelia and Odontoblasts*. PLoS One 9(9): e106330.

3.1 Introduction

Oral-facial-digital syndrome type 1 (OFD1; OMIM #311200) is an X-linked inherited disease characterized by the malformation of the face, oral cavity, hands and feet caused by heterogeneous mutations in the *OFD1* gene also known as *CXORF5*. Systemic manifestations of *OFD1* mutations include polycystic kidneys that resemble those caused by mutations in the *PKD1* or *PKD2* genes associated with autosomal dominant polycystic kidney disease (ADPKD) [84,85]. Due to the low rate of kidney transplantation, many patients with both craniofacial disorders and cystic kidney disease will eventually succumb to renal failure. Thus, there is an urgent need to clarify how the OFD1 gene product might cross-talk with the pathways regulated by the *PKD1* and *PKD2* genes to result in a common disease phenotype.

Many of the proteins associated with cystic kidney disorders, including PC1 and PC2 that underlie ADPKD, localize to and function in the primary cilium [47,71,81,86,87]. The polycystins have pivotal roles in calcium dependent signaling to multiple pathways and loss of signaling regulation when the proteins are mutant is thought to cause epithelial cell transdifferentiation and contribute to renal cyst development [85]. While the associations between defects in primary cilia, signaling and kidney disease have been recognized for over a decade, it is only recently that links between cilia, signaling, and tooth defects were revealed. Deletion of the Ofd1 gene (Ofd1Δ4-5/+-) in mice causes missing/supernumerary teeth, enamel hypoplasia, and polycystic kidney disease analogous to human oral-facial-digital syndrome type 1 [71]. The observed morphological defects in molars result from altered differentiation and polarization of odontoblasts when Ofd1 is mutant [36,71,81]. Localization of OFD1 to the primary cilium of tooth ectomesenchymal odontoblasts and renal epithelial cells is therefore speculated to be crucial for proper cellular differentiation of both cell types [71,81].

In related observations in the Tg737 mouse, ectopic teeth (premolars normally evolutionarily silenced) arise from inactivation of IFT88/polaris in the embryonic jaw and the consequential increase in sonic hedgehog signaling [88]. The Tg737 mouse was first used to illuminate the central role of IFT88/Polaris in the development of cystic kidneys [89]. The emerging molecular hierarchy requires OFD1 to recruit IFT88 as a prerequisite for ciliogenesis and ciliary hedgehog signaling that also involves the polycystins [77,90,91]. Collectively, these findings

hint that OFD1 and the polycystins are likely part of the same or overlapping protein assemblies that control similar ciliary signaling pathways in both odontoblasts and renal epithelia.

There are some striking similarities in the mechanism by which odontoblasts and renal epithelial cells respond to external stimuli with the primary cilium of odontoblasts believed to closely mimic the sensory function of cilia in renal epithelial cells [92]; thus, the primary cilium likely serves as the critical link between extracellular mechanical stimuli and initiation of responding intracellular signaling cascades in odontoblasts and renal epithelial cells. In addition to altered Hedgehog signaling, aberrant expression and signaling from the tyrosine kinase EGFR is implicated in both craniofacial disorders and ADPKD [93-95], and in primary cilia of renal epithelia, EGFR interacts with and regulates PC2 ion channel activity [87]. Collectively, these data demonstrate the need to characterize the functional interactions and molecular assemblies of complexes comprised of signaling receptors, domain-organizing proteins, and ciliary proteins, which when mutant, cause similar disease phenotypes. I therefore tested the hypothesis that OFD1 co-assembles into protein complexes constituted of PC1 and PC2, EGFR, and the flotillin lipid scaffolding proteins in the primary cilium of renal epithelia and odontoblasts. My findings provide a molecular explanation for some of the observed commonalities in the pathogenesis of multi-organ ciliopathies such as OFD1 syndrome and ADPKD.

3.2 Expression of OFD1, polycystins, flotillins and ErbB receptor family members in renal epithelia and odontoblasts

I suspected the membrane raft organizing flotillin proteins [96,97] to be key players in the organization of ciliary signaling complexes. The speculation is founded on our studies that first identified a cholesterol-rich, flotillin-organized signaling domain – constituted of polycystins, tyrosine kinases and phosphatases and cholesterol – at the basolateral membrane of renal epithelia [98,99]. Of interest is the recent finding that EGFR and downstream signaling partners are scaffolded in cholesterol-rich signaling domains by the flotillins [100]. Here, I tested if OFD1 is co-assembled into protein complexes constituted of PC1 and PC2, EGFR and the flotillin lipid scaffolding proteins in the primary cilium of renal epithelia and odontoblasts.

The expression of Erythroblastic Leukemia Viral Oncogene (ErbB) receptor proteins and the flotillins in renal epithelia and odontoblast cells is not well described. The expression of these and cystic kidney disease proteins were therefore subjected to comparative immunoblot analyses on polarized renal cortical tubular epithelial (RCTE) cells and odontoblasts (MO6-G3). PC1 **(Figure 12A, B)**, PC2 **(Figure 12C)** and OFD1 **(Figure 12D)**, along with the tyrosine kinase receptors EGFR **(Figure 12E)** and ErbB2 **(Figure 12F)** were robustly expressed in both human renal epithelial cells and mouse odontoblasts in culture. The signaling domain organizing proteins flotillin-1 **(Figure 12H)** and flotillin-2 **(Figure 12I)** were similarly expressed in both cell types, although

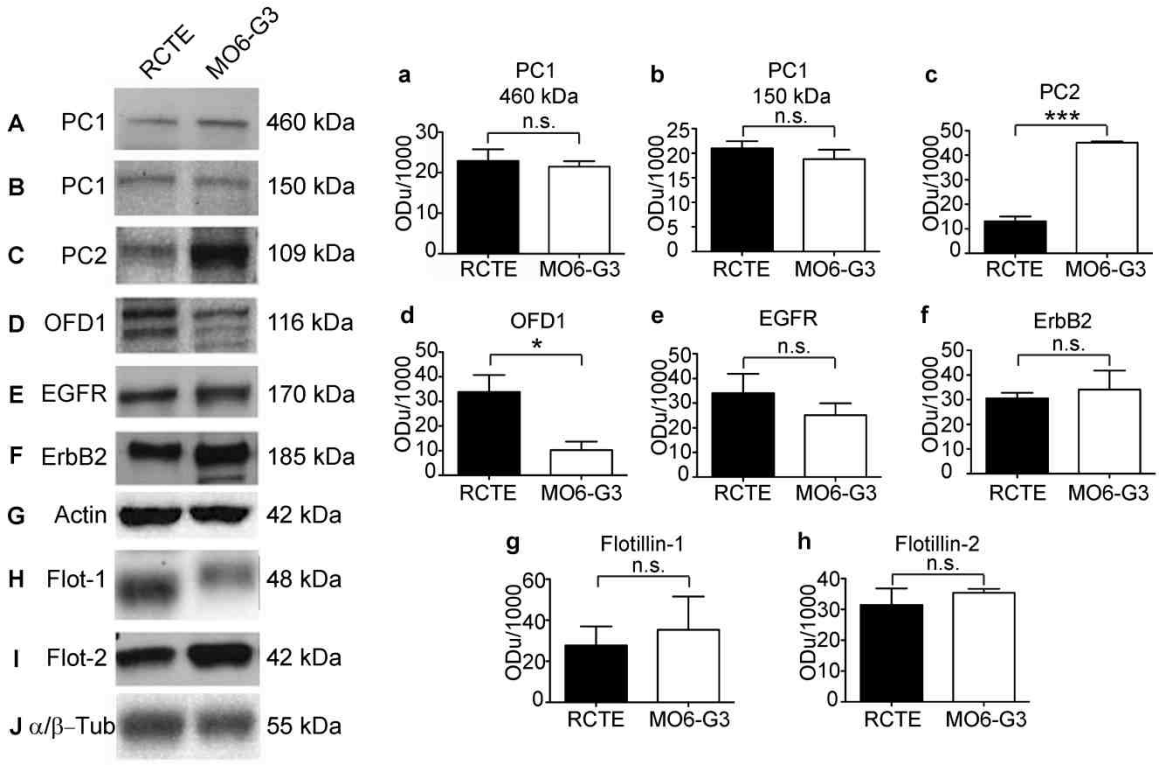

Figure 12. Key ciliary signaling proteins are expressed in RCTE and MO6-G3 cells. Renal cortical tubular epithelial (RCTE) cells and tooth derived odontoblasts (MO6-G3) cells were lysed and probed with antibodies directed against indicated proteins. PC1 using NM002 pAb (A, B), PC2 using Santa Cruz pAb (C), OFD1 using Santa Cruz pAb {Romio, 2004 #54} (D), EGFR using Santa Cruz pAb (E), ErbB2 using US Biological pAb (F), flotillin-1 using BD Transduction mAb (H), and flotillin-2 using BD Transduction mAb (I) were found to be expressed in both cell types. Actin mAb from Millipore (G) was used as a loading control for PC1, PC2, EGFR, ErbB2, and OFD1; α/β-tubulin pAb from Cell Signaling (J) was used as a loading control for flotillin-1 and flotillin-2. Actin or α/β-tubulin was used to normalize results for quantification. Bar graph showing densitometric quantification of PC1 (a, b), PC2 (c), OFD1 (d), EGFR (e), ErbB2 (f), flotillin-1 (g), flotillin-2 (h). Bar graph represents the mean ± SD of four independent experiments. (*) p=0.01 to 0.05, (***) p<0.001.

flotillin-1 exhibited a clear mobility shift in odontoblasts as compared to renal epithelial cells. The native 460 kDa PC1 is known to be cleaved in cells yielding several different C-terminal fragments that are important for physiologic functions [42,47,101]. (N.B. Available antibodies to PC1 recognize different epitopes with some recognizing the full-length 460 kDa protein while other antibodies preferentially recognize the 230-250 kDa or 150 kDa PC1 bands).

Renal epithelia and odontoblasts expressed similar levels of both the 460 kDa and the 150 kDa forms of PC1 **(Figure 12a, b)**, along with EGFR **(Figure 12e)**, ErbB2 **(Figure 12f)**, flotillin-1 **(Figure 12g)**, and flotillin-2 **(Figure 12h)**. Notably, protein expression levels of PC2 were 3.4-fold higher **(Figure 12c)**, while OFD1 levels were 3.8 fold lower in odontoblasts as compared to renal epithelia **(Figure 12d)**. These data show that key mechanosensory and signaling proteins such as the polycystin proteins, OFD1, EGFR, and the flotillins are common to both renal epithelia and odontoblasts, though there are some variations in the quantitative levels of the cation channel PC2 and OFD1.

3.3 Colocalization of OFD1, polycystins, EGFR and flotillins to the primary cilium of odontoblasts and renal epithelial cells

The primary cilium has a distinct protein composition compared to the apical surface from which it protrudes, and is enriched in signaling proteins that also function at the basolateral membrane [102,103]. The importance of the primary

cilium as a signaling command center has been suggested [87,104], yet little is known about the organization of signaling proteins within primary cilia.

Immunolocalization studies of endogenous and overexpressed proteins were performed to specifically assess ciliary protein localization patterns in odontoblasts and renal epithelial cells. Odontoblast cells and fully polarized RCTE cells are notoriously difficult to transfect via conventional techniques. To circumvent this problem, I found electroporation (iPorator) on filter surfaces routinely yielded plasmid transfection efficiencies of 40-50% (see Methods). Transiently expressed GFP-OFD1 **(Figure 13A)** and flotillin-2-GFP **(Figure 13B)** localized to primary cilia in RCTE cells with some flotillin-2 also on intracellular structures. Similarly, GFP-OFD1 **(Figure 13C)** and flotillin-2-GFP **(Figure 13D)** localized to primary cilia of odontoblast cells, though there were significant pools of flotillin-2-GFP elsewhere in the plasma membrane and intracellular structures. OFD1 is known to be associated with basal bodies and, in some renal cells, to localize along the ciliary axoneme [81]. Here I found that, particularly in odontoblasts, GFP-OFD1 staining extended beyond the region expected to contain just the basal bodies into the ciliary axoneme.

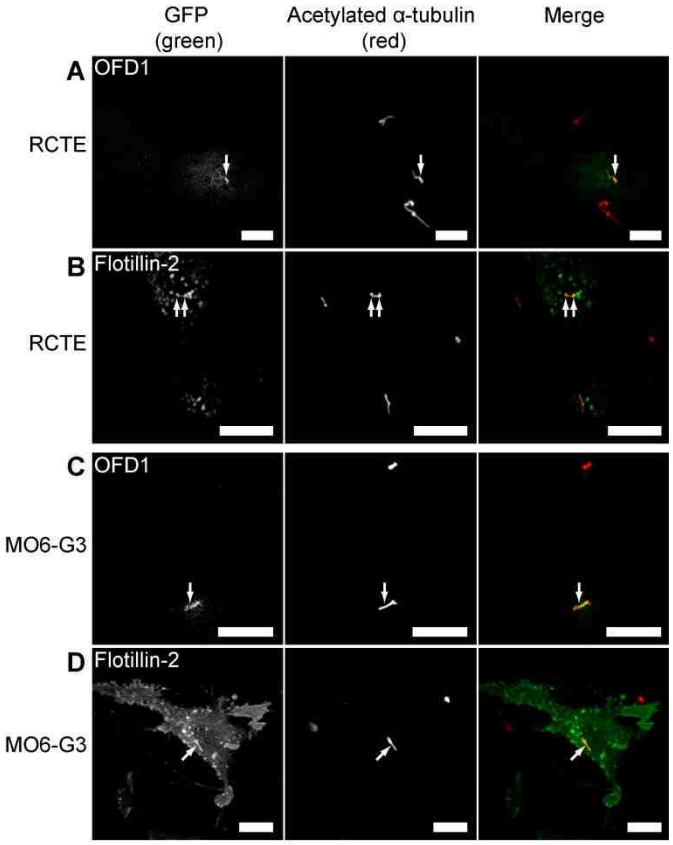

Figure 13. Transiently transfected GFP-OFD1 and flotillin-2-GFP localize to primary cilia of RCTE and MO6-G3 cells. Polarized RCTE and MO6-G3 cells were transiently transfected with either GFP-OFD1 or flotillin-2-GFP constructs. Upon 16 hours post-transfection, cells were fixed and acetylated α-tubulin (Sigma Aldrich mAb) was labeled to identify cilia. GFP-OFD1 localized to primary cilia in RCTE cells (A) and MO6-G3 cells (C). GFP-Flotillin-2 localized to primary cilia of RCTE (B) and MO6-G3 (D) cells. Images captured using a Zeiss LSM510 confocal microscope (63x objective). Images are representative of at least 3 independent experiments. Arrows denote cilia. Scale bar 10 μm.

Endogenous protein localizations were evaluated by immunofluorescence staining using antibodies specifically directed against OFD1, PC1, PC2, EGFR, and flotillin-1. In RCTE cells OFD1, PC1, PC2, and EGFR localized along the length of the primary cilium **(Figure 14A-D)**. The ciliary localization of flotillin-2-GFP prompted me to look for the flotillin-2 scaffolding partner, flotillin-1. As expected, endogenous flotillin-1 also localized to primary cilia in RCTE cells **(Figure 14E)**. Similarly, I observed endogenous OFD1, PC1, PC2, EGFR, and flotillin-1 protein localization to primary cilia in odontoblast cells **(Figure 14F-J)**.

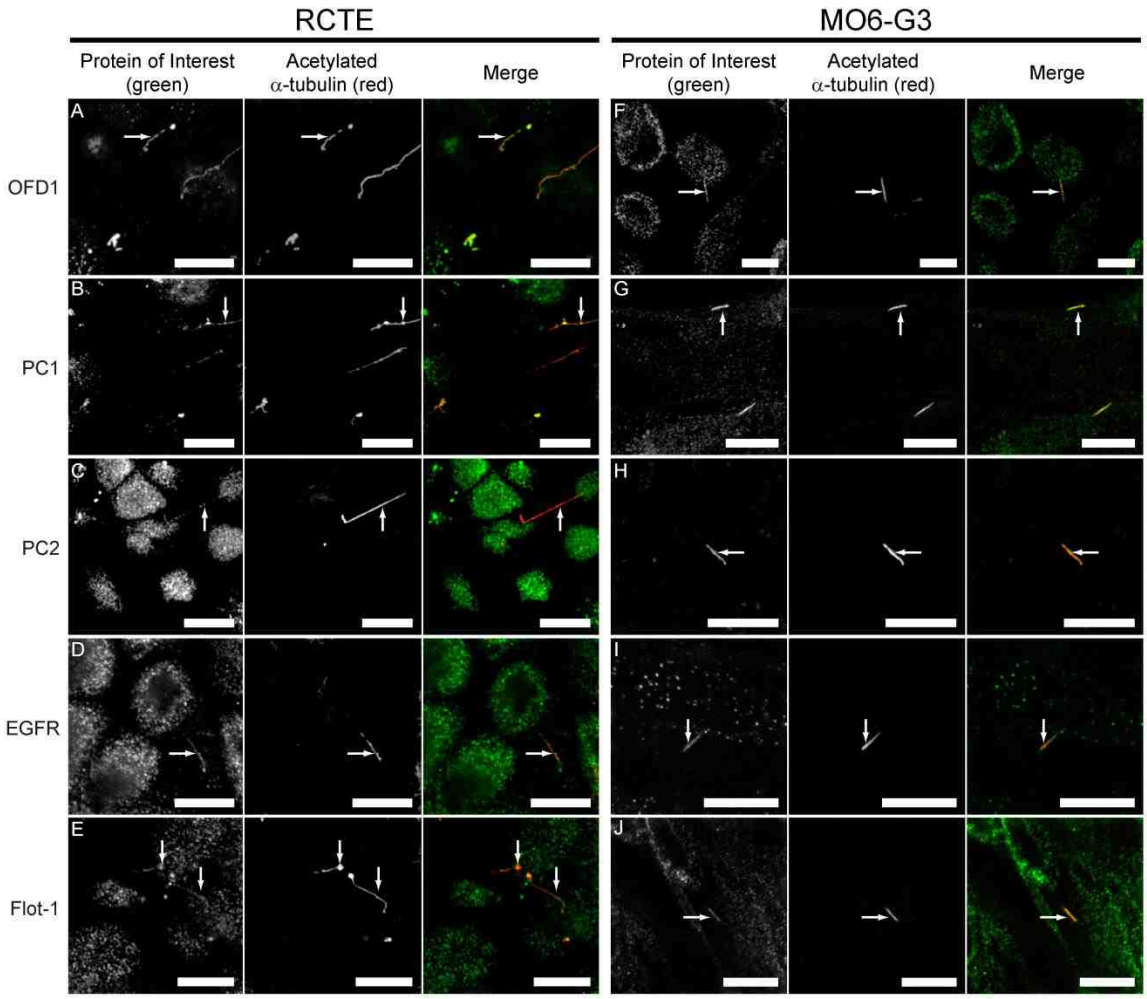

Figure 14. Endogenous OFD1, PC1, PC2, EGFR and flotillin-1 localize to primary cilia of RCTE and MO6-G3 cells. Polarized RCTE and MO6-G3 cells were fixed and stained using the indicated antibodies. OFD1 from Novus Biologicals (A, F), PC1 using pAb NM002 (B, G), PC2 using AbCam pAb (C, H), EGFR using GeneTex pAb (D, I) and flotillin-1 using AbCam pAb (E, J) were found localized to 100% of primary cilia analyzed for both cell types. Acetylated α-tubulin (Sigma-Aldrich mAb) labeling identifies cilia. Zeiss LSM510 confocal microscope images (63x objective). Arrows denote the protein of interest within a cilium. Representative results from at least 5 independent experiments. Secondary antibody only controls were negative (not shown). Scale bar 10μm.

In RCTE cells, I observed co-localization of transiently expressed Flotillin-2-GFP and PC2 in primary cilia **(Figure 15A)** as well as Flotillin-2-GFP and EGFR **(Figure 15B)**, while endogenous EGFR and PC1 co-localized to primary cilia of RCTE cells **(Figure 15C)**. The ciliary localizations of OFD1, PC1, PC2 and EGFR are consistent with previous reports showing individual proteins in different cell types [47,71,81,86,87]. However, I show for the first time the localization of all 5 proteins, including the membrane organizing flotillins, to primary cilia in a human kidney cell line. The findings that ciliary protein distributions are similar in renal epithelia and odontoblasts suggest that these proteins may be similarly organized in both cell types.

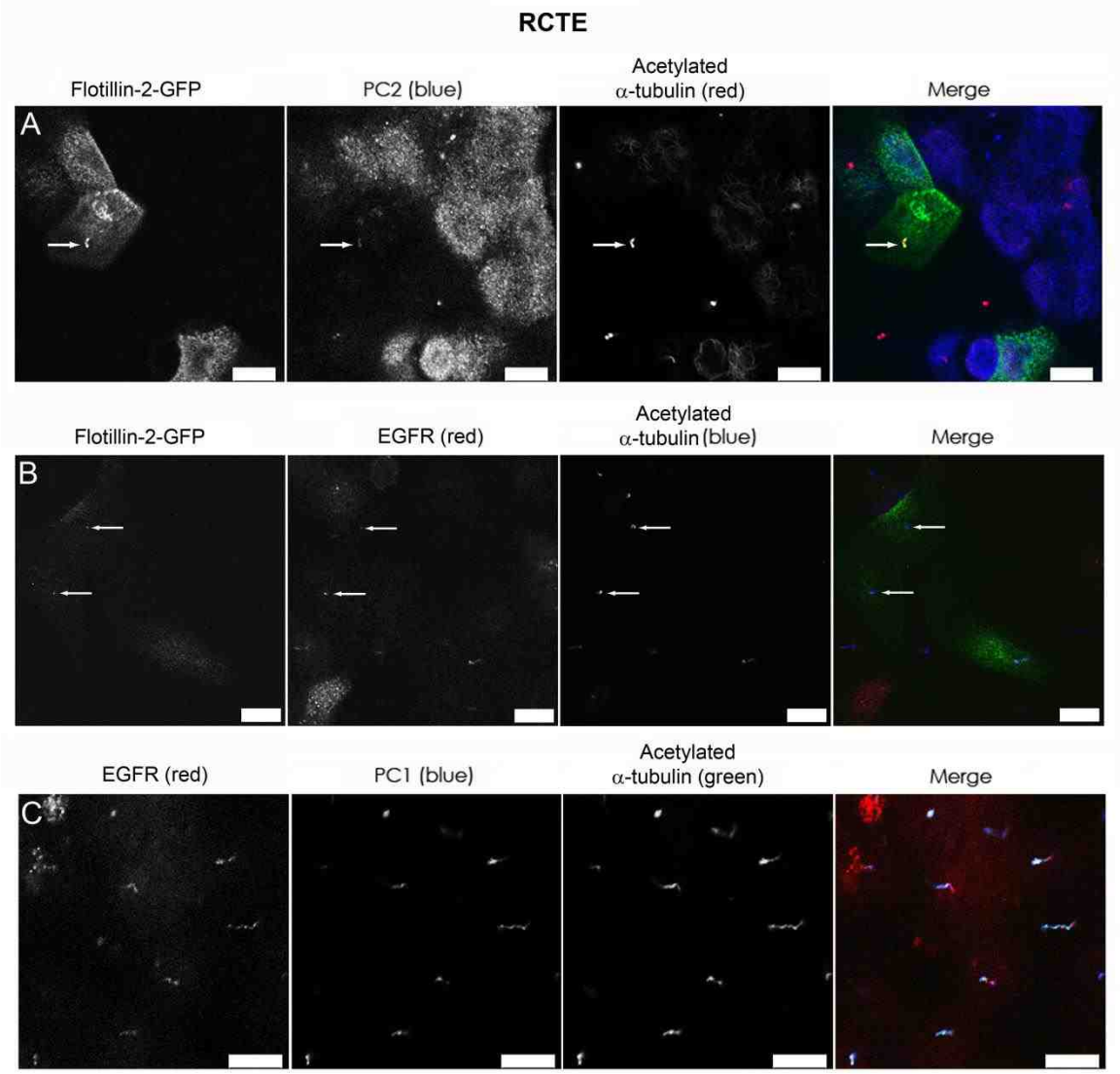

Figure 15. Two Protein Co-Localization in Primary Cilia of RCTE. Flotillin-2 was transiently transfected into polarized RCTE and cells and then fixed and stained using the AbCam pAb against PC2 (A) or the GeneTex pAb against EGFR (B) , Polarized RCTE cells were fixed and stained using the GeneTex pAb against EGFR and NM002 pAb against PC1 (C). Acetylated α-tubulin (Sigma-Aldrich mAb) labeling identifies cilia. Zeiss LSM510 confocal microscope images (63x objective). Arrows denote the protein of interest within a cilium. Representative results from at least 3 independent experiments. Secondary antibody only controls were negative (not shown). Scale bar 10 μm.

To support the microscopy data, polarized RCTE cells were deciliated using dibucaine-HCl and immunoblot analyses were performed on the ciliary enriched fraction. The ciliary marker α/β-tubulin was expressed in abundance within the collected fraction, whereas the nuclear marker lamin B was absent. Given that the nuclear membrane is often tightly coupled to cilia via a centrosomal anchoring mechanism, the data support the ciliary enrichment in the absence of nuclear contamination of the cell fraction. PC1, PC2, and EGFR were all co-enriched within the ciliary fraction of RCTE cells providing further evidence for the presence of signaling proteins within primary cilia **(Figure 16)**.

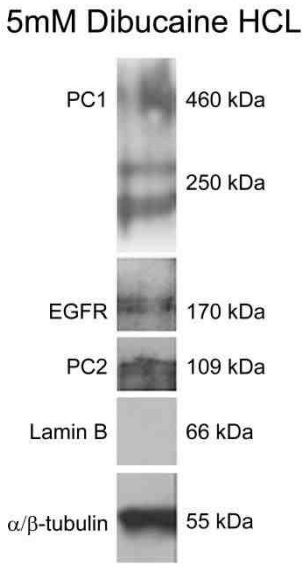

Figure 16. Deciliation of RCTE cells. Polarized renal epithelial cells were treated with 5mM Dibucaine-HCl for 15 minutes causing the cells to shed their primary cilia. Cilia were collected by fractionation and the ciliary fraction was probed. PC1 (NM032 pAb), PC2 (Santa Cruz pAb), and EGFR (Santa Cruz pAb) were expressed in the ciliary fraction of deciliated RCTE cells. The nuclear marker lamin B (Santa Cruz pAb) was not present in the ciliary fraction. Representative results from 4 independent experiments. α/β-tubulin was used as a marker of primary cilia.

3.4 Polycystins and OFD1 form protein complexes with EGFR and flotillins in odontoblasts and renal epithelial cells

To determine whether the ciliary proteins of interest are part of a multimeric complex, I performed immunoprecipitation experiments with specific antibodies against PC1 and EGFR and scored for co-precipitation of the proteins of interest. RCTE and odontoblast cells were grown to five days post-confluency to allow for polarization and ciliogenesis. PC1 was immunoprecipitated from renal epithelial and odontoblast cell lysate **(Figure 17A)** and shown to be in complex with PC2 as expected **(Figure 17C)**. The native 460 kDa PC1 contains a region with potential metalloprotease recognition sequences yielding 230-250 kDa C-terminal fragments [47,105], which were also co-precipitated **(Figure 17B)**. PC1, along with PC2, becomes tyrosine phosphorylated potentially through the actions of EGFR [87,99,106]. To test if EGFR is part of the polycystin complex, PC1 immunoprecipitates were probed for EGFR revealing that EGFR was indeed in complex with PC1 in both cell types **(Figure 17D)**. The non-transmembrane, ciliary protein OFD1 was also found to be part of the polycystin-EGFR multimeric complex in renal epithelia and odontoblast cells **(Figure 17E)**, and flotillin-2 is in complex with PC1 in both cell types **(Figure 17F)**. Quantification of replicate experiments demonstrated specific co-precipitation of PC2, EGFR, OFD1, and flotillin-2 with PC1 **(Figure 17a-f)**. In a converse experiment, EGFR was immunoprecipitated from polarized renal epithelial and odontoblast cell lysates and probed for PC1, PC2, OFD1, and flotillin-2 **(Figure 17G-K)**.

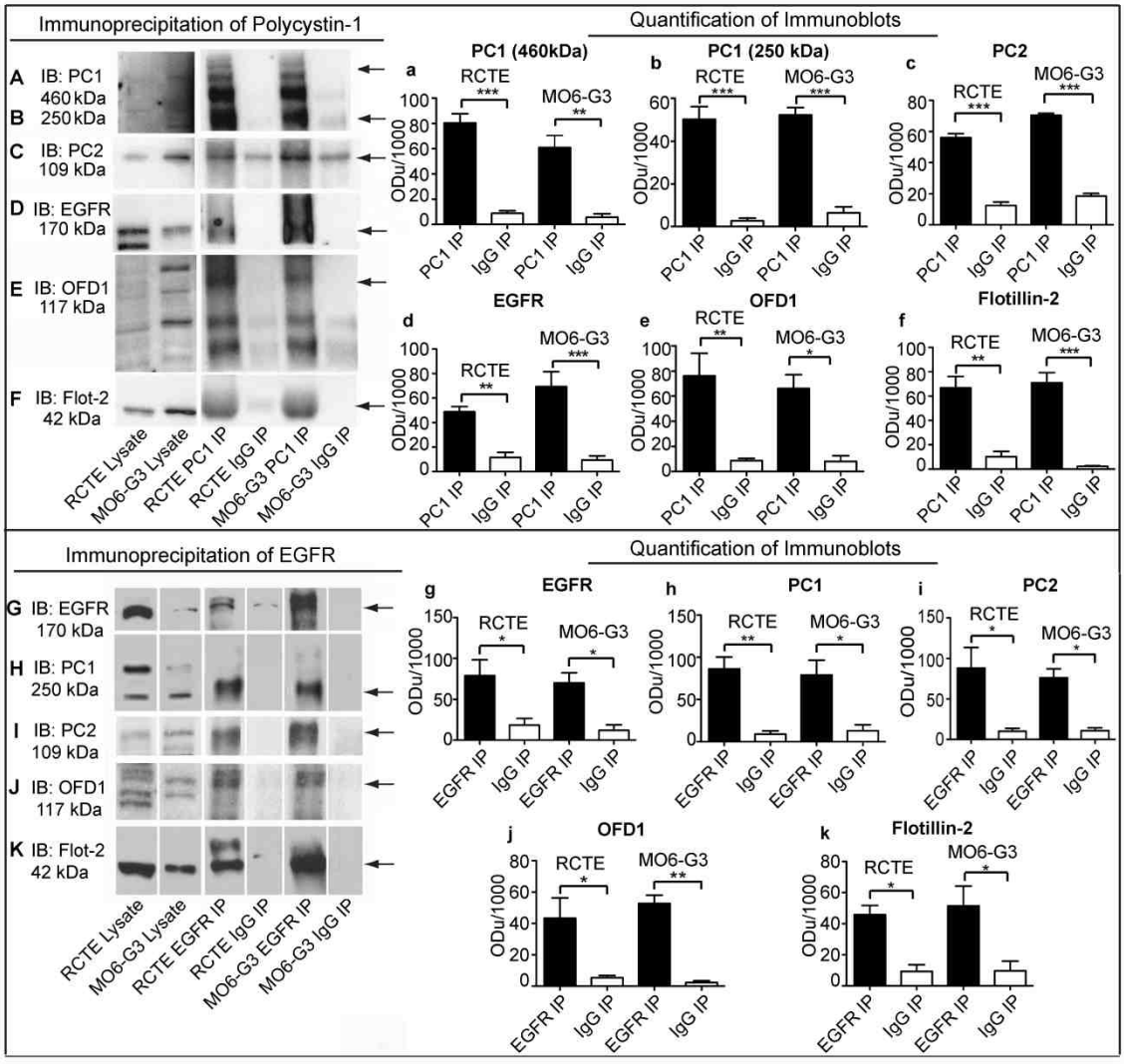
Immunoprecipitation of Polycystin-1
Quantification of Immunoblots
A IB: PC1 460 kDa
B 250 kDa
C IB: PC2 109 kDa
D IB: EGFR 170 kDa
E IB: OFD1 117 kDa
F IB: Flot-2 42 kDa
RCTE Lysate
MO6-G3 Lysate
RCTE PC1 IP
RCTE IgG IP
MO6-G3 PC1 IP
MO6-G3 IgG IP
a PC1 (460kDa)
b PC1 (250 kDa)
c PC2
d EGFR
e OFD1
f Flotillin-2
RCTE
MO6-G3
ODu/1000
PC1 IP
IgG IP
Immunoprecipitation of EGFR
G IB: EGFR 170 kDa
H IB: PC1 250 kDa
I IB: PC2 109 kDa
J IB: OFD1 117 kDa
K IB: Flot-2 42 kDa
RCTE Lysate
MO6-G3 Lysate
RCTE EGFR IP
RCTE IgG IP
MO6-G3 EGFR IP
MO6-G3 IgG IP
g EGFR
h PC1
i PC2
j OFD1
k Flotillin-2
EGFR IP
IgG IP

Figure 17. PC1, PC2, EGFR, OFD1, and flotillin-2 are part of a multimeric protein complex in RCTE and MO6-G3 cells. RCTE and MO6-G3 cells were grown 5 days post-confluency to allow for polarization and ciliogenesis. PC1 was immunoprecipitated using NM002 pAb and precipitated proteins were separated by SDS-PAGE and probed for PC1 using NM005 pAb (A, B), PC2 using AbCam pAb (C), EGFR using GeneTex pAb (D), OFD1 using Novus Biologicals pAb (E) and flotillin-2 using Cell Signaling Rabbit mAb (F). Bar graph showing a densitometric quantification of PC1 co-immunoprecipitation for PC1 (a,b), PC2 (c), EGFR (d), OFD1 (e), and flotillin-2 (f). Normal rabbit IgG was used as a negative control. In a reciprocal experiment EGFR was immunoprecipitated using Santa Cruz pAb from RCTE and MO6-G3 cell lysates. Immunoprecipitated proteins were separated by SDS-PAGE and probed for EGFR using GeneTex pAb (G), PC1 using NM002 pAb (H), PC2 using Santa Cruz pAb (I), OFD1 using Novus Biologicals pAb (J) and flotillin-2 using Cell Signaling Rabbit mAb (K). Bar graph showing a densitometric quantification of EGFR co-immunoprecipitation probed for EGFR (g), PC1 (h), PC2 (i), OFD1 (j), and flotillin-2 (k). Normal rabbit IgG was used as a negative control. Lysate lane inputs were 5% of immunoprecipitations. 25 µg of total protein was loaded into each well. Arrows indicate the quantified band of interest in each immunoblot panel. Bar represents the mean ± SD of at least three independent experiments. (*) p=0.01 to 0.05, (**) p=0.001 to 0.01, (***) p<0.001.

As seen in the PC1 immunoprecipitates, all of the proteins were co-enriched with EGFR **(Figure 17g-k)**, with a cleaved fragment of PC1 preferentially co-precipitated with EGFR. Multiple OFD1 bands are present in RCTE and MO6-G3 cell lysates and a subset of these OFD1 bands are co-precipitated with EGFR. Interestingly, the flotillin-2 bands were notably upshifted in both the PC1 and EGFR immunoprecipitates suggesting posttranslational modification within these complexes. These data indicate that key ciliary signaling proteins – PC1, PC2, EGFR and OFD1 – may well reside in a complex with membrane organizing flotillin proteins in renal and dental cell types.

3.5 Polycystin-1 and EGFR form a complex within primary cilia

I utilized an antibody-based proximity ligation assay to specifically evaluate if the protein complexes I identified by co-immunoprecipitation were resident in cilia [107]. Using antibodies directed against the extracellular domains of PC1 and EGFR, these two proteins were found to interact specifically within the primary cilium of odontoblasts **(Figure 18A)** and fully polarized renal epithelial cells **(Figure 18B)**. In both cell types the fluorescent signal was notably concentrated in puncta, suggestive of specialized domains wherein the proteins are enriched. In the relatively short cilia of odontoblasts, a less concentrated signal was also seen along the length of the shaft. Puncta associated with the cell body were largely intracellular with a small fraction at or near the basolateral membrane **(Figure 18A-B and data not shown)**. Experiments performed without primary

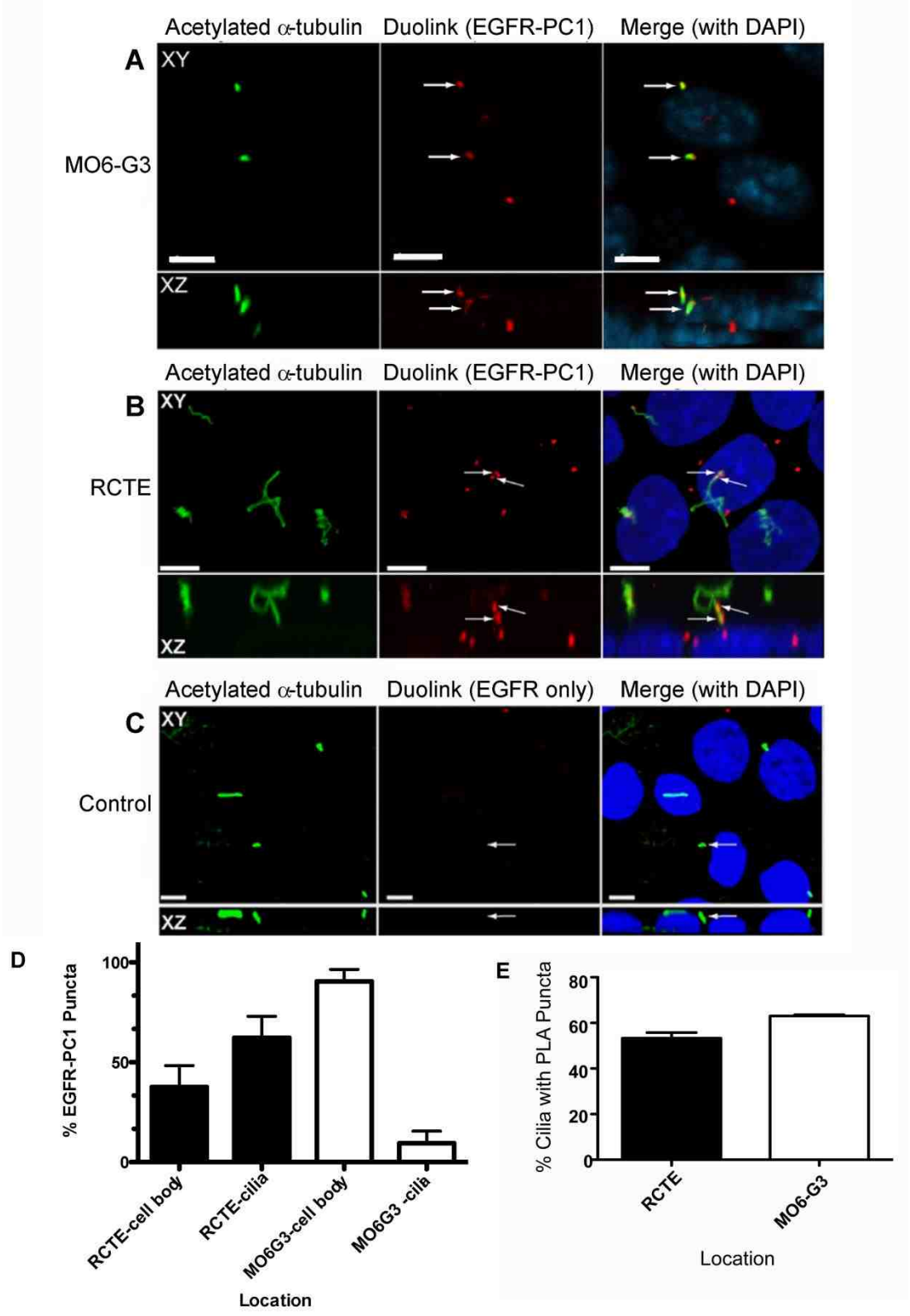
Acetylated α-tubulin
Duolink (EGFR-PC1)
Merge (with DAPI)
A
XY
MO6-G3
XZ
Acetylated α-tubulin
Duolink (EGFR-PC1)
Merge (with DAPI)
B
XY
RCTE
XZ
Acetylated α-tubulin
Duolink (EGFR only)
Merge (with DAPI)
C
XY
Control
XZ
D
% EGFR-PC1 Puncta
100
50
0
RCTE-cell body
RCTE-cilia
MO6G3-cell body
MO6G3 -cilia
Location
E
% Cilia with PLA Puncta
80
60
40
20
0
RCTE
MO6-G3
Location

Figure 18. PC1 and EGFR interact in the primary cilium of MO6-G3 and RCTE cells. Polarized MO6-G3 (A) and RCTE (B) cells were grown on coverslips 5 days post-confluency. Cells were incubated with antibodies against PC1 (Santa Cruz mAb) and EGFR (GeneTex pAb), followed by Duolink PLA Probes to identify points of PC1-EGFR interaction. Cilia identified by acetylated α-tubulin (Sigma-Aldrich mAb). Identical experiments performed without PC1 antibody are negative for fluorescent signal (C). Top panel shows XY plane, bottom panel shows XZ plane. Images from confocal microscope (63x objective). Scale bar is 5 μm. Quantification of puncta in 3 representative images (11-29 cells/field) from 2 independent experiments (D). Quantification of cilia containing PLA puncta (E). Puncta in cilia were counted based on colocalization with acetylated α-tubulin. Statistical evaluation based on two-tailed t-test. p=0.0194. Movie can be found at the following web address: http://www.plosone.org/article/info%3Adoi%2F10.1371%2Fjournal.pone.0106330#s5.

antibody against PC1 yielded no fluorescent signal verifying the specificity of the PC1-EGFR reaction **(Figure 18C)**.

Quantification of these proximity-induced fluorescent puncta showed an enrichment in the cilia (62%) as compared to the cell body (38%) of fully polarized RCTE cells **(Figure 18D)**. The pattern in odontoblasts was reversed with a greater fraction of puncta in the cell body (90%), yet retaining a quantifiable fraction in cilia (10%) **(Figure 18D)**. Both cell types had similar numbers of ciliated cells (RCTE 82%; MO6-G3 93%), although the average cilia length was different (RCTE 6.10 µm; MO6-G3 0.49 µm). Both RCTE and MO6-G3 had a similar percentage of primary cilia containing puncta: RCTE 53.4%; MO6-G3 62.6% **(Figure 18E)**. Taken in conjunction with previous data showing PC1 and PC2 interact in primary cilia [77] and PC2 forms a ciliary signaling complex with EGFR [87], these data indicate that PC1 and PC2 likely form a three way complex with EGFR in cilia.

3.6 Mutant expression of PC1 results in decreased ciliary localizations of PC2, OFD1, EGFR and flotillin-1

Given the shared disease pathologies caused by mutant OFD1 and PKD genes, I tested if the expression of a mutant component of our defined ciliary signaling complex would in turn affect the formation and/or stability of these specialized complexes. In cells from patients with ADPKD, expression of mutant PC1 often results in its absence from primary cilia [108]. Immunolocalization studies were

therefore performed on cells from human ADPKD patients with expression of mutant PC1 (Q4004X) [76]. In these cells, there was reduced expression not only of PC1, but also of the associated PC2, EGFR, and flotillin-1 proteins along the shaft of primary cilia **(Figure 19A-H)**. Quantification of multiple data sets verified statistically significant reductions ($p<0.0001$ for PC1, PC2, and flotillin-2; $p=0.0105$ for EGFR) in all components of the complex **(Figure 19I-L)**. A small residual pool of EGFR was sometimes detectable at the ciliary base. OFD1 localization to primary cilia was also significantly decreased in PKD cells as compared to RCTE cells ($p<0.0001$; data not shown).

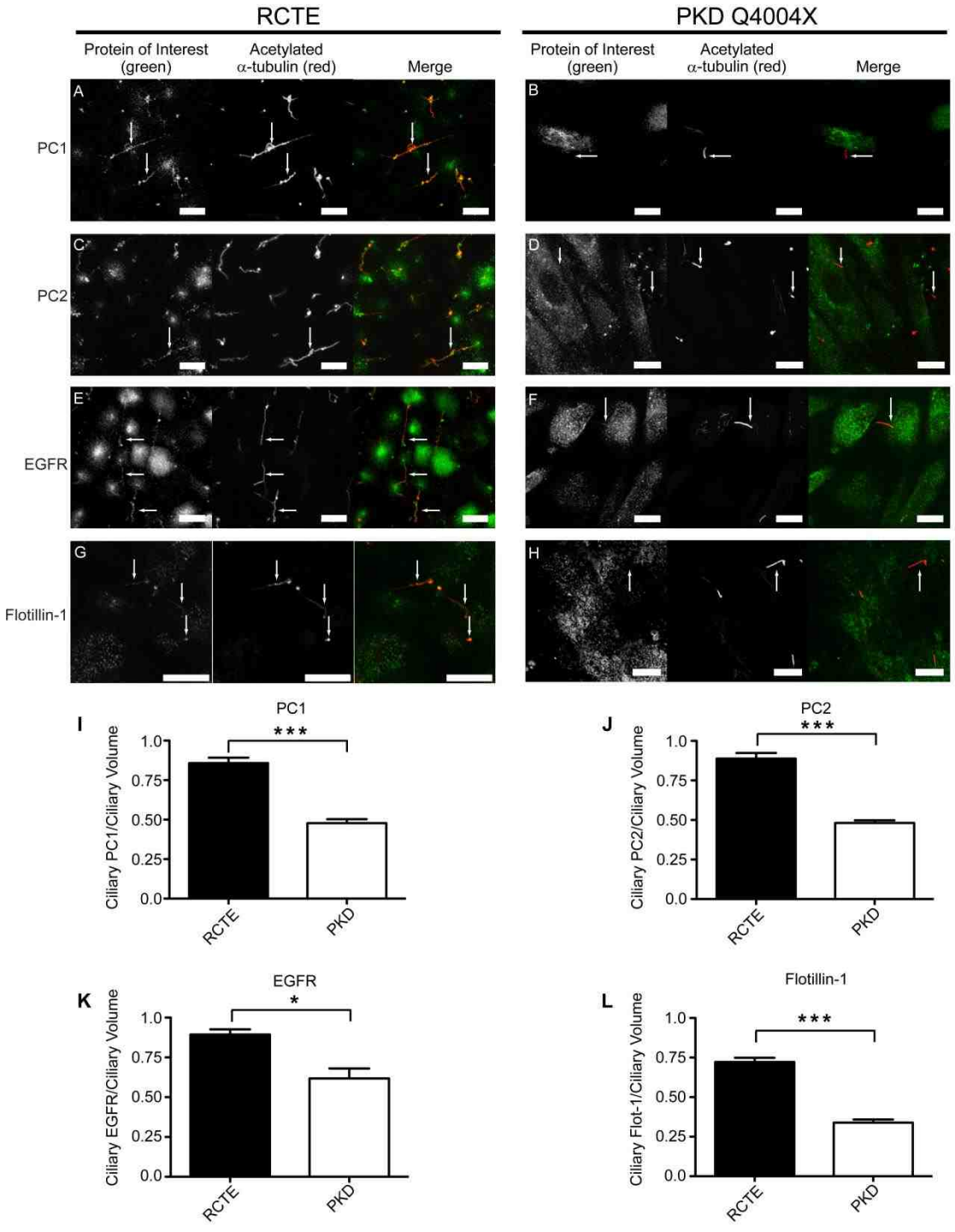
RCTE
PKD Q4004X
Protein of Interest (green)
Acetylated α-tubulin (red)
Merge
A
B
PC1
C
D
PC2
E
F
EGFR
G
H
Flotillin-1
I
PC1
***
Ciliary PC1/Ciliary Volume
1.0
0.75
0.50
0.25
0.0
RCTE
PKD
J
PC2
***
Ciliary PC2/Ciliary Volume
K
EGFR
*
Ciliary EGFR/Ciliary Volume
L
Flotillin-1
***
Ciliary Flot-1/Ciliary Volume

Figure 19. Key ciliary signaling proteins are significantly reduced in primary cilia of PKD cells. Human RCTE and PKD Q4004X cells (with expression of mutant PC1) were grown on coverslips 5 days post-confluency to permit ciliogenesis. Cells were fixed and stained using antibodies directed against indicated proteins: PC1 (NM002 pAb); PC2 (AbCam pAb); EGFR (GeneTex pAb); and flotillin-1 (AbCam pAb). PC1 (A), PC2 (C), EGFR (E) and flotillin-1(G) are present in primary cilia of RCTE cells. PC1 (B), PC2 (D), EGFR (F) and flotillin-1 (H) were lacking in primary cilia of PKD Q4004X cells. Acetylated α-tubulin (Sigma-Aldrich mAb) staining identifies cilia. Arrows denote a small residual pool of EGFR detectable at the ciliary base of PKD cells. Zeiss LSM510 confocal microscope images (63x objective). Representative results from at least 5 independent experiments. Comparative images are from a single experiment and taken under identical settings. Arrows denote cilia. Scale bar 10 μm. Quantification shows individual ciliary protein intensities normalized to the respective ciliary volume (I-L). Each protein was quantified in 30-100 cilia for each cell type. z-stack images were imported into SlideBook and a volume mask for each cilium was created based on acetylated α-tubulin staining. Staining intensities for each protein were quantified within the respective ciliary volume mask. Statistical evaluation based on two-tailed t-test. (*) $p=0.0105$, (***) $p<0.0001$.

As further confirmation, I also analyzed OFD1 localization in primary human normal kidney and PKD (46M06) cells. Whilst OFD1 localized to primary cilia of primary normal proximal tubular epithelial cells (RPTEC) cells **(Figure 20A)**, it was significantly decreased ($p<0.0036$) in primary cilia of 46M06 cells **(Figure 20B, C).** To substantiate these studies, zoomed in images of 46M06 primary cilia were taken and confirmed the absence of OFD1 in cystic renal epithelia primary cilia **(Figure 21)**.

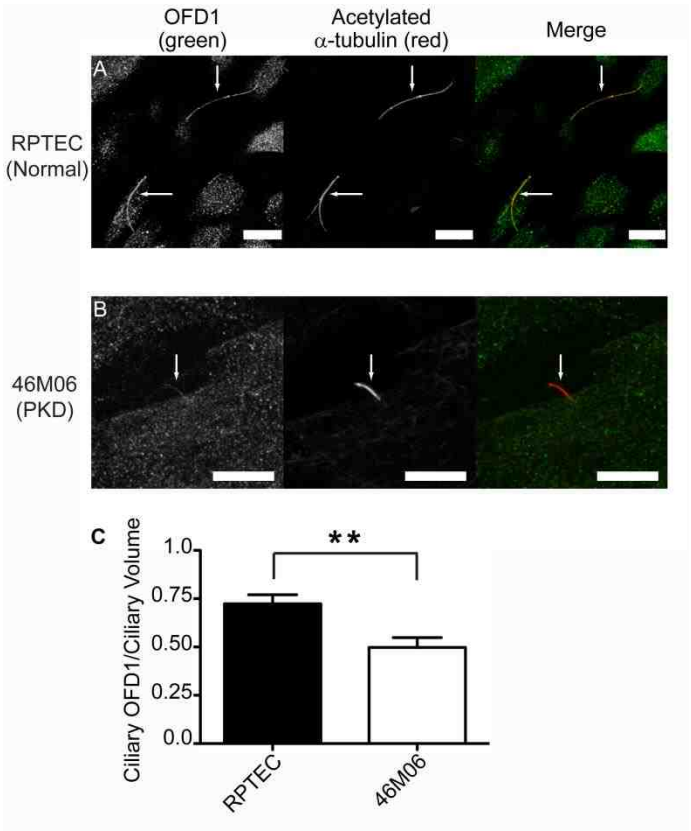

Figure 20. OFD1 ciliary localization is altered in human primary cell lines. Human primary renal proximal tubule epithelial cells (RPTEC) and PKD (44M06) cells were grown on glass coverslips 5 days post confluency to allow for ciliogenesis, fixed and stained using an antibody directed against OFD1 (Santa Cruz pAb). OFD1 localizes to primary cilia in RPTEC cells (A) but is diminished in primary cilia PKD 46M06 cells (B). Acetylated α-tubulin (Sigma-Aldrich mAb) staining identifies cilia. Zeiss LSM510 confocal microscope images (63x objective). Representative results from 3 independent experiments. Comparative images are from a single experiment and taken under identical settings. Arrows denote cilia. Scale bar 10 μm. Quantification shows OFD1 staining intensities normalized to ciliary volumes, performed as detailed in methods and Figure 6 (C). z-stack images were imported into SlideBook and a mask for the cilia was created based on acetylated α-tubulin staining. Statistical evaluation based on two-tailed t-test. (**) p=0.0036.

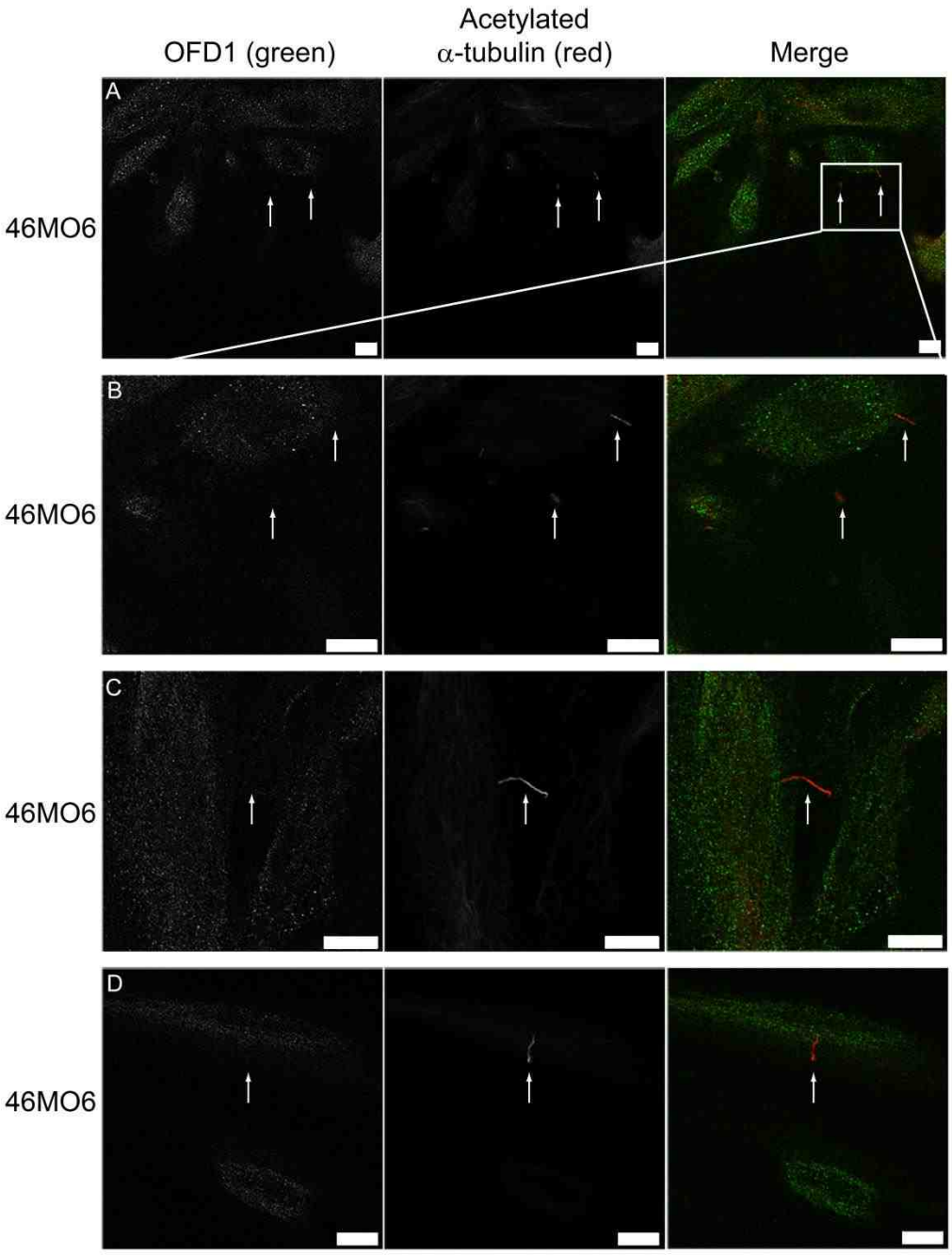

Figure 21. OFD1 is reduced in primary cilia of PKD 46M06 cells. Polarized 46M06 PKD cells were fixed and stained using an antibody directed against OFD1 (Novus Biologicals pAb). Acetylated α-tubulin (Sigma-Aldrich mAb) labeling identifies cilia. 63x objective with no zoom (A), 63x zoomed in image of panel A cilia marked with arrows (B), 63x zoomed in images of separate fields of view (C-D). Zeiss LSM510 confocal microscope images. Representative results from at least 3 independent experiments. Secondary antibody only controls were negative (not shown). Scale bar 10 μm.

Biochemical deciliation experiments were used to independently verify that all components of the identified ciliary complex were decreased in an interdependent manner when polycystin-1 is mutant. Polarized RCTE and PKD (Q4004X) cells were deciliated using Dibucaine-HCL and isolated ciliary fractions analyzed by immunoblot. Quantification of OFD1, EGFR, and flotillin-1 protein levels relative to α/β-tubulin levels confirmed that all components were reduced in the ciliary fraction of the PKD cells as compared to RCTE cells **(Figure 22)**. These data further substantiate the conclusion that the OFD1-EGFR-flotillin complex is lost from cilia in cells with mutant PC1. While siRNA-mediated ablation of OFD1 and PC1 were attempted in renal epithelia and odontoblasts, these studies were complicated by the fact that OFD1 is necessary for ciliogenesis and therefore siRNA knockdown must be performed after cells are fully polarized and have cilia. Under these conditions, a population of OFD1 remained resident in primary cilia even after 48 h of siRNA-mediated knockdown precluding accurate interpretation. The composite data demonstrate that the proteins are organized into a functional complex that is disrupted when polycystin-1 is mutant or absent.

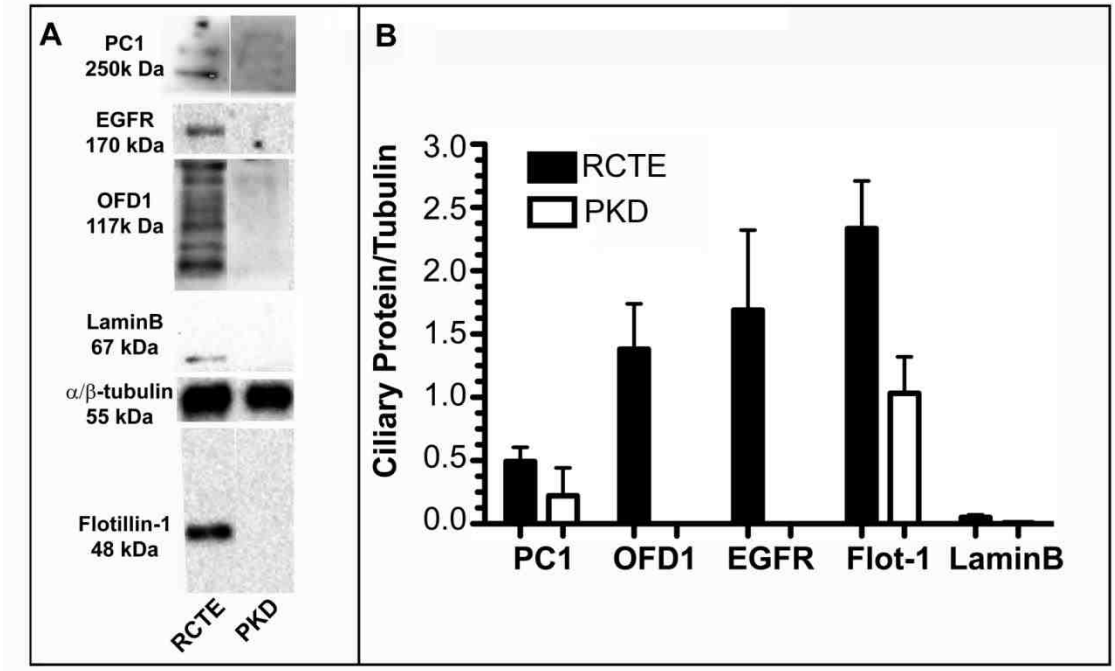

Figure 22. Expression of PC1, OFD1, EGFR, and Flotillin-1 is decreased in ciliary fractions of PKD cells compared to RCTE cells. RCTE cells and PKD Q4004X cells were grown 6 days post-confluency to allow for cell polarization and ciliogenesis and treated with 1.5 mM Dibucaine-HCl for 5 minutes to reduce cell loss and induce shedding of primary cilia. Cilia were collected by fractionation and the ciliary fraction was probed. PC1 (MN032 pAb), OFD1 (Novus Biologicals pAb), EGFR (GeneTex pAb), and flotillin-1 (BD Transduction mAb) were expressed in the ciliary fraction of deciliated RCTE cells but not PKD cells. α/β-tubulin (Cell Signaling pAb) was used as a marker of primary cilia. The nuclear marker lamin B (Santa Cruz pAb) was not present in the ciliary fraction (A). Quantification of 3 independent samples (B). Mean values were found to be statistically different ($p<0.0001$) using 1-way ANOVA.

Chapter 4: Results-OFD1 Interacts with Polycystin-1 for OFD1 Localization to Primary Ciliary

4.1 Introduction

Oral-facial-digital syndrome type1 (OFD1; OMIM #311200) is an X-linked inherited disease caused by expression of mutant OFD1 protein resulting in cognitive defects and malformations of the oral cavity, hands, and feet along with PKD. Over the past decade, advancements in renal ultrasound technology have shown that PKD is more intimately associated with OFD1 than was previously recognized and, in fact, renal symptoms often dominate the clinical course of the disease. Due to the low rate of kidney transplants, many OFD1 patients will die from ESRD due to PKD. Recent studies have shown that PKD in OFD1 patients, caused by mutation in the *OFD1* gene, very closely mimics the disease variability and kidney disease pathogenesis seen in patients with Autosomal Dominant Polycystic Kidney Disease (ADPKD), caused by mutations in the *PKD1* or *PKD2* genes, which encode PC1 or PC2 proteins, respectively. ADPKD is a common inherited disorder that affects between 1:500 to 1:1000 individuals worldwide and leads to renal failure in adulthood. Because the renal pathologies observed in OFD1 and ADPKD are virtually indistinguishable, and many of the oral, facial, and digital abnormalities are surgically corrected in childhood, it is believed that many OFD1 patient classifications may be overlooked. OFD1 is embryonic lethal in males, so it is now being recommended that an OFD1 diagnosis be suspected in families where ADPKD affects only the females.

OFD1 and ADPKD are included in an expanding list of inherited human diseases that are caused by dysfunction of primary cilia associated proteins, termed ciliopathies. This once largely ignored organelle is now being recognized for its importance in a number of cellular processes including embryonic development, organ homeostasis, and signaling events to relay messages from the extracellular environment into the cell [52,60,109,110]. In addition to *OFD1*, *PKD1,* and *PKD2*, there is a growing list of genes that have been identified to cause ciliopathies, yet there are many commonalties emerging in these genetically diverse disorders. Primary cilia are now widely considered the central cellular component involved in the pathogenesis of cystic kidney disease and ciliopathies often share similarities in extrarenal pathologies such as cardiovascular and skeletal abnormalities [111]. Growing evidence supports that commonalities observed in many ciliopathies are due to the intersection of signaling pathways harbored in the primary cilium. In fact, over the past decade, the primary cilium has emerged as the signaling hub of the cell due to the large number of signaling proteins that have been found to localize to this specialized cellular organelle. For example, in polarized renal epithelia, PC1 and PC2 interact to form a receptor-channel complex in primary cilia. There is evidence that PC1 acts as a mechanosensor in primary cilia to sense extracellular fluid flow and subsequently activate PC2 Ca^{2+} channel activity in the cilia. Furthermore, PC2 is associated with the EGFR in the primary cilium, and EGFR regulates PC2 calcium channel activity from this location [52]. Though the

amount of calcium translocated in the cilium is too small to change overall intracellular calcium levels, there is evidence that it is a pivotal signaling event with mechanistic details under active investigation [112-114]. Not surprisingly, aberrant activation and mislocaliztion of EGFR has emerged as a complicating factor in a number of known ciliopathies, including ADPKD and ARPKD, and many craniofacial disorders [54,60,93,115,116]. The connection between mislocalization of ciliary signaling proteins and human disease has revealed the need to better understand how proteins are delivered to this cellular location.

Our group, along with others, has shown the importance of a conserved peptide sequence (VxPx) that is important for the proper delivery of transmembrane proteins, such as the polycystins, to primary cilia [43,117,118]. However, the mechanism by which OFD1, a soluble protein, arrives at primary cilia remains enigmatic. OFD1 normally localizes to centrosomes during cell division where it functions to control mother/daughter centriole length and later, when cells are fully polarized, OFD1 localizes to the base of the primary cilia as well as the ciliary shaft [60,63,64]. In normal renal epithelia, OFD1 is a component of a conserved ciliary microdomain consisting of the polycystins and EGFR [60]. Human ADPKD cystic epithelial cells expressing mutant PC1 protein exhibit not only a failure of PC1 to localize to cilia, but also a decreased localization of PC2, EGFR, and OFD1 to primary cilia [60,119]. The finding that loss of ciliary PC1 leads to decreased OFD1 within the ciliary shaft suggests that PC1 might also serve to promote delivery and/or stable localization of OFD1 to primary cilia [60];

motivating a detailed mechanistic analysis of OFD1 dependence on PC1 for trafficking to cilia.

OFD1 contains five to six predicted CC domains [34,86]. Increasing evidence supports a role for CC domains in protein-protein interactions and protein trafficking to various cellular locations, and it is has been shown that these domains have roles in the localization of OFD1 to centrosomes [64]. PC1 and PC2 also contain CC domains that mediate their intracellular interaction. Studies have shown that PC2 interaction with PC1 via the CC domains is required for PC2 to correctly localize to primary cilia [120]. Although PC2 can arrive at the ciliary membrane independently of PC1 [117], the stable expression of PC2 in primary cilia is dependent on PC1 [60].

Based on previous findings, there are four plausible routes for OFD1 ciliary delivery **(Figure 23)**. The first possibility is that OFD1 is packaged in vesicles with PC1 beginning at the ER and/or at the Golgi and the two proteins are delivered together to the cilia utilizing the VxPx ciliary targeting motif found in PC1 **(Figure 23A)**. Second, OFD1 could require a direct interaction with PC1 via the CC domains in both proteins to “hitchhike” with PC1 for delivery to primary cilia **(Figure 23B)**. Third, OFD1 may arrive at the base of the primary cilium

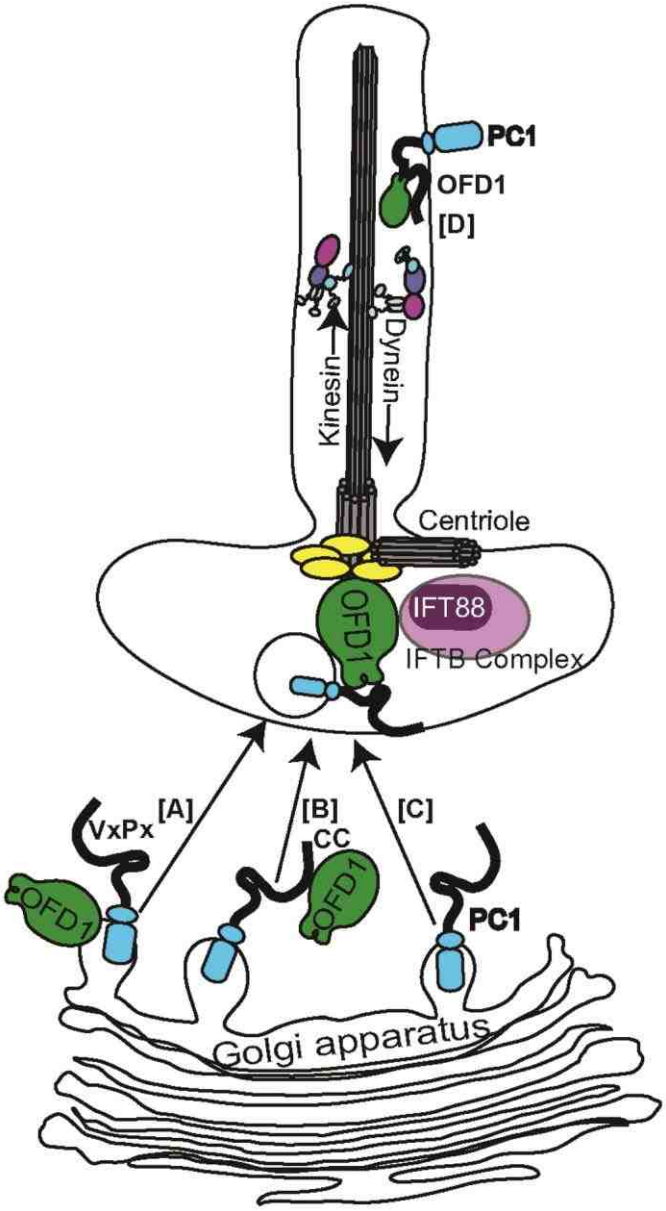

Figure 23. Proposed models for OFD1 trafficking to primary cilium. We propose four possible routes for OFD1 ciliary delivery. (A) OFD1 is packaged in vesicles with PC1 at the Golgi and the two proteins are delivered together to the cilia utilizing the VxPx motif found in PC1. (B) OFD1 interacts with PC1 via CC domains for ciliary delivery. (C) OFD1 arrives at the base of the primary cilium independently of PC1 and is involved in the docking of vesicles for integration into the primary cilium. (D) OFD1 arrives at the primary cilium independently and is subsequently organized into a ciliary microdomain containing PC1. Utilization of the iDimerize (pink cassettes = DmrD domains) CD16.7-PC1 C-terminal tail constructs will allow for analysis of spatial and temporal interaction of OFD1 with PC1 at various subcellular locations.

independently of PC1 and be involved in the docking of vesicles for integration into the primary cilium **(Figure 23C)**. Lastly, OFD1 might arrive at the primary cilium independently and subsequently become organized into a ciliary microdomain containing PC1 **(Figure 23D)**. Characterization of the molecular basis for the interaction between membrane proteins (such as polycystins) and soluble proteins (such as OFD1) is important to distinguish the role of PC1 in ciliary protein transport and/or stabilization within the ciliary shaft.

4.2 iDimerize-CD16.7-PC1-WT, but not iDimerize-CD16.7-PC1-359 mutant lacking the VxPx targeting motif, localizes to primary cilia of renal epithelial cells

Previous studies showed that a conserved amino acid motif (VxPx) is vital for recognition of ciliary membrane proteins, such as PC1, PC2, and rhodopsin (a photoreceptor expressed in retinal epithelia) by a GTPase driven trafficking machinery and ciliary transport fidelity [43,117,118]. When the VxPx motif is mutant or absent from PC1 or PC2, these proteins are excluded from the primary cilia. The VxPx sorting motif is recognized by the small GTPase Arf4, which functions as an important regulator of protein trafficking from the Golgi apparatus to the base of the cilium [43,118]. In a previous study from our lab, the C-terminus of PC1 containing the VxPx motif was demonstrated to be required for PC1 targeting to primary cilia of renal epithelia by utilizing a series of PC1 fusion proteins [43]. The chimeric protein constructs consisted of an N-terminal ectoplasmic domain derived from human CD16 (which facilitates protein retrieval

and analyses as well as selective immunolocalization) and the transmembrane domain of human CD7 followed by the membrane distal C-terminus of human PC1. Successive deletion of more and more of the PC1 tail, starting from the extreme C-terminal end of PC1 tested the importance of various sequences in the ciliary localization of PC1 **(Figure 24)**. The CD16.7-PC1-WT tail fusion protein localized to primary cilia of RCTE cells, while a CD16.7-PC1-359 truncation mutant construct lacking the last 20 amino acids, including the ciliary targeting VxPx motif, failed to localize to primary cilia [47].

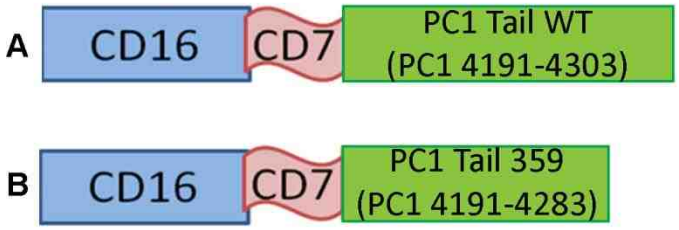

Figure 24. Cartoon representation of CD16.7-PC1 fusion proteins. The chimeric protein constructs consisted of an N-terminal ectoplasmic domain derived from human CD16 (which facilitates protein retrieval and analyses as well as selective immunolocalization) and the transmembrane domain of human CD7 followed by the membrane distal wild-type 112 amino acids of the PC1 cytoplasmic C-terminal tail (A). The last 20 amino acids of the CD16.7-PC1-WT tail were deleted to produce the CD16.7-PC1-359 truncation mutant lacking the ciliary targeting VxPx motif (B).

In the present study, I took advantage of these previously characterized constructs to determine if PC1 was required for OFD1 localization to primary cilia. In order to accomplish this, I utilized a reversible dimerization system (iDimerize) to test several possibilities for the spatio-temporal assembly of OFD1 with the polycystins (described in Figure 23). The 'iDimerizeTM' cassettes containing an ER targeting signal (Clontech, custom synthesis detailed in Materials and Methods) cause protein oligomerization and trapping in the ER that can be released with the addition of a ligand (called solubilizer and based on the reversible, ligand-dependent relief of the oligomerization of the FKB508 protein [121,122]). The addition of ligand allows disaggregation and synchronous plasma membrane transport, which can be monitored by immunofluorescence staining **(Figure 25)**.

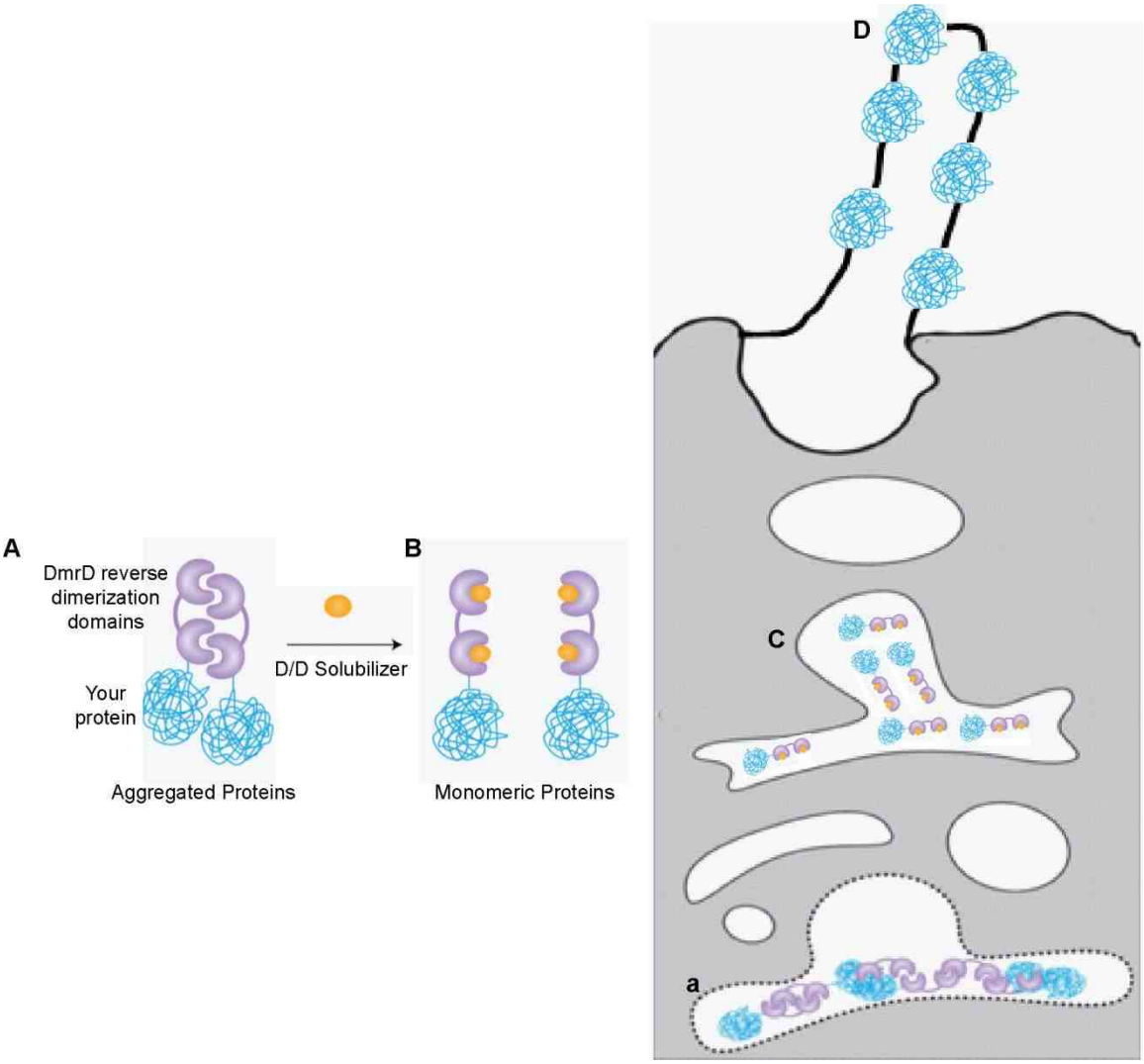

Figure 25. Schematic showing the iDimerize reversible dimerization system. The 'iDimerizeTM' cassettes contain an ER targeting signal (Clontech) and cause protein oligomerization and trapping in the ER (A, a) that can be released with the addition of a solubilizing ligand (B). The addition of ligand allows disaggregation and synchronous release of iDimerize-CD16.7-PC1 fusion protein from ER. Cells can then be placed at 20˚C to accumulate protein in Golgi (C) or keep cells at 37˚C to allow for plasma membrane transport (D), which can be monitored by immunofluorescence staining.

The iDimerizeTM' cassettes were cloned in frame in front of the N-terminus of the CD16.7-PC1-WT and CD16.7-PC1-359 chimeras. The iDimerize-CD16.7-PC1-WT and iDimerize-CD16.7-PC1-359 fusion constructs **(Figure 26A)** were transfected into polarized RCTE cells. Before addition of solubilizing ligand, both the iDimerize-CD16.7-PC1-WT and iDimerize-CD16.7-PC1-359 constructs exhibit perinuclear staining indicative of being trapped in the ER **(Figure 26B and data not shown)**. Treatment of cells with 250 nM solubilizer causes the disruption of iDimerize protein oligimerization in the ER and synchronous release of iDimerize fusion proteins to the Golgi where the iDimerize cassettes are cleaved off during protein processing, allowing for proper packaging of CD16.7-PC1 constructs by the subsequent cellular sorting pathways. The iDimerize-CD16.7-PC1-WT construct successfully localized to primary cilia **(Figure 26C)**, while the iDimerize-CD16.7-PC1-359 construct failed to localize to primary cilia of RCTE cells **(Figure 26D)**. The significant reduction in ciliary localization of iDimerize-CD16.7-PC1-359 mutant protein lacking the ciliary targeting VxPx motif compared to the iDimerize-CD16.7-PC1-WT construct **(Figure 26E)** corroborates our previous finding that the VxPx motif is essential for trafficking of PC1 to primary cilia of renal epithelial cells. These studies verified the fidelity of the iDimerize-CD16.7-PC1-WT and iDimerize-CD16.7-PC1-359 constructs for the study of OFD1 and PC1 protein-protein interactions en route to primary cilia; starting with PC1 synthesis in the ER and subsequent transport through the secretory pathway from the Golgi apparatus to primary cilia.

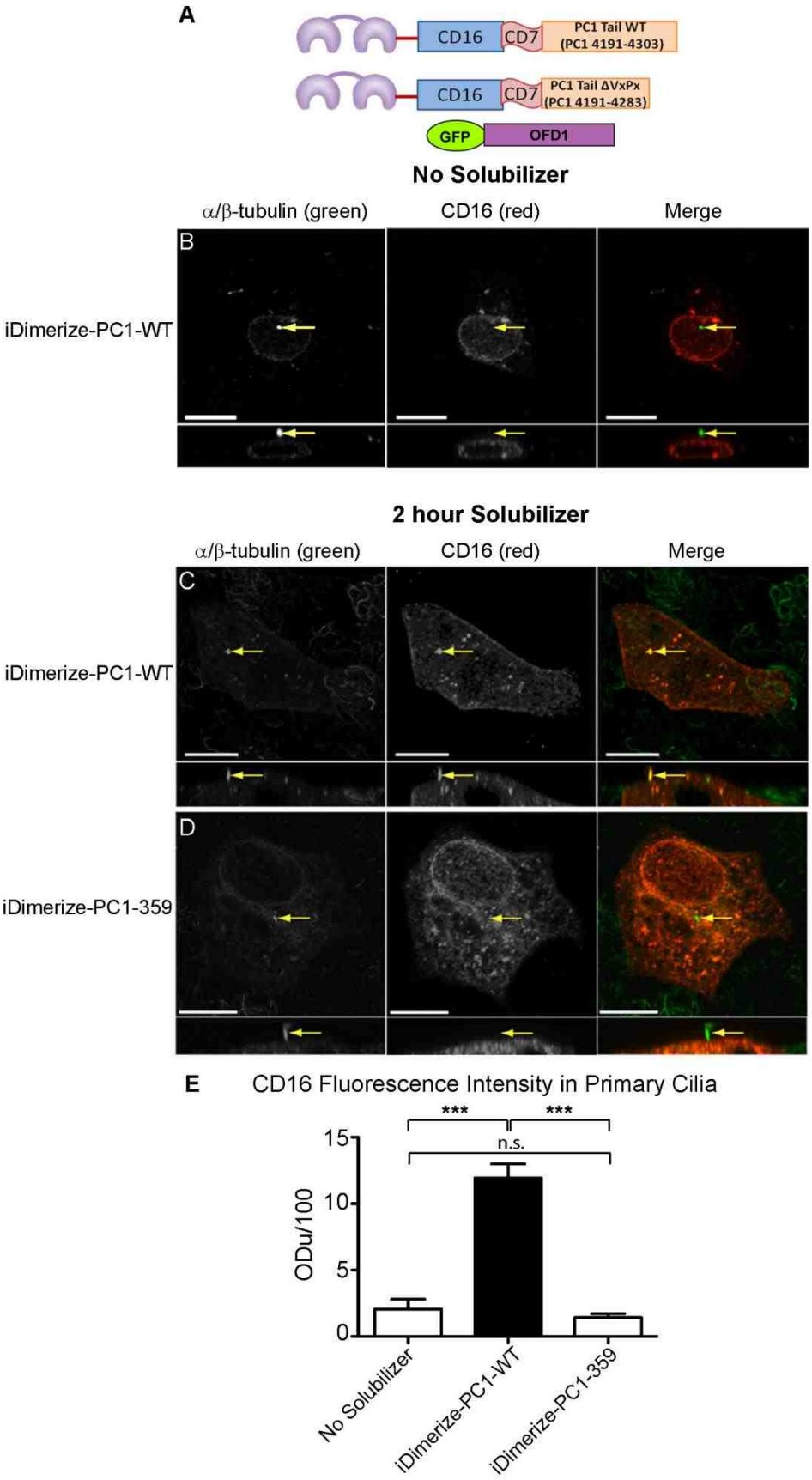
A
CD16
CD7
PC1 Tail WT
(PC1 4191-4303)
CD16
CD7
PC1 Tail ΔVxPx
(PC1 4191-4283)
GFP
OFD1
No Solubilizer
α/β-tubulin (green)
CD16 (red)
Merge
B
iDimerize-PC1-WT
2 hour Solubilizer
α/β-tubulin (green)
CD16 (red)
Merge
C
iDimerize-PC1-WT
D
iDimerize-PC1-359
E
CD16 Fluorescence Intensity in Primary Cilia
***
***
n.s.
15
10
5
0
ODu/100
No Solubilizer
iDimerize-PC1-WT
iDimerize-PC1-359

Figure 26. iDimerize-CD16.7-PC1-WT, but not iDimerize-CD16.7-PC1-359, localizes to primary cilium. Schematic of iDimerize PC1 fusion proteins and GFP OFD1. iDimerize PC1 fusion proteins consist of an 'iDimerizeTM' cassette containing an ER targeting signal (Clontech) fused to the NH_2-terminal ectoplasmic domain of human CD16 followed by the transmembrane domain of human CD7 and the membrane distal C-terminus of human PC1 C-terminal tail with or without the VxPx ciliary targeting motif. GFP-OFD1 consists of eGFP fused to the N-terminus of full-length OFD1 (A). RCTE cells were grown on 0.4 μm filter supports 4 days post confluency to allow for polarization and transfected with the iDimerize-CD16.7-PC1-WT or iDimerize-CD16.7-PC1-359 truncation mutant construct. Post-transfection (16 hours) cells were incubated +/- solubilizer and stained with antibody against CD16. Perinuclear staining of iDimerize-CD16.7-PC1-WT construct locked in endoplasmic reticulum due to absence of solubilizer (B).Following 2 hour treatment with solubilizer, iDimerize-CD16.7-PC1-WT localizes to primary cilia (C) while iDimerize-CD16.7-PC1-359 fails to localize to cilia (D). α/β-tubulin labeling identifies cilia. Arrows denote the protein of interest within a cilium. Zeiss META confocal microscope images (63x objective). Secondary antibody only controls were negative (not shown). Scale bar 10 μm. Quantification shows ciliary protein intensities normalized to the respective ciliary volume (E). Each protein was quantified in 30-100 cilia for each cell type. z-stack images were imported into SlideBook and a volume mask for each cilium was created based on α/β-tubulin staining. Staining intensities for each protein were quantified within the respective ciliary volume mask. Mean values were found to be statistically different ($p<0.0001$) using 1-way ANOVA.

4.3 Expression of iDimerize-CD16.7-PC1-359 mutant impairs the ability of GFP-OFD1 to localize to primary cilia

To address the possibility that OFD1 ciliary localization is dependent on the VxPx ciliary targeting motif in PC1, I tested if OFD1 expression with a PC1 VxPx mutant would affect the ciliary localization of OFD1. I have previously shown overexpressed GFP-OFD1 localization to primary cilia of RCTE cells [60]. Here, I co-transfected RCTE cells with GFP-OFD1 and either the iDimerize-CD16.7-PC1-WT or iDimerize-CD16.7-PC1-359 VxPx mutant. This allowed analysis of how newly synthesized OFD1 protein localization to primary cilia is affected by PC1 ciliary localization. Before addition of solubilizing ligand, the iDimerize-CD16.7-PC1-WT construct exhibits a nuclear envelope and contiguous perinuclear staining indicative of the iDimerize-CD16.7-PC1 protein aggregation in the ER **(Figure 27A)**. As expected, there was no ciliary localization of the iDimerize-CD16.7-PC1 construct before addition of solubilzer due to protein accumulation in the ER. GFP-OFD1 successfully localized to primary cilia of cells that did not co-express iDimerize-CD16.7-PC1 constructs (data not shown), corroborating our previous studies showing ciliary localization of GFP-OFD1 in cells expressing only endogenous PC1 [60]. Interestingly, GFP-OFD1 failed to localize to primary cilia in cells where iDimerize-PC1 was trapped in the ER, suggesting that OFD1 requires PC1 for ciliary delivery. Upon addition of solubilizing ligand, iDimerize-CD16.7-PC1-WT localizes to primary cilia, along with GFP-OFD1 **(Figure 27B)**. However, iDimerize-CD16.7-PC1-359 fails to localize to cilia upon addition of solubilizer. In the cells expressing iDimerize-

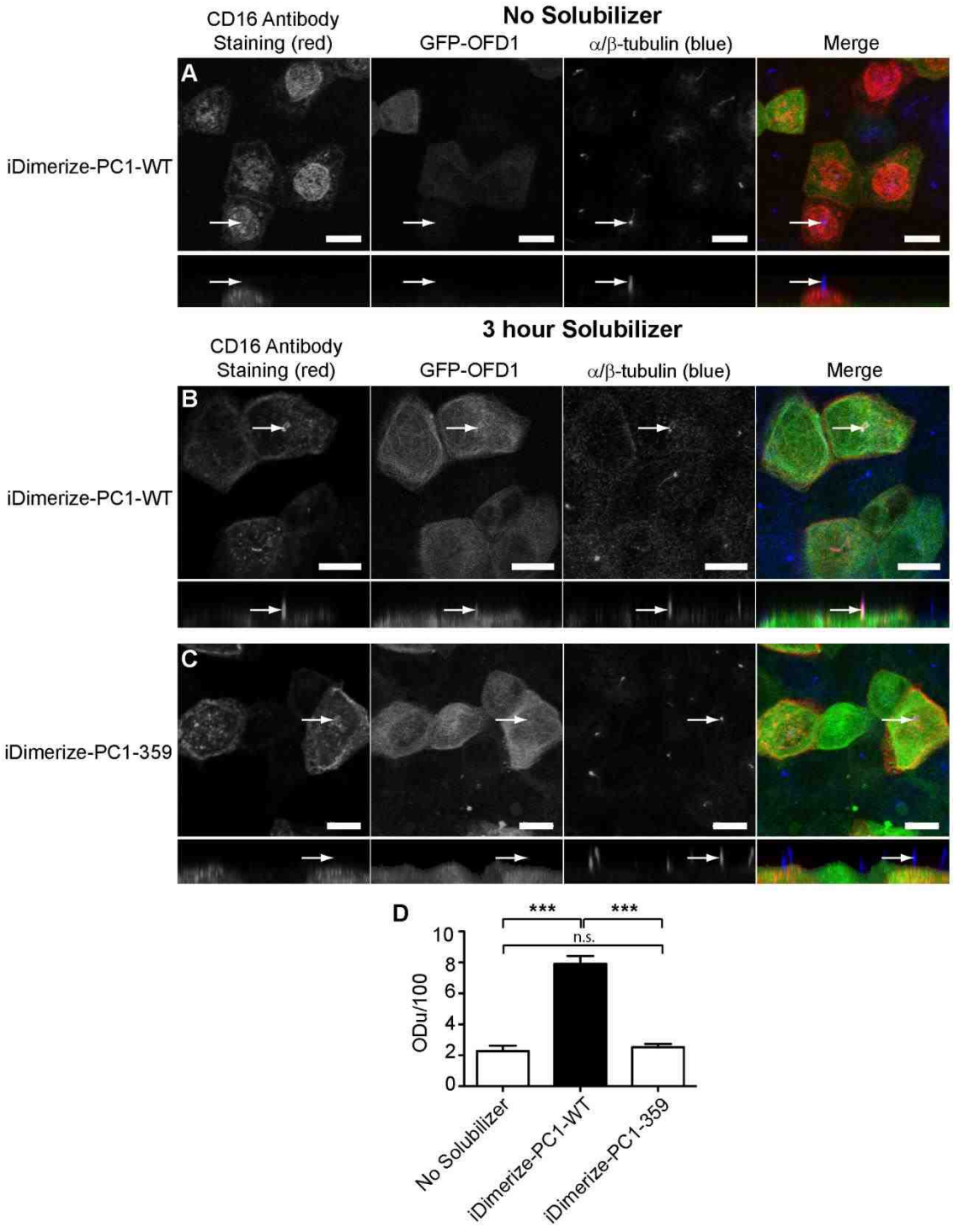
No Solubilizer
CD16 Antibody Staining (red)
GFP-OFD1
α/β-tubulin (blue)
Merge
A
iDimerize-PC1-WT
3 hour Solubilizer
CD16 Antibody Staining (red)
GFP-OFD1
α/β-tubulin (blue)
Merge
B
iDimerize-PC1-WT
C
iDimerize-PC1-359
D
***
***
n.s.
ODu/100
10
8
6
4
2
0
No Solubilizer
iDimerize-PC1-WT
iDimerize-PC1-359

Figure 27. GFP-OFD1 fails to localize to cilia of cells expressing the iDimerize-CD16.7-PC1-359 mutant. Polarized RCTE grown on 0.4 μm filter supports were co-transfected with GFP-OFD1 and either the iDimerize-CD16.7-PC1-WT or iDimerize-CD16.7-PC1-359 truncation mutant construct. Post-transfection (16 hours) cells were incubated +/- solubilizer and stained with antibody against CD16. GFP-OFD1 exhibits cytoplasmic localization but fails to localize to primary cilia in cells without solubilizer when iDimerize-PC1-CD16.7-PC1 construct is locked in ER (A). Following 3 hour treatment with solubilizer, iDimerize-CD16.7-PC1-WT along with GFP-OFD1 localize to primary cilia (B) while GFP-OFD1 is absent from cilia in cells expressing iDimerize-CD16.7-PC1-359 (also absent from cilia) (C). α/β-tubulin labeling identifies cilia. Arrows denote the protein of interest within a cilium. Secondary antibody only controls were negative (not shown). Zeiss LSM META confocal microscope images (63x objective). Scale bar 10 μm.Quantification shows ciliary protein intensities normalized to the respective ciliary volume as detailed in Figure 1 (D). Mean values were found to be statistically different ($p<0.0001$) using 1-way ANOVA.

CD16.7-PC1-359, there is also a significant decrease of GFP-OFD1 localized to primary cilia **(Figure 27C, D)**. The reduction in ciliary GFP-OFD1 is similar between the cells expressing the iDimerize-CD16.7-PC1-359 mutant and those without solubilizer where the iDimerize-CD16.7-PC1 construct is trapped in the ER **(Figure 27D)**. These data suggest that OFD1 requires PC1 for correct ciliary localization and/or stabilization of OFD1 in the ciliary shaft.

To further confirm the findings, the proteins were accumulated in the Golgi using a 20°C temperature block as described previously [83]. Briefly, I co-transfected RCTE cells with GFP-OFD1 and either the iDimerize-CD16.7-PC1-WT or iDimerize-CD16.7-PC1-359 mutant and allowed the iDimerize-CD16.7-PC1 constructs to accumulate in the ER for 16 hours. Before addition of solubilizer, the iDimerize-CD16.7-PC1-WT protein was concentrated in the nuclear envelope and contiguous perinuclear ER affirming efficacy of transfection and experimental protocol **(Figure 28A)**. Upon addition of solubilizer, cells were transferred to a reduced temperature (20°C) water bath to cause the iDimerize constructs to synchronously exit from the ER and accumulate in the Golgi. After 1 hour at 20°C, both the iDimerize-CD16.7-PC1-WT **(Figure 28B)** and iDimerize-CD16.7-PC1-359 **(Figure 28C)** largely disappeared from the ER/nuclear envelope and were instead found in punctate structures in a crescent around the nucleus suggestive of transport to the Golgi. The iDimerize-CD16.7-PC1-359 mutant exhibits greater residual PC1 ER staining suggesting that the iDimerize-CD16.7-PC1-359 mutant while able to exit the ER to the Golgi, may do so more slowly

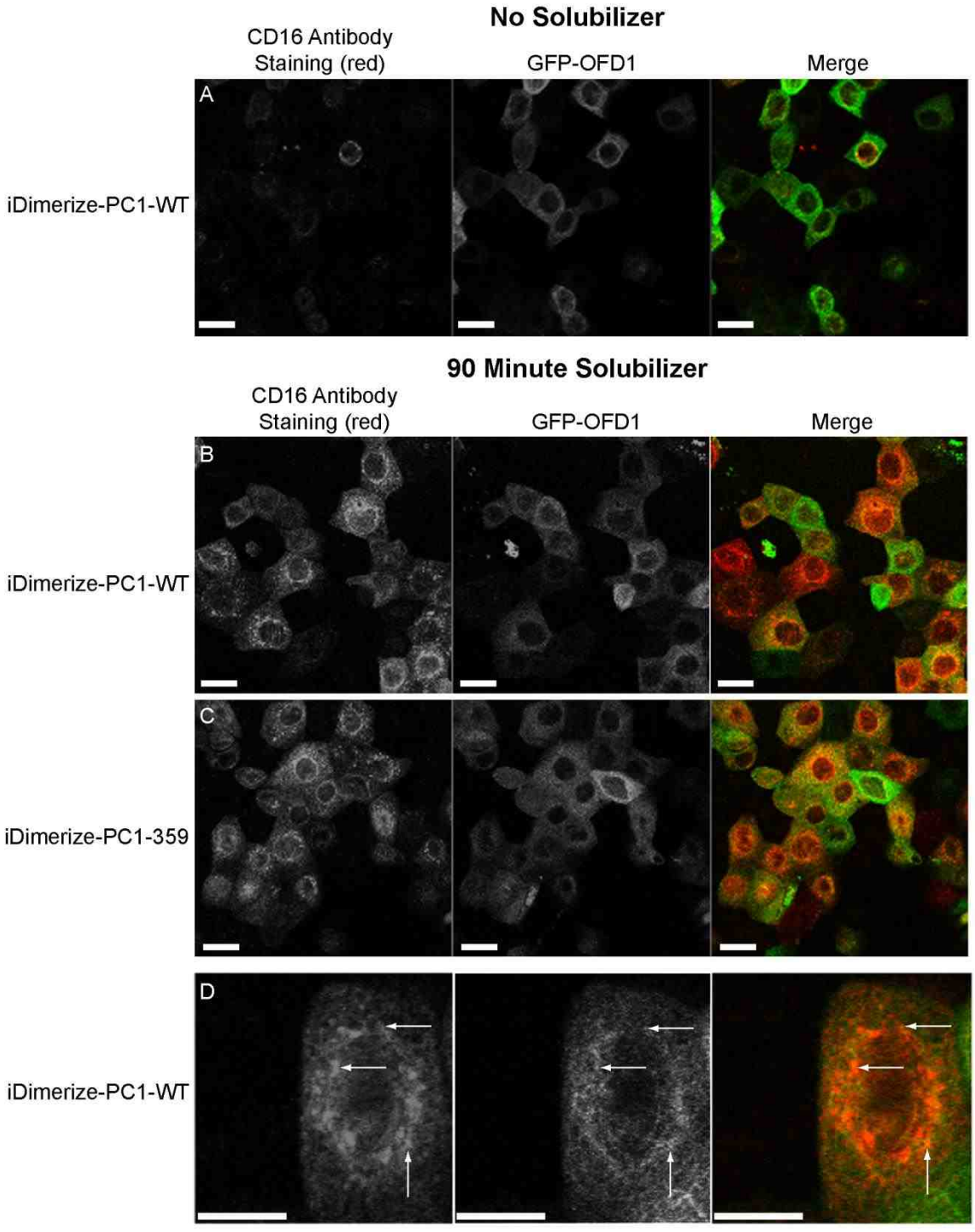
No Solubilizer
CD16 Antibody Staining (red)
GFP-OFD1
Merge
A
iDimerize-PC1-WT
90 Minute Solubilizer
CD16 Antibody Staining (red)
GFP-OFD1
Merge
B
iDimerize-PC1-WT
C
iDimerize-PC1-359
D
iDimerize-PC1-WT

Figure 28. Golgi accumulation of iDimerize-CD16.7-PC1 constructs. Polarized RCTE cells grown on 0.4 µm filter supports were co-transfected with GFP-OFD1 and either the iDimerize-CD16.7-PC1-WT or iDimerize-CD16.7-PC1-359 truncation mutant construct. Post-transfection (16 hours) cells were incubated +/- solubilizer and placed at 20 degrees Celsius for 60-90 minutes to lock proteins in Golgi. Cells were then fixed and stained with antibody against CD16. Before addition of solubilizer, iDimerize-CD16.7-PC1 construct are locked in ER while GFP-OFD1 is localized to cytoplasm (A). After treatment with solubilizer, iDimerize-CD16.7-PC1-WT (B) and CD16.7-PC1-359 (C) constructs exhibit punctate staining in area surrounding ER indicative of accumulation in Golgi. GFP-OFD1 co-localizes with iDimerize-CD16.7-PC1 intracellularly (D). Arrows denote areas of GFP-OFD1 and iDImerize-CD16.7-PC1 co-localization. Zeiss LSM META confocal microscope images (63x objective). Secondary antibody only controls were negative (not shown). Scale bar 10 µm.

than the iDimerize-CD16.7-PC1-WT protein. GFP-OFD1 was largely cytoplasmic; however, there were discrete puncta showing GFP-OFD1 co-localized with iDimerize-CD16.7-PC1 in the area surrounding the perinuclear region upon release from ER **(Figure 28D)**. In cells where PC1 is locked in the ER or mutant, GFP-OFD1 cannot localize to primary cilia but does co-localize with PC1 intracellularly. This suggests that the failure of GFP-OFD1 to localize to cilia may be due to OFD1 being trapped with the iDimerize-CD16.7-PC1-359 VxPx mutant in the ER or Golgi. Taken together, these data suggest that stable expression of OFD1 in primary cilia is dependent on PC1 ciliary localization.

4.4 CD16.7-PC1-L152P coiled coil mutant causes a reduction in OFD1 localization to primary cilia

The interaction of the polycystin proteins, PC1 and PC2, via CC domains is required for PC2 stabilization in the ciliary membrane [120]. Therefore, it was of interest to test the possibility that OFD1 ciliary localization is dependent on interaction with PC1 via the CC domains present in both proteins. We have previously shown that the PC1 tripartite fusion proteins CD16.7-PC1-WT and PC1 CC domain mutant CD16.7-PC1-L152P both correctly localize to primary cilia of kidney epithelial cells [43,119]. To test if the expression of the CD16.7-PC1-L152P CC mutant might affect OFD1 ciliary localization, we co-transfected RCTE cells with GFP-OFD1 and either CD16.7-PC1-WT or CD16.7-PC1-L152P. In the positive control sample, GFP-OFD1 localized to primary cilia in cells expressing CD16.7-PC1-WT protein **(Figure 29A)**. However, in cells

overexpressing the CD16.7-PC1-L152P CC mutant GFP-OFD1 failed to localize to primary cilia **(Figure 29B)**. These data indicate that the CC domain in PC1 is crucial for OFD1 interaction and for stable OFD1 ciliary localization.

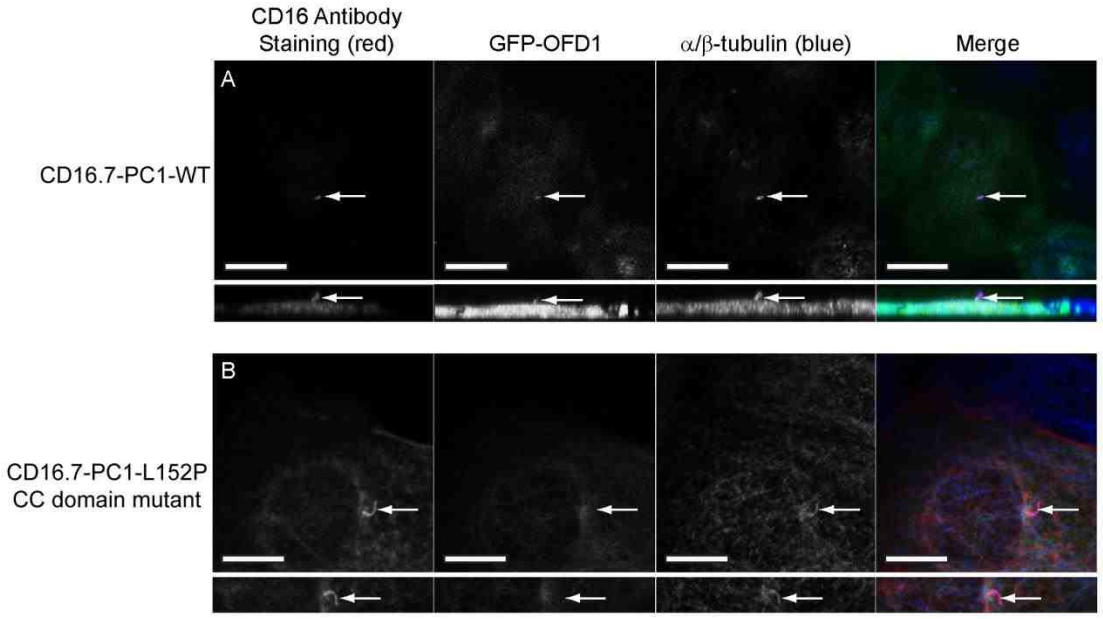

Figure 29. GFP-OFD1 fails to localize to cilia in cells expressing the CD16.7-PC1-L152P coiled coil mutant. Polarized RCTE cells grown on 0.4 µm filter supports were co-transfected with GFP-OFD1 and either the CD16.7-PC1-WT or CD16.7-PC1-L152P coiled coil mutant construct. Post-transfection (16 hours) cells were then fixed and stained with antibody against CD16. CD16.7-PC1-WT and GFP-OFD1 localize to primary cilia (A). While the CD16.7-PC1-L152P mutant is able to localize to cilia, GFP-OFD1 fails to co-localize to cilia in cells expressing the CD16.7-PC1-L152P coiled coil mutant (B). α/β-tubulin labeling identifies cilia. Arrows denote the protein of interest within a cilium. Zeiss LSM META confocal microscope images (63x objective). Secondary antibody only controls were negative (not shown). Scale bar 10 µm.

4.5 OFD1 interacts with PC1 via coiled coil domains

I previously showed that OFD1 interacts with PC1, but the domains important for this interaction remained unknown [60]. For reciprocal confirmation of an interaction between PC1 and OFD1 dependent on the CC domains, in vitro binding experiments were conducted using a CC deletion mutant of OFD1. OFD1 is comprised of a short N-terminus containing a LisH motif and a much longer C-terminus with five to six predicted CC domains **(Figure 30A)**.

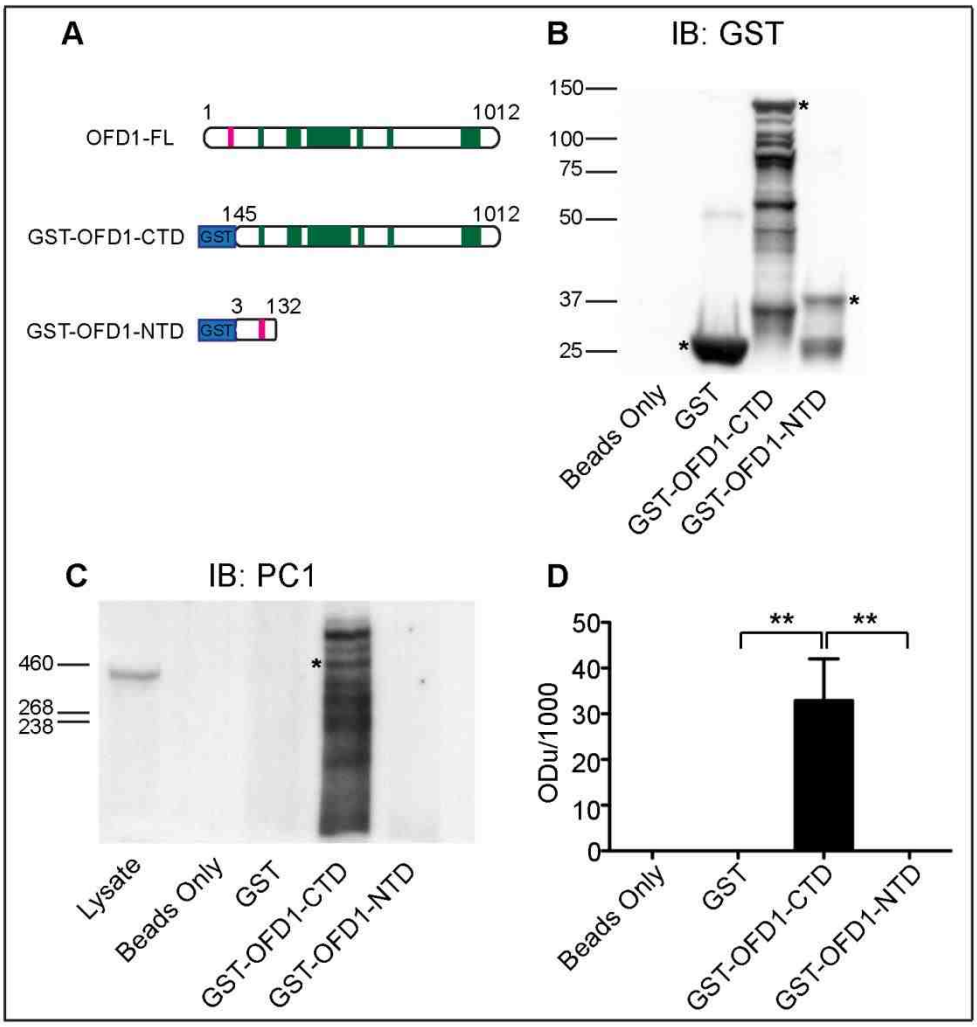

Figure 30. PC1 interacts with coiled coil domains of OFD1. Cartoon depicted full-length OFD1 with a N-terminal LisH motif and a longer C-terminus comprised of six predicted coiled coil domains. Constructs used for this study consisted of a GST tag fused to either the C-terminus of OFD1 containing the coiled coil domains or GST fused to the N-terminus of OFD1 without coiled coil domains (A). Glutathione resin-bound GST (~25kDa), GST-OFD1-CTD (~129 kDa) and GST-OFD1-NTD (~44kDa) was incubated with cell lysate of polarized RCTE cells. After washing, the pulled-down complexes were subjected to SDS-PAGE and analyzed by Western blotting using anti-GST and anti-PC1 antibodies. While all GST constructs (and GST alone) were present in GST pulldowns at their correct sizes (B) only the GST-OFD1-CTD was found in complex with full length ~460 kDa PC1 (C). Quantification shows mean values were found to be statistically different ($p=0.0005$) using 1-way ANOVA (D).

GST-OFD1 fusion proteins with or without the CC domains were used to investigate the importance of OFD1 CC domains for interaction with PC1. GST-OFD1-NTD (44kDa) is comprised of GST fused to the N-terminus of OFD1 containing the LisH motif **(Figure 30A)**. GST-OFD1-CTD (129kDa) consists of GST fused to the C-terminal portion of OFD1 containing the CC domains **(Figure 30A)**. GST only, GST-OFD1-CTD, or GST-OFD1-NTD purified protein were incubated with RCTE cell lysate and glutathione beads were used to recover the GST fusion proteins and any bound proteins from the cell lysates. The glutathione-bead-bound-proteins were resolved by SDS-PAGE, and immunoblotted. Probing for GST identified recovery of GST only and both GST-OFD1 fusion proteins **(Figure 30B)**. Probing for full length PC1 (~460kDa) showed GST-OFD1-CTD containing the CC domains was able to interact with PC1 but GST-OFD1-NTD and GST alone failed to pulldown PC1 from RCTE cell lysates **(Figure 30C; Quantification: Figure 30D)**. These data show that the CC domains of OFD1 are required for OFD1 interaction with PC1 and coupled with the PC1 CC mutant analyses shown above make it likely that there is a reciprocal interaction between the CC domains of PC1 and OFD1.

Chapter 5: Discussion

The data presented here identify the presence of a ciliary signaling complex that is conserved between cells of kidney tubules and the oral cavity. I show that this complex consists of the polycystins (PC1 and PC2), the OFD1 ciliopathy disease gene product, the EGFR receptor tyrosine kinase and the membrane raft organizing flotillin proteins. Moreover, I demonstrated that when one of these proteins is mutant it changes the assembly or stability of the entire ciliary signaling complex in the affected cell types, suggestive of co-assembly into a common domain. Indeed, the decreased expression of OFD1 in primary cilia when PC1 is mutant offers a molecular basis for some of the common pathologies of OFD1 and ADPKD.

The demonstration that the flotillins localize to primary cilia of renal epithelia and odontoblasts and flotillin-2 interacts with the polycystins, EGFR and OFD1 in both cell types is extremely exciting for several reasons. The presence of the flotillins in cilia supports previous speculation regarding commonalities between basolateral membrane, immune synapse and cilia membrane organization [47,123,124]. Flotillins are important in the formation of ordered membrane domains in hematopoietic cells where they are critical for cell polarization and lymphoid immune synapse formation [96,125,126]. In polarized Madin-Darby canine kidney cells, both flotillin-1 and -2 have a non-polarized distribution. Additionally, the flotillins were suggested to have a role in polarization that is

restricted to hematopoietic cells [125]. However, as we showed in human renal epithelial cells flotillins bind cholesterol and organize the polycystins, E-cadherin, tyrosine kinases and phosphatases at the lateral membrane [98]. As shown in this work, flotillins may also organize the polycystins, EGFR and OFD1 in primary cilia into specialized domains. The fact that ciliary EGFR levels were less compromised than the other components is interesting and suggests that the tyrosine kinase may move in and out of cholesterol based raft domains organized by flotillins and that this is likely to have functional importance in regulating ciliary signaling.

Flotillins play a major role in the fidelity of cell signaling and EGFR function [80,127,128]. Knockdown of flotillin-2 disrupts localization and phosphorylation of EGFR and activation of downstream MAPK signaling components [100]. However, in breast cancer cells with mutant PIK3CA, a well-known downstream target of EGFR signaling, knockdown of flotillin-1 causes an upregulation of EGFR and hyperactivation of MAPK signaling. These data indicate that the flotillins have dual roles in enabling receptor tyrosine kinase activation and downstream signaling, as well as in restraining signaling components such as PIK3CA in an inactive state [129]. Furthermore, the polycystins have been shown to interact with both receptor tyrosine kinases and phosphatases within primary cilia [87, 99]. The importance of ciliary organization of EGFR signaling is further reinforced by recent studies showing that when cilia are ablated, EGFR mediated activation of apical calcium channels is increased 64-fold [130]. Similarly, in

IMCD-3 cells, primary cilia were found to restrain interaction and cross-talk between G-protein coupled receptors, which are also known to cross-talk with receptor tyrosine kinases [110,131]. Hence, it appears likely that the flotillins have an important role in the control of ciliary signaling that extends beyond a purely scaffolding function. Notably, the upshift in molecular weight of flotillin proteins in the complex is suggestive of post-translational modifications that may be important in their regulation of specific signaling events.

In addition to EGFR, there are growing numbers of receptor tyrosine kinases identified in primary cilia of epithelia, neuronal cells and fibroblasts [110]. Of particular interest are the expression of RON kinase in motile cilia of airway epithelia and the documented cooperation between EGFR, RON and Met [132-134]. Emerging data from studies in human embryonic kidney cells and in breast, lung and colorectal cancer cells indicate that the RON kinase interacts with EGFR and may contribute to direct transcriptional regulation [135,136]. Counterbalancing the activities of receptor tyrosine kinases are receptor protein phosphatases, with members of the LAR family shown to be present in cilia of renal epithelia [99]. Additional regulation may occur at the level of proteasomal degradation at the ciliary base [136]. The connections between RON, Met and EGFR are intriguing because both Met and EGFR are pivotal in cystogenesis [137-139]. Based on the fact that the decreased levels of OFD1, PC2 and flotillins were more significantly affected than EGFR in cells expressing mutant PC1, it is possible that OFD1, PC2 and the flotillins are highly dependent on

functional PC1 for ciliary delivery and stabilization whereas EGFR may arrive at the primary cilium independently of PC1 but relies on functional PC1 for integration into ciliary signaling protein assemblies.

There are two molecular explanations for the finding that mutant PC1 results in reductions of OFD1 and other key signaling proteins in primary cilia that immediately come to mind. First, PC1 and OFD1 may have interdependent roles in the ciliary transport and/or targeting of the proteins in the complex. Second, PC1 may be essential for stabilizing the complex within the ciliary membrane. The data presented here demonstrate that localization and/or stable expression of OFD1 in primary cilia is dependent on PC1 ciliary localization. From what we have learned from past studies, there appears to be an ordered sequence of events for ciliary protein trafficking. First, integral membrane ciliary cargo is sorted in the Golgi, followed by vesicle budding, translocation to the base of the primary cilia, docking at the basal bodies, and subsequent vesicle fusion for incorporation into the ciliary membrane [118,140-142]. Our previous studies on the ciliary trafficking of the polycystins demonstrated that PC1 is dependent on a conserved VxPx motif, which is recognized by the small GTPase Arf4 at the Golgi, for targeting to the ciliary membrane. Truncation of the PC1 C-terminal tail containing the VxPx motif disrupts the ability of Arf4 to bind PC1 and negatively affects PC1 localization to primary cilia. The data shown here suggests that OFD1, a soluble protein that does not have a VxPx ciliary targeting motif, depends on an interaction with PC1 for localization to the primary cilia. GFP-

OFD1 localized to primary cilia in cells expressing iDimerize-CD16.7-PC1-WT but was lacking in cells expressing the iDimerize-CD16.7-PC1-359 VxPx mutant. Additionally, GFP-OFD1 failed to localize to cilia in cells where iDimerize-CD16.7-PC1 was accumulated in the ER or Golgi. Our previous studies show that in renal epithelial cells mutant PC1 protein lacking the VxPx motif accumulates in the Golgi, with possible backup in the ER [43], which suggests that the absence of ciliary targeting signals causes mutant PC1 to fail to be properly escorted out of the Golgi. The ciliary trafficking of endogenous wild-type PC1 may be negatively affected by the accumulation of overexpressed PC1 constructs intracellularly in the ER or Golgi. Native PC1 may oligomerize with overexpressed iDimerize-CD16.7-PC1 at these intracellular locations resulting in the inability of endogenous PC1 to facilitate OFD1 ciliary delivery and/or stabilization. This speculation is supported by our previous studies showing accumulation of mutant PC1 in the Golgi of ADPKD cystic epithelia results in dysfunction of basolateral cellular trafficking, which shares numerous similarities with ciliary trafficking [143]. I show here that GFP-OFD1 co-localized with iDimerize-CD16.7-PC1 intracellularly when PC1 is accumulated in the Golgi. This suggests that OFD1 may be recruited with PC1 to the Golgi for delivery to primary cilia and may explain why GFP-OFD1 failed to traffic to cilia in cells where PC1 was lacking in primary cilia.

The fact that loss of ciliary PC1 led to decreased OFD1 localization to the ciliary shaft suggests that PC1 interaction with OFD1, likely via CC domains found in

both proteins, may be required for ciliary delivery or stable association of OFD1 within the ciliary membrane. Support for this speculation is provided by previous reports showing PC1 and PC2 also contain CC domains that mediate their interaction, and are important for their ciliary localization [144,145]. These studies show that OFD1 interaction with PC1 is dependent on CC domains. Furthermore, GFP-OFD1 localizes to primary cilia of normal RCTE cells [60]; however GFP-OFD1 failed to localize to primary cilia of cells expressing a CC mutant of PC1. The fact that endogenous PC1 expressed in these cells was not sufficient to stabilize OFD1 in primary cilia suggests that the overexpressed CD16.7-PC1-L152P CC mutant may have a dominant negative effect on OFD1 ciliary localization. Further characterizing the molecular basis for the interaction between membrane proteins (such as polycystins) and soluble proteins (such as OFD1) en route to primary cilia and within the ciliary shaft will be important to distinguish the role(s) of PC1 in transport and/or stabilization of other ciliary proteins.

OFD1 has known functions at the base of cilia to control ciliogenesis. Furthermore, OFD1 may be involved in vesicle docking machineries and recruitment of intraflagellar transport (IFT) proteins at the base of the cilium. IFT88 is a crucial component of the IFT complex B, which is involved in moving proteins along the ciliary axoneme and is required for primary cilia formation. The CC domains of OFD1 are crucial for the recruitment of IFT88 to centrosomes and loss of either OFD1 or IFT88 results in failure of cells to produce cilia

[36,63,71,88,89]. OFD1 plays an important role at the centrosome to control centriole distal appendage formation and to stabilize centriolar microtubules at a defined length [63]. Distal appendages are also implicated in the trafficking and docking of ciliary vesicles carrying membrane constituents [146-149]. It is possible that OFD1 is involved in the docking of vesicles containing ciliary membrane proteins such as PC1 and simultaneously facilitating interactions with IFT88 for transfer along the ciliary shaft. In the process, PC1 transfer to cilia may enable OFD1 entry and/or stabilization. If ciliary vesicle docking at the distal appendages requires an interaction between PC1 and OFD1, it is conceivable that the ciliary localizations of multiple components of a preassembled complex would be similarly affected. Thus, the diminished OFD1 localization to cilia when PC1 is mutant may adversely affect both ciliogenesis and ciliary function based on the dual roles OFD1 has in regulating intraflagellar transport components and membrane vesicles.

In these studies, I show the existence of a protein complex containing the polycystins, flotillins, EGFR and OFD1 in cilia of both renal and dental cells providing evidence for the existence of conserved ciliary signaling microdomains in multiple cell types that may account for the shared pathologies. Furthermore, I show that the stabilization of OFD1 in the ciliary membrane is dependent on interaction with PC1, which is facilitated by CC domains found in both proteins. These data show that when PC1 is mutant, the ciliary localization of PC2, EGFR, the flotillins, and OFD1 are concomitantly decreased. The requirement of PC1 for

the ciliary trafficking of OFD1 and integrity of the ciliary microdomain provides a plausible molecular rationale for the similarities between craniofacial disorders and cystic kidney disease. These findings provide a molecular explanation for some of the observed commonalities in the pathogenesis of multi-organ ciliopathies such as OFD1 and ADPKD and inform strategies for the development of potential therapeutic interventions that stabilize protein complexes.

Future Directions

OFD1 and ADPKD share many similarities in cystic kidney disease pathogenesis, yet the molecular basis for these commonalities is just beginning to be unraveled. Experiments investigating how key ciliary signaling proteins interact will be essential to gain information about the mechanisms by which overlapping signaling pathways intersect to result in shared disease phenotypes. The iDimerize-CD16.7-PC1 constructs will allow us further dissection of the sequence of events involved in OFD1 ciliary protein targeting, docking, and microdomain assembly in the primary cilia. For example, the system can be used to identify specific trafficking machinery components important for transport and will allow immunoprecipitation of complexes that form discrete subcellular locales during transport. The studies will provide us new and vital information on the sequence of events involved in the spatiotemporal assembly and delivery of ciliary OFD1. The present work suggests that OFD1 and PC1 first interact at the Golgi for delivery to primary cilia. However, further studies should utilize the Golgi lock experiment combined with subsequent release to primary cilia to determine whether OFD1 and PC1 first interact at the Golgi, basal bodies at the base of the cilium, or after both proteins are integrated into the ciliary membrane. The use of the iDimerize constructs will pave the way for the identification of the cohort of proteins that are also delivered via the same pathway and the sequence in which they join the assembly. The present studies lay the groundwork for how receptor tyrosine kinases may be organized in cilia and warrant an expanded

characterization to determine how receptor protein kinases and phosphatases along with other signaling proteins may interact with or be co-assembled with the flotillin-EGFR-polycystin-OFD1 protein complexes characterized here.

Establishing the flotillins as critical organizers of ciliary microdomains will set the stage for analyzing the role of the flotillins in the coordinated transport of associated proteins to cilia. The importance of the flotillins in immune synapse formation, which is dependent on highly targeted membrane protein insertion, suggests that they are likely to play a similarly pivotal role in ciliogenesis through their interactions with OFD1 and the polycystins. I hypothesize that OFD1 associates with flotillin-organized ciliary microdomains enabling stabilization of this cytosolic protein in specialized areas of the cilia. The flotillin proteins contain cholesterol binding CRAC domains that are important for flotillin binding cholesterol to organize lipid raft domains. Future studies using methyl β-cyclodextrin (known to disrupt flotillin protein assemblies of PC1) will determine how cholesterol depletion will disrupt the OFD1 ciliary microdomains organized by the flotillins. Alternatively, flotillin siRNA knockdown could be used to investigate the effect on OFD1, PC1, PC2, and EGFR ciliary localization and interactions. I predict that the reduction in flotillins will impair ciliary microdomain formation and disrupt OFD1 ciliary localization.

The delivery of proteins to the primary cilium relies on variety of trafficking chaperones and machinery to arrive at this destination. Because the iDimerize-

CD16.7-PC1-359 VxPx mutant caused a significant impairment in the trafficking of OFD1 to the primary cilium, it should be investigated whether or not OFD1 also depends on the small GTPase Arf4, which recognizes the VxPx motif in PC1, for transport to the cilium using Arf4 siRNA. Significant decreases in cellular Arf4 should cause a significant reduction in the amount of OFD1 present in the cilium if transport depends on PC1. In the event that PC1 is not required for OFD1 ciliary delivery, we predict that OFD1 traffics to the basal body and cilium via an alternative route, likely through interaction with the IFT-B complex. Alternatively, because OFD1 has been shown to recruit the intraflagellar transport protein IFT88 to the base of the cilium, there exists the possibility that OFD1 is a chaperone in this pathway and may be responsible for docking polycystin-containing vesicles at the base of the cilium instead of co-trafficking with PC1 from the Golgi. Polarized RCTE cells transfected with siRNA against OFD1 to deplete OFD1 protein will allow analysis of OFD1 functions distinct from those described to be important for ciliogenesis, and will help dissect if PC1 may also rely on OFD1 for ciliary delivery.

The important role of OFD1 in regulation of primary cilia is supported by the finding that OFD1 co-localizes with other ciliopathy disease proteins at centriolar satellites including BBS4 and CEP290 [34]. At this cellular location, OFD1 interacts with the key centriolar satellite component PCM-1 via the CC domains of OFD1. The CC domains 2 through 4 of OFD1 are crucial for the recruitment of IFT88 to centrosomes. At this cellular location, OFD1 interacts with the key

centriolar satellite component PCM-1 via the 5th CC domain of OFD1. This finding supports the functional importance of the various CC domains found in OFD1 and suggests that OFD1 mutations that affect different domains may contribute to clinically diverse phenotypes. This is evidenced by the observation that in human patients, OFD1 CC mutants were associated with tooth abnormalities, while splice variants were associated with kidney disease [150]. Furthermore, mutations predicted to affect the extreme C-terminus of OFD1 including the 5th CC domain are found in rare male patients with mental retardation and digital abnormalities [34]. Further studies on which CC domains of OFD1 are required for interaction with PC1 will be essential to dissect how these proteins are assembled into ciliary microdomains together.

In summary, further studies to determine how OFD1 and PC1 interact en route to primary cilia and how they are assembled into ciliary microdomains will be an important next step in these studies. Additionally, the trafficking machinery required for OFD1 ciliary delivery has yet to be determined. The flotillins role in the assembly of ciliary signaling domains will be important to establish how these unique microdomains are organized and how disruption of these domains results in human diseases with multi-organ pathologies.

References

1. Levey AS, Atkins R, Coresh J, Cohen EP, Collins AJ, et al. (2007) Chronic kidney disease as a global public health problem: Approaches and initiatives - a position statement from Kidney Disease Improving Global Outcomes. Kidney International 72: 247-259.

2. Nahas ME (2005) The global challenge of chronic kidney disease. Kidney International 68: 2918-2929.

3. Katabathina VS, Kota G, Dasyam AK, Shanbhogue AK, Prasad SR (2010) Adult renal cystic disease: a genetic, biological, and developmental primer. Radiographics 30: 1509-1523.

4. Chen PM, Lai TS, Chen PY, Lai CF, Yang SY, et al. (2014) Multidisciplinary Care Program for Advanced Chronic Kidney Disease: Reduces Renal Replacement and Medical Costs. Am J Med.

5. Smith DH, Gullion CM, Nichols G, Keith DS, Brown JB (2004) Cost of medical care for chronic kidney disease and comorbidity among enrollees in a large HMO population. J Am Soc Nephrol 15: 1300-1306.

6. Laliberte F, Bookhart BK, Vekeman F, Corral M, Duh MS, et al. (2009) Direct All-Cause Health Care Costs Associated With Chronic Kidney Disease in Patients With Diabetes and Hypertension: A Managed Care Perspective. Journal of Managed Care Pharmacy 15: 312-322.

7. Vupputuri S, Kimes TM, Calloway MO, Christian JB, Bruhn D, et al. (2014) The economic burden of progressive chronic kidney disease among patients with type 2 diabetes. Journal of Diabetes and Its Complications 28: 10-16.

8. Bissler JJ, Dixon BP (2005) A mechanistic approach to inherited polycystic kidney disease. Pediatr Nephrol 20: 558-566.

9. Hildebrandt F (2010) Genetic kidney diseases. Lancet 375: 1287-1295.

10. Igarashi P, Somlo S (2002) Genetics and pathogenesis of polycystic kidney disease. J Am Soc Nephrol 13: 2384-2398.

11. Kurschat CE, Muller RU, Franke M, Maintz D, Schermer B, et al. (2014) An approach to cystic kidney diseases: the clinician's view. Nat Rev Nephrol 10: 687-699.

12. Torres V, Harris P (2009) Autosomal dominant polycystic kidney disease: the last 3 years. Kidney Int 76: 149-168.

13. Grantham J, Cook L, Torres V, Bost J, Chapman A, et al. (2008) Determinants of renal volume in autosomal-dominant polycystic kidney disease. Kidney Int 73: 108-116.

14. Grantham J, Cook L, Wetzel L, Cadnapaphornchai M, Bae K (2010) Evidence of extraordinary growth in the progressive enlargement of renal cysts. Clin J Am Soc Nephrol 5: 889-896.

15. Bertram J, Douglas-Denton R, Diouf B, Hughson M, Hoy W (2011) Human nephron number: implications for health and disease. Pediatr Nephrol 26: 1529-1533.

16. Chapman A, Bost J, Torres V, Guay-Woodford L, Bae K, et al. (2012) Kidney volume and functional outcomes in autosomal dominant polycystic kidney disease. Clin J Am Soc Nephrol 7: 479-486.

17. Wilson P (2004) Polycystic kidney disease. N Engl J Med 350: 151-164.

18. Chapman A, Stepniakowski K, Rahbari-Oskoui F (2010) Hypertension in autosomal dominant polycystic kidney disease. Adv Chronic Kidney Dis 17: 153-163.

19. Grantham J, Bennett W, Perrone R (2011) mTOR inhibitors and autosomal dominant polycystic kidney disease. N Engl J Med 364: 286-287; author reply 287-289.

20. Nauli S, Kawanabe Y, Kaminski J, Pearce W, Ingber D, et al. (2008) Endothelial cilia are fluid shear sensors that regulate calcium signaling and nitric oxide production through polycystin-1. Circulation 117: 1161-1171.

21. AbouAlaiwi W, Takahashi M, Mell B, Jones T, Ratnam S, et al. (2009) Ciliary polycystin-2 is a mechanosensitive calcium channel involved in nitric oxide signaling cascades. Circ Res 104: 860-869.

22. Fick G, Johnson A, Hammond W, Gabow P (1995) Causes of death in autosomal dominant polycystic kidney disease. J Am Soc Nephrol 5: 2048-2056.

23. Sharif-Naeini R, Folgering J, Bichet D, Duprat F, Lauritzen I, et al. (2009) Polycystin-1 and -2 dosage regulates pressure sensing. Cell 139: 587-596.

24. Norman J (2011) Fibrosis and progression of autosomal dominant polycystic kidney disease (ADPKD). Biochim Biophys Acta 1812: 1327-1336.

25. Hassane S, Leonhard W, van der Wal A, Hawinkels L, Lantinga-van Leeuwen I, et al. (2010) Elevated TGFbeta-Smad signalling in experimental Pkd1 models and human patients with polycystic kidney disease. J Pathol 222: 21-31.

26. Happe H, de Heer E, Peters D (2011) Polycystic kidney disease: the complexity of planar cell polarity and signaling during tissue regeneration and cyst formation. Biochim Biophys Acta 1812: 1249-1255.

27. Chapin HC, Caplan MJ (2010) The cell biology of polycystic kidney disease. J Cell Biol 191: 701-710.

28. Bacallao R, McNeill H (2009) Cystic kidney diseases and planar cell polarity signaling. Clin Genet 75: 107-117.

29. Grantham J, Ye M, Gattone Vn, Sullivan L (1995) In vitro fluid secretion by epithelium from polycystic kidneys. J Clin Invest 95: 195-202.

30. Liu Y (2011) Cellular and molecular mechanisms of renal fibrosis. Nat Rev Nephrol.

31. Eddy A (2000) Molecular basis of renal fibrosis. Pediatr Nephrol 15: 290-301.

32. Hahm K, Lukashev ME, Luo Y, Yang WJ, Dolinski BM, et al. (2007) Alphav beta6 integrin regulates renal fibrosis and inflammation in Alport mouse. Am J Pathol 170: 110-125.

33. Grantham J, Mulamalla S, Swenson-Fields K (2011) Why kidneys fail in autosomal dominant polycystic kidney disease. Nat Rev Nephrol 7: 556-566.

34. Lopes C, Prosser S, Romio L, Hirst R, O'Callaghan C, et al. (2011) Centriolar satellites are assembly points for proteins implicated in human ciliopathies, including oral-facial-digital syndrome 1. J Cell Sci 124: 600-612.

35. Feather SA, Woolf AS, Donnai D, Malcolm S, Winter RM (1997) The oral-facial-digital syndrome type 1 (OFD1), a cause of polycystic kidney disease and

associated malformations, maps to Xp22.2-Xp22.3. Hum Mol Genet 6: 1163-1167.

36. Zullo A, Iaconis D, Barra A, Cantone A, Messaddeq N, et al. (2010) Kidney-specific inactivation of Ofd1 leads to renal cystic disease associated with upregulation of the mTOR pathway. Hum Mol Genet 19: 2792-2803.

37. Thivichon-Prince B, Couble M, Giamarchi A, Delmas P, Franco B, et al. (2009) Primary cilia of odontoblasts: possible role in molar morphogenesis. J Dent Res 88: 910-915.

38. Feather S, Woolf A, Donnai D, Malcolm S, Winter R (1997) The oral-facial-digital syndrome type 1 (OFD1), a cause of polycystic kidney disease and associated malformations, maps to Xp22.2-Xp22.3. Hum Mol Genet 6: 1163-1167.

39. Oatley P, Stewart A, Sandford R, Edwardson J (2012) Atomic force microscopy imaging reveals the domain structure of polycystin-1. Biochemistry 51: 2879-2888.

40. Dalagiorgou G, Basdra E, Papavassiliou A (2010) Polycystin-1: function as a mechanosensor. Int J Biochem Cell Biol 42: 1610-1613.

41. Lal M, Song X, Pluznick J, Di Giovanni V, Merrick D, et al. (2008) Polycystin-1 C-terminal tail associates with beta-catenin and inhibits canonical Wnt signaling. Hum Mol Genet 17: 3105-3117.

42. Qian F, Boletta A, Bhunia AK, Xu H, Liu L, et al. (2002) Cleavage of polycystin-1 requires the receptor for egg jelly domain and is disrupted by human

autosomal-dominant polycystic kidney disease 1-associated mutations. Proc Natl Acad Sci U S A 99: 16981-16986.

43. Ward H, Brown-Glaberman U, Wang J, Morita Y, Alper S, et al. (2011) A conserved signal and GTPase complex are required for the ciliary transport of polycystin-1. Mol Biol Cell 22: 3289-3305.

44. Santoso N, Cebotaru L, Guggino W (2011) Polycystin-1, 2, and STIM1 interact with IP(3)R to modulate ER Ca release through the PI3K/Akt pathway. Cell Physiol Biochem 27: 715-726.

45. Casuscelli J, Schmidt S, DeGray B, Petri E, Celic A, et al. (2009) Analysis of the cytoplasmic interaction between polycystin-1 and polycystin-2. Am J Physiol Renal Physiol 297: F1310-1315.

46. Celic A, Petri E, Benbow J, Hodsdon M, Ehrlich B, et al. (2012) Calcium-induced conformational changes in the C-terminal tail of polycystin-2 are necessary for channel gating. J Biol Chem.

47. Ward HH, Brown-Glaberman U, Wang J, Morita Y, Alper SL, et al. (2011) A conserved signal and GTPase complex are required for the ciliary transport of polycystin-1. Mol Biol Cell 22: 3289-3305.

48. Hogan M, Manganelli L, Woollard J, Masyuk A, Masyuk T, et al. (2009) Characterization of PKD protein-positive exosome-like vesicles. J Am Soc Nephrol 20: 278-288.

49. Nadella R, Blumer J, Jia G, Kwon M, Akbulut T, et al. (2010) Activator of G protein signaling 3 promotes epithelial cell proliferation in PKD. J Am Soc Nephrol 21: 1275-1280.

50. Parnell S, Magenheimer B, Maser R, Zien C, Frischauf A, et al. (2002) Polycystin-1 activation of c-Jun N-terminal kinase and AP-1 is mediated by heterotrimeric G proteins. J Biol Chem 277: 19566-19572.

51. Terryn S, Ho A, Beauwens R, Devuyst O (2011) Fluid transport and cystogenesis in autosomal dominant polycystic kidney disease. Biochim Biophys Acta 1812: 1314-1321.

52. Ma R, Li W, Rundle D, Kong J, Akbarali H, et al. (2005) PKD2 functions as an epidermal growth factor-activated plasma membrane channel. Mol Cell Biol 25: 8285-8298.

53. Xu T, Wang N, Fu L, Ye C, Yu S, et al. (2012) Celecoxib inhibits growth of human autosomal dominant polycystic kidney cyst-lining epithelial cells through the VEGF/Raf/MAPK/ERK signaling pathway. Mol Biol Rep.

54. Zheleznova N, Wilson P, Staruschenko A (2011) Epidermal growth factor-mediated proliferation and sodium transport in normal and PKD epithelial cells. Biochim Biophys Acta 1812: 1301-1313.

55. Wu G, Markowitz G, Li L, D'Agati V, Factor S, et al. (2000) Cardiac defects and renal failure in mice with targeted mutations in Pkd2. Nat Genet 24: 75-78.

56. Liang G, Yang J, Wang Z, Li Q, Tang Y, et al. (2008) Polycystin-2 down-regulates cell proliferation via promoting PERK-dependent phosphorylation of eIF2alpha. Hum Mol Genet 17: 3254-3262.

57. Talbot J, Shillingford J, Vasanth S, Doerr N, Mukherjee S, et al. (2011) Polycystin-1 regulates STAT activity by a dual mechanism. Proc Natl Acad Sci U S A 108: 7985-7990.

58. Mekahli D, Sammels E, Luyten T, Welkenhuyzen K, van den Heuvel L, et al. (2012) Polycystin-1 and polycystin-2 are both required to amplify inositol-trisphosphate-induced Ca(2+) release. Cell Calcium.

59. Wallace D (2011) Cyclic AMP-mediated cyst expansion. Biochim Biophys Acta 1812: 1291-1300.

60. Jerman S, Ward HH, Lee R, Lopes CA, Fry AM, et al. (2014) OFD1 and flotillins are integral components of a ciliary signaling protein complex organized by polycystins in renal epithelia and odontoblasts. PLoS One 9: e106330.

61. Romio L, Wright V, Price K, Winyard PJ, Donnai D, et al. (2003) OFD1, the gene mutated in oral-facial-digital syndrome type 1, is expressed in the metanephros and in human embryonic renal mesenchymal cells. J Am Soc Nephrol 14: 680-689.

62. Ferrante M, Giorgio G, Feather S, Bulfone A, Wright V, et al. (2001) Identification of the gene for oral-facial-digital type I syndrome. Am J Hum Genet 68: 569-576.

63. Singla V, Romaguera-Ros M, Garcia-Verdugo J, Reiter J (2010) Ofd1, a human disease gene, regulates the length and distal structure of centrioles. Dev Cell 18: 410-424.

64. Romio L, Fry A, Winyard P, Malcolm S, Woolf A, et al. (2004) OFD1 is a centrosomal/basal body protein expressed during mesenchymal-epithelial transition in human nephrogenesis. J Am Soc Nephrol 15: 2556-2568.

65. Ferrante MI, Zullo A, Barra A, Bimonte S, Messaddeq N, et al. (2006) Oral-facial-digital type I protein is required for primary cilia formation and left-right axis specification. Nat Genet 38: 112-117.

66. Tang Z, Lin MG, Stowe TR, Chen S, Zhu M, et al. (2013) Autophagy promotes primary ciliogenesis by removing OFD1 from centriolar satellites. Nature 502: 254-257.

67. Praetorius HA, Spring KR (2001) Bending the MDCK cell primary cilium increases intracellular calcium. J Membr Biol 184: 71-79.

68. Ohazama A, Haycraft C, Seppala M, Blackburn J, Ghafoor S, et al. (2009) Primary cilia regulate Shh activity in the control of molar tooth number. Development 136: 897-903.

69. Magloire H, Couble ML, Romeas A, Bleicher F (2004) Odontoblast primary cilia: facts and hypotheses. Cell Biol Int 28: 93-99.

70. Allard B, Couble ML, Magloire H, Bleicher F (2000) Characterization and gene expression of high conductance calcium-activated potassium channels displaying mechanosensitivity in human odontoblasts. J Biol Chem 275: 25556-25561.

71. Thivichon-Prince B, Couble ML, Giamarchi A, Delmas P, Franco B, et al. (2009) Primary cilia of odontoblasts: possible role in molar morphogenesis. J Dent Res 88: 910-915.

72. Davenport J, Yoder B (2005) An incredible decade for the primary cilium: a look at a once-forgotten organelle. Am J Physiol Renal Physiol 289: F1159-1169.

73. Otto E, Hurd T, Airik R, Chaki M, Zhou W, et al. (2010) Candidate exome capture identifies mutation of SDCCAG8 as the cause of a retinal-renal ciliopathy. Nat Genet 42: 840-850.

74. Hurd T, Hildebrandt F (2011) Mechanisms of nephronophthisis and related ciliopathies. Nephron Exp Nephrol 118: e9-14.

75. MacDougall M, Thiemann F, Ta H, Hsu P, Chen LS, et al. (1995) Temperature sensitive simian virus 40 large T antigen immortalization of murine odontoblast cell cultures: establishment of clonal odontoblast cell line. Connect Tissue Res 33: 97-103.

76. Herbert BS, Grimes BR, Xu WM, Werner M, Ward C, et al. (2013) A telomerase immortalized human proximal tubule cell line with a truncation mutation (Q4004X) in polycystin-1. PLoS One 8: e55191.

77. Yoder B, Hou X, Guay-Woodford L (2002) The polycystic kidney disease proteins, polycystin-1, polycystin-2, polaris, and cystin, are co-localized in renal cilia. J Am Soc Nephrol 13: 2508-2516.

78. Ishikawa H, Thompson J, Yates JR, 3rd, Marshall WF (2012) Proteomic analysis of mammalian primary cilia. Curr Biol 22: 414-419.

79. Nelson DL (1995) Preparation of cilia and subciliary fractions from Paramecium. Methods Cell Biol 47: 17-24.

80. Neumann-Giesen C, Fernow I, Amaddii M, Tikkanen R (2007) Role of EGF-induced tyrosine phosphorylation of reggie-1/flotillin-2 in cell spreading and signaling to the actin cytoskeleton. J Cell Sci 120: 395-406.

81. Romio L, Fry AM, Winyard PJ, Malcolm S, Woolf AS, et al. (2004) OFD1 is a centrosomal/basal body protein expressed during mesenchymal-epithelial transition in human nephrogenesis. J Am Soc Nephrol 15: 2556-2568.

82. Vandorpe DH, Chernova MN, Jiang L, Sellin LK, Wilhelm S, et al. (2001) The cytoplasmic C-terminal fragment of polycystin-1 regulates a Ca2+-permeable cation channel. J Biol Chem 276: 4093-4101.

83. Matlin KS, Simons K (1983) Reduced temperature prevents transfer of a membrane glycoprotein to the cell surface but does not prevent terminal glycosylation. Cell 34: 233-243.

84. Feather SA, Winyard PJ, Dodd S, Woolf AS (1997) Oral-facial-digital syndrome type 1 is another dominant polycystic kidney disease: clinical, radiological and histopathological features of a new kindred. Nephrol Dial Transplant 12: 1354-1361.

85. Jerman S, Wandinger-Ness, A., Ward H.H. (2013) Polycystins and the Pathophysiology of ADPKD. In: Bacallao RL, and Gattone II., V.H., editor. Polycystic Kidney Disease 1st edition electronic book. UK: Future Science Group.

86. Giorgio G, Alfieri M, Prattichizzo C, Zullo A, Cairo S, et al. (2007) Functional characterization of the OFD1 protein reveals a nuclear localization and physical interaction with subunits of a chromatin remodeling complex. Mol Biol Cell 18: 4397-4404.

87. Ma R, Li WP, Rundle D, Kong J, Akbarali HI, et al. (2005) PKD2 functions as an epidermal growth factor-activated plasma membrane channel. Mol Cell Biol 25: 8285-8298.

88. Ohazama A, Haycraft CJ, Seppala M, Blackburn J, Ghafoor S, et al. (2009) Primary cilia regulate Shh activity in the control of molar tooth number. Development 136: 897-903.

89. Yoder BK, Tousson A, Millican L, Wu JH, Bugg CE, Jr., et al. (2002) Polaris, a protein disrupted in orpk mutant mice, is required for assembly of renal cilium. Am J Physiol Renal Physiol 282: F541-552.

90. Singla V, Romaguera-Ros M, Garcia-Verdugo JM, Reiter JF (2010) Ofd1, a human disease gene, regulates the length and distal structure of centrioles. Dev Cell 18: 410-424.

91. Tran PV, Talbott GC, Turbe-Doan A, Jacobs DT, Schonfeld MP, et al. (2014) Downregulating Hedgehog Signaling Reduces Renal Cystogenic Potential of Mouse Models. J Am Soc Nephrol.

92. Nait Lechguer A, Couble ML, Labert N, Kuchler-Bopp S, Keller L, et al. (2011) Cell differentiation and matrix organization in engineered teeth. J Dent Res 90: 583-589.

93. Miettinen PJ, Chin JR, Shum L, Slavkin HC, Shuler CF, et al. (1999) Epidermal growth factor receptor function is necessary for normal craniofacial development and palate closure. Nat Genet 22: 69-73.

94. Otto EA, Ramaswami G, Janssen S, Chaki M, Allen SJ, et al. (2011) Mutation analysis of 18 nephronophthisis associated ciliopathy disease genes using a

DNA pooling and next generation sequencing strategy. J Med Genet 48: 105-116.

95. Suda N, Kitahara Y, Ohyama K (2006) A case of amelogenesis imperfecta, cleft lip and palate and polycystic kidney disease. Orthod Craniofac Res 9: 52-56.

96. Salzer U, Prohaska R (2001) Stomatin, flotillin-1, and flotillin-2 are major integral proteins of erythrocyte lipid rafts. Blood 97: 1141-1143.

97. Neumann-Giesen C, Falkenbach B, Beicht P, Claasen S, Luers G, et al. (2004) Membrane and raft association of reggie-1/flotillin-2: role of myristoylation, palmitoylation and oligomerization and induction of filopodia by overexpression. Biochem J 378: 509-518.

98. Roitbak T, Surviladze Z, Tikkanen R, Wandinger-Ness A (2005) A polycystin multiprotein complex constitutes a cholesterol-containing signalling microdomain in human kidney epithelia. Biochem J 392: 29-38.

99. Boucher CA, Ward HH, Case RL, Thurston KS, Li X, et al. (2011) Receptor protein tyrosine phosphatases are novel components of a polycystin complex. Biochim Biophys Acta 1812: 1225-1238.

100. Amaddii M, Meister M, Banning A, Tomasovic A, Mooz J, et al. (2012) Flotillin-1/reggie-2 protein plays dual role in activation of receptor-tyrosine kinase/mitogen-activated protein kinase signaling. J Biol Chem 287: 7265-7278.

101. Merrick D, Bertuccio CA, Chapin HC, Lal M, Chauvet V, et al. (2013) Polycystin-1 cleavage and the regulation of transcriptional pathways. Pediatr Nephrol.

102. Vieira OV, Gaus K, Verkade P, Fullekrug J, Vaz WL, et al. (2006) FAPP2, cilium formation, and compartmentalization of the apical membrane in polarized Madin-Darby canine kidney (MDCK) cells. Proc Natl Acad Sci U S A 103: 18556-18561.

103. Kang RS, Folsch H (2009) An old dog learns new tricks: novel functions of the exocyst complex in polarized epithelia in animals. F1000 Biol Rep 1: 83.

104. Goetz SC, Anderson KV (2010) The primary cilium: a signalling centre during vertebrate development. Nat Rev Genet 11: 331-344.

105. Van Adelsberg J, Chamberlain S, D'Agati V (1997) Polycystin expression is temporally and spatially regulated during renal development. Am J Physiol 272: F602-609.

106. Geng L, Burrow CR, Li HP, Wilson PD (2000) Modification of the composition of polycystin-1 multiprotein complexes by calcium and tyrosine phosphorylation. Biochim Biophys Acta 1535: 21-35.

107. Thymiakou E, Episkopou V (2011) Detection of signaling effector-complexes downstream of bmp4 using PLA, a proximity ligation assay. J Vis Exp.

108. Xu C, Rossetti S, Jiang L, Harris PC, Brown-Glaberman U, et al. (2007) Human ADPKD primary cyst epithelial cells with a novel, single codon deletion in the PKD1 gene exhibit defective ciliary polycystin localization and loss of flow-induced Ca2+ signaling. Am J Physiol Renal Physiol 292: F930-945.

109. Goetz S, Anderson K (2010) The primary cilium: a signalling centre during vertebrate development. Nat Rev Genet 11: 331-344.

110. Christensen ST, Clement CA, Satir P, Pedersen LB (2012) Primary cilia and coordination of receptor tyrosine kinase (RTK) signalling. J Pathol 226: 172-184.

111. Cai Y, Fedeles SV, Dong K, Anyatonwu G, Onoe T, et al. (2014) Altered trafficking and stability of polycystins underlie polycystic kidney disease. J Clin Invest 124: 5129-5144.

112. Delling M, DeCaen PG, Doerner JF, Febvay S, Clapham DE (2013) Primary cilia are specialized calcium signalling organelles. Nature 504: 311-314.

113. DeCaen PG, Delling M, Vien TN, Clapham DE (2013) Direct recording and molecular identification of the calcium channel of primary cilia. Nature 504: 315-318.

114. Paavola J, Schliffke S, Rossetti S, Kuo IY, Yuan S, et al. (2013) Polycystin-2 mutations lead to impaired calcium cycling in the heart and predispose to dilated cardiomyopathy. J Mol Cell Cardiol 58: 199-208.

115. Wilson PD (2011) Apico-basal polarity in polycystic kidney disease epithelia. Biochim Biophys Acta 1812: 1239-1248.

116. Arbeiter A, Buscher R, Bonzel KE, Wingen AM, Vester U, et al. (2008) Nephrectomy in an autosomal recessive polycystic kidney disease (ARPKD) patient with rapid kidney enlargement and increased expression of EGFR. Nephrol Dial Transplant 23: 3026-3029.

117. Geng L, Okuhara D, Yu Z, Tian X, Cai Y, et al. (2006) Polycystin-2 traffics to cilia independently of polycystin-1 by using an N-terminal RVxP motif. J Cell Sci 119: 1383-1395.

118. Mazelova J, Astuto-Gribble L, Inoue H, Tam B, Schonteich E, et al. (2009) Ciliary targeting motif VxPx directs assembly of a trafficking module through Arf4. EMBO J 28: 183-192.

119. Xu C, Rossetti S, Jiang L, Harris P, Brown-Glaberman U, et al. (2007) Human ADPKD primary cyst epithelial cells with a novel, single codon deletion in the PKD1 gene exhibit defective ciliary polycystin localization and loss of flow-induced Ca2+ signaling. Am J Physiol Renal Physiol 292: F930-945.

120. Hanaoka K, Qian F, Boletta A, Bhunia A, Piontek K, et al. (2000) Co-assembly of polycystin-1 and -2 produces unique cation-permeable currents. Nature 408: 990-994.

121. Rollins CT, Rivera VM, Woolfson DN, Keenan T, Hatada M, et al. (2000) A ligand-reversible dimerization system for controlling protein-protein interactions. Proc Natl Acad Sci U S A 97: 7096-7101.

122. Rivera VM, Wang X, Wardwell S, Courage NL, Volchuk A, et al. (2000) Regulation of protein secretion through controlled aggregation in the endoplasmic reticulum. Science 287: 826-830.

123. Griffiths G, Tsun A, Stinchcombe J (2010) The immunological synapse: a focal point for endocytosis and exocytosis. J Cell Biol 189: 399-406.

124. Baldari CT, Rosenbaum J (2010) Intraflagellar transport: it's not just for cilia anymore. Curr Opin Cell Biol 22: 75-80.

125. Rajendran L, Beckmann J, Magenau A, Boneberg EM, Gaus K, et al. (2009) Flotillins are involved in the polarization of primitive and mature hematopoietic cells. PLoS One 4: e8290.

126. Lui-Roberts WW, Stinchcombe JC, Ritter AT, Akhmanova A, Karakesisoglou I, et al. (2012) Cytotoxic T lymphocyte effector function is independent of nucleus-centrosome dissociation. Eur J Immunol 42: 2132-2141.
127. Banning A, Tomasovic A, Tikkanen R (2011) Functional aspects of membrane association of reggie/flotillin proteins. Curr Protein Pept Sci 12: 725-735.
128. Meister M, Tomasovic A, Banning A, Tikkanen R (2013) Mitogen-Activated Protein (MAP) Kinase Scaffolding Proteins: A Recount. Int J Mol Sci 14: 4854-4884.
129. Kurrle N, Ockenga W, Meister M, Vollner F, Kuhne S, et al. (2013) Phosphatidylinositol 3-Kinase dependent upregulation of the epidermal growth factor receptor upon Flotillin-1 depletion in breast cancer cells. BMC Cancer 13: 575.
130. Zhang ZR, Chu WF, Song B, Gooz M, Zhang JN, et al. (2013) TRPP2 and TRPV4 form an EGF-activated calcium permeable channel at the apical membrane of renal collecting duct cells. PLoS One 8: e73424.
131. Marley A, Choy RW, von Zastrow M (2013) GPR88 reveals a discrete function of primary cilia as selective insulators of GPCR cross-talk. PLoS One 8: e70857.
132. Manzanares D, Monzon ME, Savani RC, Salathe M (2007) Apical oxidative hyaluronan degradation stimulates airway ciliary beating via RHAMM and RON. Am J Respir Cell Mol Biol 37: 160-168.

133. McCleese JK, Bear MD, Kulp SK, Mazcko C, Khanna C, et al. (2013) Met interacts with EGFR and Ron in canine osteosarcoma. Vet Comp Oncol 11: 124-139.

134. Benvenuti S, Lazzari L, Arnesano A, Li Chiavi G, Gentile A, et al. (2011) Ron kinase transphosphorylation sustains MET oncogene addiction. Cancer Res 71: 1945-1955.

135. Peace BE, Hill KJ, Degen SJ, Waltz SE (2003) Cross-talk between the receptor tyrosine kinases Ron and epidermal growth factor receptor. Exp Cell Res 289: 317-325.

136. Liu HS, Hsu PY, Lai MD, Chang HY, Ho CL, et al. (2010) An unusual function of RON receptor tyrosine kinase as a transcriptional regulator in cooperation with EGFR in human cancer cells. Carcinogenesis 31: 1456-1464.

137. Horie S, Higashihara E, Nutahara K, Mikami Y, Okubo A, et al. (1994) Mediation of renal cyst formation by hepatocyte growth factor. Lancet 344: 789-791.

138. Qin S, Taglienti M, Cai L, Zhou J, Kreidberg JA (2012) c-Met and NF-kappaB-dependent overexpression of Wnt7a and -7b and Pax2 promotes cystogenesis in polycystic kidney disease. J Am Soc Nephrol 23: 1309-1318.

139. Zheleznova NN, Wilson PD, Staruschenko A (2011) Epidermal growth factor-mediated proliferation and sodium transport in normal and PKD epithelial cells. Biochim Biophys Acta 1812: 1301-1313.

140. Deretic D (2013) Crosstalk of Arf and Rab GTPases en route to cilia. Small GTPases 4: 70-77.

141. Nachury M, Seeley E, Jin H (2010) Trafficking to the ciliary membrane: how to get across the periciliary diffusion barrier? Annu Rev Cell Dev Biol 26: 59-87.
142. Jin H, White SR, Shida T, Schulz S, Aguiar M, et al. (2010) The conserved Bardet-Biedl syndrome proteins assemble a coat that traffics membrane proteins to cilia. Cell 141: 1208-1219.
143. Charron AJ, Bacallao RL, Wandinger-Ness A (2000) ADPKD: a human disease altering Golgi function and basolateral exocytosis in renal epithelia. Traffic 1: 675-686.
144. Hanaoka K, Qian F, Boletta A, Bhunia AK, Piontek K, et al. (2000) Co-assembly of polycystin-1 and -2 produces unique cation-permeable currents. Nature 408: 990-994.
145. Nauli SM, Alenghat FJ, Luo Y, Williams E, Vassilev P, et al. (2003) Polycystins 1 and 2 mediate mechanosensation in the primary cilium of kidney cells. Nat Genet 33: 129-137.
146. Tanos BE, Yang HJ, Soni R, Wang WJ, Macaluso FP, et al. (2013) Centriole distal appendages promote membrane docking, leading to cilia initiation. Genes Dev 27: 163-168.
147. Joo K, Kim CG, Lee MS, Moon HY, Lee SH, et al. (2013) CCDC41 is required for ciliary vesicle docking to the mother centriole. Proc Natl Acad Sci U S A 110: 5987-5992.
148. Kim J, Krishnaswami SR, Gleeson JG (2008) CEP290 interacts with the centriolar satellite component PCM-1 and is required for Rab8 localization to the primary cilium. Hum Mol Genet 17: 3796-3805.

149. Sillibourne JE, Hurbain I, Grand-Perret T, Goud B, Tran P, et al. (2013) Primary ciliogenesis requires the distal appendage component Cep123. Biol Open 2: 535-545.

150. Thauvin-Robinet C, Cossee M, Cormier-Daire V, Van Maldergem L, Toutain A, et al. (2006) Clinical, molecular, and genotype-phenotype correlation studies from 25 cases of oral-facial-digital syndrome type 1: a French and Belgian collaborative study. Journal of Medical Genetics 43: 54-61.